Geoprocessing Approaches to Delineate Impoundments and Characterize Subcatchments within Kansas Reservoir Drainages

By

Andrew Charles Duncan Cleary

Submitted to the graduate degree program in Geography

and the Graduate Faculty of the University of Kansas in partial fulfillment of the

requirements for the degree of Master of Science.

_____

Chair Stephen Egbert

_____

Xingong Li

_____

Frank deNoyelles

_____

Edward Martinko

Date Defended: January 13, 2017

The Thesis Committee for Andrew C. D. Cleary
certifies that this is the approved version of the following thesis:

Geoprocessing Approaches to Delineate Impoundments and Characterize Subcatchments within Kansas Reservoir Drainages

_____
Chair Stephen Egbert

_____
Xingong Li

Date approved: January 13, 2017

ABSTRACT

Andrew C. D. Cleary, M.S.
Department of Geography, 2017
University of Kansas

Federal reservoirs in Kansas are presently undergoing infill at varying rates and represent a growing concern, as these features are integral to the state's infrastructure and projected dredging required to restore capacities are substantial. Kansas exhibits a unique hydrography by having some of the highest densities of small impoundments in the United States. Previous studies have highlighted the potential of impoundments to act as significant sinks for sediment. However, their significance within Kansas reservoir drainages and potential service in mitigating downstream reservoir sediment yields is not well understood. This thesis seeks to improve understanding of small impoundments distributions and significance in relation to reservoir sediment yield through two stages.

Chapter 2 applies elevation-based methods of impoundment identification using newly available LiDAR-derived Digital Elevation Models (DEM) in order to enhance Kansas reservoir drainage inventories relative to relying solely on the National Hydrography Dataset (NHD). The two DEM-based methodologies resulted in the identification of features absent in the NHD, and accuracy testing showed both DEM-based methodologies produce more accurate surface area geometries. In turn, the two approaches can be used to update and improve accuracy of inventories relative to using the NHD exclusively.

Chapter 3 delineates small impoundment catchment areas within nine eastern Kansas reservoir drainages and compares erosion-related traits in the context of impoundment catchment

and direct runoff. The majority of sediment presently infilling Kansas reservoirs has been noted as originating from channel-bank erosion sources, not overland sources. Since impoundments are potentially positioned in the path of channel-bank eroded material, better understanding both their distribution and their potential sediment trapping is an important aspect of reservoir drainage yield modeling and management. By investigating erosion-related factors for reservoir drainages and addressing impoundment catchment, several possible trends were observed. For example, contrasting impoundment size distributions were observed in the highest and lowest drainage sediment yields. Impoundments tend to be more abundant in reaches and grassland areas, while they decrease in abundance closer to reservoirs and in cropland areas. Additionally, average catchment area for small impoundments in the region is much smaller than previous estimates, which may suggest smaller sediment loads reaching impoundments.

This thesis demonstrates new approaches to investigating potential trends relating to reservoir sedimentation and suggests several avenues for further research. As LiDAR-derived DEMs become increasingly available, methods such as those demonstrated in Chapter 2 are particularly valuable. Not only does this project highlight potential inaccuracies of the NHD, but it presents automated and easily repeatable methods to enhance NHD-based inventories in other regions. Chapter 3 considers the significance of small impoundments when investigating potential sources of difference in Kansas reservoir drainage yields, which is a component often absent in drainage scale erosion modeling. Given the abundance of small impoundments for the region and the projected costs of reservoir restoration, this study provides insight into the significance of small impoundments in connection to a growing concern. By better assessing the factors responsible for differing rates of infill among reservoir drainages, reservoir drainage management may make more informed decisions. Additionally, this project also capitalizes on

the growing abundance of LiDAR-derived DEMs, and demonstrates their value in delineating small impoundment catchment to better understand their role as mitigators of downstream sediment yield.

ACKNOWLEDGMENTS

There are many that I am indebted to for assisting me throughout this project and my graduate studies. My committee members, Steve Egbert, Xingong Li, Jerry deNoyelles, and Ed Martinko, all provided wonderful guidance and a great deal of patience. Ed Martinko has been a mentor to me since I first came to the University of Kansas and has always been a voice of reason and source of encouragement in my graduate studies. Jerry deNoyelles, the resident reservoir infill expert at the University of Kansas, has provided invaluable “food for thought”, and consistently helped me see the broad picture when I became bogged down in the details. I have Xingong Li to thank for teaching me just about everything I know related to GIS and programming. His courses and guidance fueled my interest in GIS and made this project possible. Finally, Steve Egbert has provided much needed notes throughout the process and offered greatly appreciated optimism and reassurance during the particularly stressful times.

Thank you to the staff and faculty of the Kansas Biological Survey (KBS) for making it a habit to leave their doors open to precocious graduate students. Jude Kastens has been especially helpful with this project. His help in attaining the DEMs, introducing me to the Topographic Wetland Identification Process (TWIP), and guidance in navigating the geoprocessing made this project feasible and saved me a great deal of trial and error. Thank you to Vahid Rahmani for providing me the reservoir infill data, which was a major source of direction for this project. Scott Campbell and Paul Liechti are owed thanks for allowing me to participate in reservoir sediment coring and always making time to discuss sedimentation and research with me. Additionally, I am indebted to Jerry Whistler for salvaging my laptop data after a crash early on

in the project. Finally, thank you to Bob Hagen for granting me my first opportunity to teach, and for demonstrating a passion for ecology and education that has forever left an impression on me.

There are several family members that have been truly accommodating and encouraging throughout my graduate career. I owe my aunt and uncle, Jerry and Gwen Dobson, tremendous thanks for introducing me to KU and showing me the value in studying geography. Thank you to my parents, who have been continuous sources of support, and demonstrated degrees of patience that I hope to never ask of them again. Thank you to my brother and his wife for all of their confidence and support. Finally, thank you to my grandmother and grandfather, who have been limitless sources of encouragement and two of my greatest influences.

TABLE OF CONTENTS

Abstract iii

Acknowledgments vi

List of Figures x

List of Tables xii

Chapter 1: **Introduction**

Introduction 1
Background
Abundance of Impoundments and Impoundments Characterization in Kansas 2
Kansas Reservoir Fill Concerns and Factors Influencing Downstream Sediment Yield 4
Methods of Impoundment Identification 10
Problem Summary and Research Objectives 14
Significance 16
References 18

Chapter 2: **Approaches in Identifying New Water Bodies and Improving Geometries Relative to the NHD**

Introduction 21
Hydrological, Sedimentation, and Geochemical Effects of Impoundments 21
Ecological Effects of Impoundments 26
Current Water Body Inventories 33
Water Body Identification Associated with LiDAR-derived Data 38
Project Summary 41
Methodology
Study Area and Data Sources 43
Preliminary Processing 44
Topographic Wetland Identification Process Model (TWIP) and Zero Slope Method (ZS) 46
Accuracy Assessment 48
Combined Dataset 48
Results
NHD Results 49
TWIP Results 49

Zero Slope Results 50
Combined Dataset 51
Surface Area Difference 51
Accuracy Assessment 52
Discussion
TWIP Accuracy and Limitations 52
Zero Slope Effectiveness and Efficiency 54
Summary and Significance of Combined Dataset 56
Conclusions 59
References 60

Chapter 3: **Comparing Impoundment Abundance, Distribution, and Catchment Traits among Eastern Kansas Reservoir Drainages**

Introduction 82
Reservoir Fill Concerns in Kansas 83
Kansas Landscape Factors Related to Erosion and Sedimentation 86
Obstacles to Incorporating Small Water Features into Reservoir Drainage Modeling 91
High Resolution Subcatchment Delineation and Data Availability for Kansas 95
Project Summary 96
Methodology
Study Area & Data Sources 98
Preliminary Processing 100
Water Body Size Distribution and Catchment Calculations 100
Erosion-related Landscape Traits 101
Results
Individual Drainage Summaries 102
Combined Results 103
Discussion
Similarities and Differences in Erosion-related Traits 105
Cumulative Data, Subcatchment, and Direct Runoff Area Trends 108
Conclusions 110
References 113

Chapter 4: **Conclusions**

Summary 141
Further Research 144
Significance 146
References 147

Appendix 149

List of Figures

Chapter 2

Figure 1. Reservoir Drainage Areas....64

Figure 2. John Redmond Reservoir Drainage Boundary....65

Figure 3. Overview of Processing....66

Figure 4. Drainage DEM Extraction....68

Figure 5. Extraction of NHD Data for Individual Reservoir Drainages....68

Figure 6. Road and Railroad Removal....69

Figure 7. TWIP....70

Figure 8. Effect of Zero Slope Buffer....71

Figure 9. Accuracy Assessment for Zero Slope....72

Figure 10. Accuracy Assessment Equation....73

Figure 11. Joining of NHD Feature Fragments....74

Figure 12. Fragmented Zero Slope Feature Joined by TWIP Procedure....75

Chapter 3

Figure 1. Reservoir Drainage Areas....118

Figure 2. Annual Precipitation for Kansas....119

Figure 3. Catchment Delineation....120

Figure 4. Land Use Extraction for Drainage, Subcatchment, and Direct Runoff Area....120

Figure 5. Soil Data Extraction for Drainage, Subcatchment, and Direct Runoff Area....121

Figure 6. Slope Summary Statistics....122

Figure 7. Catchment Fragmentation during Conversion from Raster to Polygon....123

Figure 8. Results for Marion Reservoir Drainage....124

Figure 9. Results for El Dorado Reservoir Drainage.....125

Figure 10. Results for Council Grove Reservoir Drainage.....126

Figure 11. Results for Pomona Reservoir Drainage 127

Figure 12. Results for Melvern Reservoir Drainage.....128

Figure 13. Results for Clinton Reservoir Drainage 129

Figure 14. Results for Fall River Reservoir Drainage 130

Figure 15. Results for Toronto Reservoir Drainage.....131

Figure 16. Results for Perry Reservoir Drainage.....132

Figure 17. Surface–Area–to–Catchment–Area Ratio for Absent NHD Feature.....133

List of Tables

Chapter 2

Table 1. NHD Results 76

Table 2. TWIP Results 77

Table 3. Zero Slope Results 78

Table 4. Combined Dataset Results 79

Table 5. Surface Area 80

Table 6. Accuracy Assessment Results 81

Chapter 3

Table 1. Reservoir Sedimentation Summary 134

Table 2. Water Body Surface Area Distribution 135

Table 3. Water Body Catchment Sizes Summary 135

Table 4. Surface–Area–to–Catchment–Area Ratios 136

Table 5. Percentage Subcatchment 136

Table 6. Land Use Distribution 137

Table 7. Soil Erosion Class Distribution 138

Table 8. Soil Runoff Classification Distribution 139

Table 9. Slope Summary Statistics 140

Chapter 1

Introduction

Introduction

The decline of water resources is a global problem exacerbated by climate change and unprecedented population growth. On a regional scale, water problems are more localized, reflecting the land use history, physical environment, and policy decisions of the area. In Kansas, federal reservoirs, which provide municipal, agricultural, flood control, and recreational services, are experiencing capacity loss due to sedimentation. Projected costs of capacity restoration are substantial, and research investigating factors that mitigate the impacts of sedimentation could prove valuable in developing more efficient management strategies. One such factor, small impoundment distribution in Kansas reservoir drainages, has been relatively understudied in terms of reducing reservoir sediment yield.

Newly available high-resolution digital elevation models (DEMs) covering most of the state allow application of automated approaches to identifying small impoundments and a means to improving an important and popular water body dataset. This enhanced elevation dataset has been produced over the past six years and therefore includes impounded features constructed since the completion of the National Hydrology Dataset (NHD) in 2007. Deriving water bodies' geometries and positions in the context of recent high-resolution elevation data not only identifies features absent in the NHD, but it also provides compatible pour points for subcatchment delineation using the same elevation data. In turn, a more current and accurate

water body dataset can be developed for Kansas reservoir drainages, offering a new resource to study the relationship between impoundment distribution and reservoir sediment yield.

Furthermore, traits fundamental to erosion and runoff modeling can be quantified within impoundment catchments areas and compared with downstream reservoir fill rates. While landscape and climate traits have been characterized for reservoir drainage areas in Kansas, distinguishing the influence of these factors according to subcatchment area versus unimpeded reservoir catchment area may illuminate a landscape factor worthy of consideration when addressing current reservoir sedimentation concerns and future management strategies.

Abundance of Impoundments and Impoundment Characterization in Kansas

Historically, environmental analysis of lentic systems, or still water features, on a global level has been hindered by fragmentary data on the size and distribution of the world's lakes and impoundments. However, advancements in remote sensing and satellite imagery resolution offer more accurate tools for estimation. In a study by Downing et al. (2006), enhanced spatial resolution coupled with novel analytical approaches estimated the world's lakes and impoundments to exceed 304 million. Lakes and reservoirs cover 4.2 million square kilometers and are comprised of millions of lakes covering less than 1 sq. kilometer. In terms of farm ponds, the estimated aggregated area exceeds 77,000 square kilometers globally, with between 0.1–6.0% of total agricultural land area covered by small impoundment surface area (Downing et al., 2006).

In the conterminous United States, the majority of the water surface area is attributed to artificial water bodies with distribution and functionality differing by local climate and land use

traits. When excluding the Great Lakes, unaltered natural lakes account for only a small percentage of water area across the conterminous U.S. (Smith et al., 2002). Of this total surface area occupied by artificial water bodies, impoundments less than 4 ha or roughly less than 10 acres account for 20% of lentic water surface area (Smith et al., 2002). Nationally, the number of water bodies covering less than 10 acres exceeds the number of larger bodies by an estimated factor of 70, and the trend for these smaller waterbodies is one of overall increase, with numbers estimated to grow 1-3% annually across the U.S. (Smith et al., 2002). The number of impoundments is much higher east of the continental divide, with the lowest density but often larger average surface areas occurring in arid regions of the southwest (Smith et al., 2002). Agricultural portions of the Midwest tend to have the highest densities of impoundments and the smallest mean surface areas (Smith et al., 2002). Specifically, the eastern portion of the Great Plains exhibits the greatest abundance of impoundments (Smith et al., 2002) due to agricultural water supply needs. Oklahoma, for example, has double the average density of waterbodies of Minnesota, which are primarily comprised of natural lakes. Furthermore, many of Oklahoma's impoundments emerged in the past century (Smith et al., 2002). Not surprisingly, findings by Smith et al. (2002) demonstrated an east to west decreasing gradation of impoundments between 95 – 103° W due to rain shadow effects of the Rockies and increasing precipitation moving east. Kansas falls within this longitudinal range and is representative of this gradient.

Kansas exemplifies the agricultural industry's tendency both towards constructing small impoundments and a dependence on reservoir water services. Kansas alone boasts over 200,000 impoundments under 40 hectares, which combined cover approximately 288 square miles and store an estimated 1,299,000 acre/feet of water (NHD, 2016; Callihan, 2013). The density gradient for small impoundments as estimated by Smith et al. (2002) ranges from less than 0.03

impoundments per km^2 in western portions of the state to an average of 1-3 water bodies per km^2 in the eastern third. Regarding large reservoirs, Kansas has over 200 reservoirs with surface areas exceeding 20 hectares, mostly state or federally owned (deNoyelles & Kastens, 2016). Eighty of these provide primary or backup drinking water for 60% of the state's population and provide flood control services, which was the primary purpose for construction of the state's 24 federal reservoirs. While these larger reservoirs provide municipal, flood control, and recreational services, smaller impoundments also provide a variety of services including livestock watering, irrigation, domestic water, and recreation (deNoyelles & Kastens, 2016). For a region with natural lentic systems limited to ephemeral playas predominately in western Kansas and relatively few oxbow and sinkhole lakes statewide (Martinko et al., 2014), this extensive landscape modification has substantially altered hydrological and physical processes.

Kansas Reservoir Fill Concerns and Factors Influencing Downstream Sediment Yield

Water resources loss is a global issue, and like other declining resources, population growth and climate change have been identified and studied as factors influencing projected water resources loss. A paper by Vorosmarty et al. (2000) modeled the loss of water resources on a global scale in relation to climate change and population growth rates. Using census and climate data from 1985 – 2000, researchers predicted climate change and population growth leading up to 2025. Statistical analysis found population growth to be more influential on water resources stress than climate change. While it is difficult to accurately model and quantify change in global stress on water resources, the overall pattern is one of "pandemic increase" (Vorosmarty et al., 2000). Kansas has experienced a population increase of 164,000 people

between 2000 and 2010 (U.S. Census Bureau, 2015), which represents an increased demand of nearly 1.8 M m^3 of drinking water per year (Rahmani et al., 2017). In addition to population growth and climate change consequences, an arguably more immediate and potentially financially taxing water resources problem is presently garnering concern in Kansas.

Many reservoirs of eastern Kansas are approaching the end of their usable life as sediment fill approaches 50%. By 2030, the first three federal reservoirs in Kansas, Tuttle Creek, Toronto, and John Redmond – will reach 50% infilling and require dredging to maintain functionality (deNoyelles & Kastens, 2016). If current fill rates remain constant, another 8 of the state's 24 federal reservoirs will be half in-filled by 2105, and 44% of the total storage will be lost for the combined 24 (deNoyelles & Kastens, 2016). As reservoirs lose storage capacity to sedimentation, shallow zones expand, and the relatively young and unstable biotic communities can shift towards excess cyanobacteria growth, which can be detrimental to water quality (deNoyelles & Jakubauskus, 2008; deNoyelles & Kastens, 2016). In addition, capacity loss impairs a reservoir's function as a flood deterrent. As the state considers plans for dredging action to recover reservoir capacity, projected costs are staggering. At a present-day cost of roughly $6 for removal of one cubic yard of sediment, restoring the 24 federal reservoirs to their original volume by the end of the century would cost $13.8 billion (deNoyelles & Kastens, 2016). Furthermore, 1.4 million acres of one foot deep sediment would have to be disposed of, and costs and methods of disposal are difficult to ascertain (deNoyelles & Kastens, 2016).

Reservoir sediment yield is dependent on several landscape factors, which naturally are related to sediment load in reservoir tributaries. Streamflow is the main source of sediment for reservoirs, and higher rates of sedimentation correlate with drainage areas experiencing higher precipitation rates (Langbein & Schumm, 1958). Increased runoff results in greater discharge and

sediment carrying capacity. In turn, potential runoff and sediment load are dependent on drainage area, watershed slope, soil type and permeability, and land use (Bedient et al., 2013; deNoyelles & Jakubauskus, 2008). Drainage area determines the volume of water generated by a precipitation event (Bedient et al., 2013), the impacts of which are as follows. Watershed slope reflects the change in elevation with distance in an overland flow area and influences overland flow velocity. Soil type determines infiltration rate and water-holding capacity of the landscape. Finally, land use and land cover have significant effects on watershed response by influencing overland flow velocity, infiltration, and susceptibility to erosion. Under the "Rational Method" common in hydrological modeling, land cover types ranking from least to greatest runoff potential are as follows: woodland or forest, meadow or grassland, pasture or range land, cultivated land, and urban areas with increasing percent imperviousness (Bedient et al., 2013).

The present-day Kansas landscape is the product of a history of intensive land use and modified fluvial systems, which has resulted in higher than pre-settlement sediment loads and lentic body sedimentation rates exceeding those of most natural lakes. Prior to Euro-American settlement, Kansas watersheds were dominated by native grasslands, and riparian vegetation effectively stabilized soil and slowed runoff (deNoyelles & Kastens, 2016). However, current federal reservoir watersheds can be characterized by nutrient rich and erodible soils, which in many cases have experienced row crop production for the last 125 – 150 years (deNoyelles & Kastens, 2016). Infill rates for natural lakes of comparable size are not as high as rates for Kansas's federal reservoirs, in part due to the greater watershed-to-basin area ratio typical of Kansas reservoirs (deNoyelles & Kastens, 2016). Furthermore, drainage modifications have been implemented in the form of straightened stream channels and constructed bank levees (Juracek & Zeigler, 2007). While the purpose for these modifications is based on channel position

stabilization and local flooding mitigation, the changes have resulted in "high water flows, reduced residence time, increased in-channel erosion, and increased sediment carrying capacity compared to pre-European settlement conditions" (deNoyelles & Kastens, 2016). In a study highlighting the source of sediment infilling for Perry Lake, Juracek and Zeigler (2007) used chemical tracers to measure sediment origins from channel banks and surface soils. Results indicated that the majority of sediment infilling the reservoir originated from channel-bank sources (Juracek & Zeigler, 2007).

In catchment areas with similar precipitation patterns, landscape factors clearly influence specific sedimentation yields. However, an additional factor, one relatively understudied on reservoir catchment scale and placed so as to intercept channel-bank eroded material, may be mitigating Kansas reservoir sedimentation. Given the abundance of small impoundments in the state, it is likely that they play a significant role in trapping sediment that would otherwise contribute to downstream reservoirs. Therefore, better characterization of their function as sediment sinks may augment reservoir watershed management knowledge.

Studies have shown that small impoundments act as sediment sinks on a scale comparable to major lakes and reservoirs. Dams have been described as "significant features of every river and watershed of the nation" (Gaff, 1999). While the effects of sediment and particulate trapping in rivers is well documented (Trimble and Bube, 1990; Meade, 1990), the effects of upstream sediment trapping by small impoundments has often been overlooked (Mulholland & Elwood, 1982; Stallard, 1998; Smith et al., 2001). An estimated two thirds of annual erosion in the United States, or 600 t km^{-2} $year^{-1}$ (Smith et al., 2001), is deposited in lentic systems. However, this accumulation is thought to be split fairly evenly between large and small (<4 ha) water bodies (Smith et al., 2002). A 2005 study by Renwick et al. examining small

impoundments in the conterminous United States estimated total catchment area and sediment load trapped by small impoundments. Estimates from the study estimated that 25% of total sheet and rill erosion settle in small impoundments, which capture 21% of the total watershed areas for the subcontinental United States. Furthermore, using three separate models to compare small impoundment sediment load to that of reservoirs, total sediment rates in U.S. ponds ranged from 0.43 – 1.78 x $10^9 m^3 yr^{-1}$, which potentially matches or exceeds estimated total reservoir accumulation of 1.67 x $10^9 m^3 yr^{-1}$ and supports the conclusions of Smith et al. (Renwick et al., 2005). This wide range of projected small impoundment sediment yields reflects the difficulty of measuring cumulative small impoundment accumulation with precision. This may be due in part to the shear abundance of small water bodies, limited high resolution data and methods, and the multitude of factors involved in hydrological and sediment modeling. Nevertheless, it is accepted that small impoundments are significant sinks and reducers of downstream sediment load, although their value in moderating downstream reservoir sediment yields is still not well understood.

Given that sediment is itself a sink for nutrients, impoundments also serve as nutrient sinks, reducing riverine nutrient transport. A spatial modeling study (Bosch, 2008) of two Michigan watersheds investigated impoundment size and positioning in relation to total phosphorous (TP) and total nitrogen transport (TN). Results showed TP and TN transport doubling after impoundments were removed from the model. As expected, impoundments were most effective at reducing TP and TN transport when positioned near the mouth of the river or in nitrogen and phosphorous source areas (Bosch, 2008). In the Midwest, Smith et al. (2002) has attributed the tendency of small impoundments to trap disproportionate amounts of nutrients to their proneness to occur in proximity to agricultural sources of nutrient loading. Finally, Bosch

(2008) found that multiple smaller impoundments caused a greater cumulative reduction in transport than a single large reservoir. Given the high density of small impoundments in Kansas and the current issues surrounding reservoir filling and eutrophication occurrences, the results from Bosch evoke the question: To what extent are small impoundments reducing the likelihood of eutrophication in downstream reservoirs by serving as nutrient sinks? If farm ponds are in fact catchments for high nitrogen and phosphorous source areas (i.e., fertilized crop land), the reduction in nutrient transport could provide a significant service in managing downstream reservoir water quality.

An additional service often overlooked in small impoundment valuation is the burial of organic carbon (OC). This process may be considered more significant in reducing atmospheric carbon dioxide levels than regulating downstream water quality. Downing et al. (2008) assessed OC burial in 40 impoundments in an intensively farmed region of Iowa. Results indicated that impoundments buried a higher concentration of OC than natural lakes due to heavier sedimentation and sediment aggregate transport, and OC burial proportions were significantly higher in small impoundments (Downing et al., 2008). As in the case of nitrogen and phosphorus, this effect can be attributed to the tendency for rapid vertical accretion by small impoundments.

Because small impoundments are sinks for sediment, nutrients, and organic carbon, they provide a service in reducing downstream accumulation, including in managed reservoirs. However, it should be noted that, like reservoirs, impoundments eventually fill. There is relatively little research on how and when a small impoundment may turn from sink to source, but it could be assumed that impoundments are experiencing similar specific yields to nearby reservoirs due to similarity in landscape factors. Should the shift occur, the re-release of contents

into a stream system would likely disturb the lotic reach and contribute an abundance of sediment, nutrients, and carbon to the downstream lentic body. This deleterious effect on water quality and increased sediment and nutrient transport would reflect a reverse in the aforementioned sink services of small impoundments. However, operating under the assumption that small impoundments retain their sink functionality, effectively identifying their occurrence and characterizing their catchments may provide insight into their influence on downstream reservoir sedimentation.

Methods of Impoundment Identification

Historically, GIS water feature datasets have been created through manual geoprocessing with source data including topographic maps, land use raster data, and aerial imagery. The process of identification and digitization has often been hindered by spatial resolution, time, and resources available for manual geoprocessing. The National Hydrology Dataset (NHD) was developed using topographic quadrangle digitization coupled with visual identification using orthoimagery. Since the onset of its production, higher spatial resolution aerial imagery has become more common, and more recently, LiDAR has offered unprecedented digital elevation data resolution for select regions. LiDAR-derived DEMs combined with GIS tools and programming languages now offer novel approaches to identify small water features in the landscape, automating the geoprocessing and reducing inconsistencies resulting from human error.

Following the advent of GIS, features of topographic maps could be digitized for cataloguing and analysis purposes, and aerial imagery aided in the validation of digitized water

features. As described above, the NHD is the product of digitized water features drawn from topographic maps supplemented with aerial imagery. NHD source topographic maps range from the 1950s to present, and geometry validation during digitization (beginning in the 1990's) was restricted by the temporal and spatial resolution of orthoimagery available at the time (USGS, 2009). In addition to dated source maps and imagery, another limitation of NHD accuracy can be attributed to manual photointerpretation methods, which are subject to human error and inconsistencies (Carpenter et al., 2011). While the NHD includes much of the long-term impoundments exceeding 100 square feet in relative geometric accuracy (USGS, 2009), introducing new methodologies and more recent data may allow not only the identification of more recently constructed water bodies, but produce updated, improved geometries as well.

A study by Smith and researchers further emphasizes potential spatial resolution and manual geoprocessing limitations of manual water feature identification and dataset generation. Smith et al. (2002) first used the United States Geological Survey (USGS) Land Cover Dataset to vectorize 30-m pixels representative of water bodies to estimate impoundment abundance in the conterminous United States. This dataset resulted in an estimate of 2.6×10^6 water bodies with a lower surface area limit of 1000 m^2 (Smith et al., 2002). When using higher resolution data offered by the USGS Digital Line Graph dataset and a feature resolution limit of 25 m^2, researchers turned to extrapolation rather than the massive manual geoprocessing resources that would have been required. The resulting number for total water bodies in the conterminous U.S. was estimated at 9×10^6 (Smith et al., 2002). While enhanced raster resolution offered identification of finer water features, the geoprocessing that would have been required by manual geoprocessing forced researchers to extrapolate regional findings and potentially compromise accuracy.

Using LiDAR-derived elevation data, researchers have been able to automatically distinguish water bodies in largely consistent, efficient, and easily duplicated approaches. A popular approach demonstrated by Leonard et al. (2012), uses neighborhood analysis to distinguish depressions. The study incorporated 2 meter LiDAR elevation data into custom relief models to identify localized concavity and potential wetland locations. Each raster cell value was divided by the mean of the adjacent cell values. Should the ratio be < 1.0, concavity is indicated. Results showed an 85.1% accuracy rate in the automated wetland identification after field validation. Wu et al. (2014) further demonstrated advantages of depression analysis using LiDAR-derived DEMs and developed an approach to identify vernal pools more accurately and efficiently than previous photointerpretation methods. Wu and colleagues developed a semi-automated approach to extract surface depressions from a 1 meter resolution DEM, which alleviated inconsistencies and repeatability issues inherent in manual geoprocessing (Wu et al., 2014). Furthermore, boundaries of vernal pools identified using DEMs can be extracted as polygon features, automating characterization of geometric properties (Wu et al., 2014). While photointerpretation and manual feature tracing have historically been popular approaches to the identification of minor lentic bodies, these recent studies demonstrate the possible improvements in consistency and efficiency associated with automated geoprocessing using LiDAR-derived DEMs.

In a regional study occurring in western Kansas, photointerpretation using 1-m and 2-m imagery led to the successful identification of new ephemeral water body features relative to previous catalogs. By combining the high-resolution aerial imagery, raster graphics, soils data, and manual feature delineation, Bowen et al. (2010) conducted playa identification to augment previous datasets for 46 counties in western Kansas. The resulting dataset included 22,045

playas, more than doubling that of previous inventories, with a field validation accuracy assessment of 98% (Bowen et al., 2010). Bowen attributed the success in identifying new features and the failure of past inventories to the enhanced spatial resolution of the imagery data. Since this study's publication, equally high-resolution elevation data have been made available for the study area as well as much of the rest of the state. With this new 2-m LiDAR-derived elevation data, an alternative approach to playa identification has successfully demonstrated automatic feature identification and reduced manual processing relative to Bowen's approach.

Kastens et al. (2016) identified playas by extracting sinks meeting depth threshold criteria from LiDAR-derived DEMs, naming the model the Topographic Wetland Identification Process (TWIP). Researchers found that DEM preparation prior to running TWIP, including applying a median focal filter and burning interpolated elevation values into buffered road and railroad areas, resulted in fewer false positives in the model results. The TWIP works by first creating a sink depth map by subtracting prepared DEM from a filled DEM and selecting sink depth pixels with a value less than or equal to a given depth threshold. These pixels are vectorized into polygons representing water bodies, the elevation values inside the polygons "punched" from the DEM, and the process repeated with new features appended to the dataset until no new features are identified. After establishing suitable DEM preparation and applying various depth thresholds, researchers identified 37.3% of features present in the Playa Lakes Joint Venture (PLJV) dataset (Kastens et al., 2016). Given the broad study area, ephemeral nature of playas, extensive number of features not intersecting with the PLJV, and the purpose of the funding, exact determination of which additional features identified were undocumented playas and which were false positives was not carried out. However, the study demonstrated a novel automated approach to identifying subtle water lentic features over a broad area of Kansas, and the steps

involved have been scripted in Python and packaged as an ArcGIS tool for easy duplication and application to other study areas. Furthermore, researchers were able to delineate playa catchment areas by making use of the ArcGIS toolset and 2 meter DEMs, a task previously impossible to complete accurately for the smallest playas due to absence of high-resolution DEMs.

Since the compilation of the NHD for the area covering Kansas, new imagery and elevation data have been developed. Recent studies have demonstrated success in water feature identification via automated depression or sink analysis using 1-m and 2-m DEMs (Leonard et al., 2012; Wu et al., 2014; Kastens et al., 2016). With LiDAR-derived DEMs now available for the majority of Kansas, there is an opportunity to apply similar geoprocessing methods focused on water feature identification and recognition of recently constructed water bodies absent in the NHD as well as update preexisting feature geometries. Furthermore, an automated geoprocessing approach may offer a more efficient, consistent, and easily duplicated alternative to previous photointerpretation and topographic map digitization.

Problem Summary and Research Objectives

The dense distribution of small impoundments in eastern Kansas reflects Kansans' dependence on the various services provided by impoundments and reflects major anthropogenic alteration of natural processes. A consequence of this alteration is the infilling of artificial water bodies. With growing concern surrounding reservoir infilling, research tied to limiters of downstream sediment yield could offer valuable insight into reservoir management on a drainage scale. To better understand the role impoundments may play as sinks within a reservoir drainage, there first is a need to update and improve the accuracy of available water body distribution data.

Automated geoprocessing techniques combined with newly available high-resolution elevation data provide alternative means of identifying water bodies and offer improved efficiency and consistency when compared to previous manual approaches. Furthermore, delineating impoundment subcatchments using newly available elevation data and characterizing subcatchment traits related to erosion potential may identify subcatchment trends connected to reservoir sediment yield.

In order to better characterize the distribution of small impoundments and their significance as sources of subcatchment within Kansas reservoir drainages, this research has three central objectives: 1) Conduct two automated water feature identification approaches – the TWIP approach taken from Kastens et al. (2016) and the Zero Slope method – and gauge their efficiencies using aerial imagery, the NHD, and an accuracy assessment index, 2) Update the water body data of the NHD for select drainage regions by incorporating newly identified features and amending less accurate geometries, 3) Delineate subcatchment areas for select reservoirs, analyze landscape traits which influence erodibility, and compare impoundment distributions and subcatchment traits among reservoir drainages.

The first and second objectives are addressed in Chapter Two. Using LiDAR-derived DEMs generated from 2010 – 2016, two automated methods are applied in efforts to identify recently impounded water bodies and update NHD feature geometries. The first method, the Topographic Wetland Identification Process (TWIP), uses sink mapping with a sink depth threshold to identify elevation patches potentially representative of water bodies. The second method, the Zero Slope approach (ZS), identifies hydro-flattened patches potentially representative of water bodies. The results of these methodologies are validated in the context of aerial imagery, and an accuracy assessment index quantifies geometry accuracy of the TWIP,

ZS, and NHD. Features from each dataset are merged into a single new dataset by order of highest accuracy index.

Chapter 3 addresses the final objective by delineating impoundment drainage areas, summarizing land use, soil, and slope traits for cumulative subcatchment areas, and characterizing the water body and subcatchment distribution for ten reservoir drainages in eastern Kansas. The resulting water body dataset from Chapter 2 serves as pour points for identifying subcatchment areas, which are then merged to measure total subcatchment for each reservoir drainage. Land use raster data from the 2005 Kansas Land Cover Patterns dataset, soil data from gridded Soil Survey Geographic Data shapefiles (gSSURGO), and slope rasters are then clipped according to subcatchment and unimpeded area masks and analyzed to identify landscape trends in the context of subcatchment and possible relation to downstream reservoir sediment yield.

Significance

Automated geoprocessing methods paired with recent LiDAR-derived elevation data offer an opportunity to augment data taken from the NHD and advance our understanding of water body distribution within Kansas reservoir drainages. The accuracy of the current NHD is limited by dated topographic source material (with the earliest beginning in the 1950s) and orthoimagery available at the time of digitization, which began in the 1990s (NHD Feature Catalog, 2009). With impoundment numbers increasing yearly, the use of more current data sources in identifying water bodies will likely show new impoundments and altered geometries relative to the NHD. Several studies have investigated impoundment distribution on a national

scale (Smith et al., 2002; Renwick et al., 2005), but have had to sacrifice regional detail and accuracy in favor of broader characterization. Efforts have also been made to characterize impoundment abundance for Kansas (Callahan, 2013), but methodologies and conclusions have been limited to available datasets at the time of the studies (i.e., NHD and National Elevation Dataset). However, with recent LiDAR-derived elevation data collected from 2010 – 2015 covering most of the state, and with Kastens et al. (2016) demonstrating their utility in water body identification, there now is an opportunity to apply relatively novel methodologies to enhance and modernize water body inventories for the region. By developing a more current and precise water impoundment dataset for reservoir drainages, the influences of impoundment distribution on reservoir sedimentation may be more rigorously explored.

Subcatchment delineation and trait characterization may provide further insight into the connection between the impoundment distribution of a reservoir drainage and reservoir sediment yield. Combining the NHD with the results of the geoprocessing approaches explored in Chapter 2 will offer a more complete and potentially compatible pour point dataset for subcatchment delineation. The anticipation is that since the water bodies are delineated from elevation data, the features may be more suited for raster processing, such as watershed delineation, than rasterized features drawn from topographic maps or aerial imagery. Additionally, most of the reservoirs of eastern Kansas have not had impoundment subcatchments delineated nor their land use, soil, or slope characterized and compared for subcatchments and unimpeded contributing areas. By doing so, trends may be recognized related to subcatchment landscape factors and downstream sediment yield, a little studied dynamic related to reservoir infill for the region.

Finally, as LiDAR-derived elevation data become more common, this study will provide a methodology that can be easily repeated and applied to other regions. The automated aspect of

much of the geoprocessing may reduce sources of human error as well as time and costs related to manual water body identification and geoprocessing. Much of the methodology is scripted and packaged as ArcGIS tools, which will be openly available to other researchers. The overarching goal of this project is to demonstrate novel and easily duplicated methods in water body inventorying and subcatchment characterization, which may be suitable for adoption in investigating and managing the various effects of impoundments.

References

Bedient, P. B., Huber, W. C., & Vieux, B. E. (2013). Chapter 2: Hydrologic analysis. *Hydrology and Floodplain Analysis 5th Edition*, 88-169.

Bosch, N. S. (2008). The influence of impoundments on riverine nutrient transport: An evaluation using the Soil and Water Assessment Tool. *Journal of Hydrology 355*(1), 131 147.

Bowen, M. W., Johnson, W. C., Egbert, S. L., & Klopfenstein, S. T. (2010). A GIS-based approach to identify and map playa wetlands on the High Plains, Kansas, USA. *Wetlands 30*(4), 675-684.

Callihan, R. A. (2013). Distribution, proliferation and significance of small impoundments in Kansas. (M.S.), University of Kansas, Lawrence, KS.

Carpenter, L., Stone, J., & Griffin, C. (2011) Accuracy of aerial photography for locating seasonal (vernal) pools in massachusetts. *Wetlands 31*, 573–581.

deNoyelles, F. & Jakubauskus, M. (2008). Current state, trend, and spatial variability of sediment in Kansas reservoirs. *Sedimentation in Our Reservoirs: Causes and Solutions*, 9-23.

deNoyelles, F. & Kastens, J. H. (2016) Reservoir sedimentation challenges in Kansas. *Transactions of the Kansas Academy of Science, 119(1)*, 69-81.

Downing, J.A., Prairie, Y. T., Cole, J. J., Duarte, C. M., Tranvik, L. J., Striegl, R. G., McDowell, W. H., Kortelainen, P., Caraco, N.F., Melack, J. M., & Middelburg, J. J. (2006). The global abundance and size distribution of lakes, ponds, and impoundments. *Limnology and Oceanography, 51*(5), 2388-2397.

Downing, J. A., Cole, J. J., Middleburg, J. J., Striegl, R. G., Duarte, C. M., Kortelainen, P., Prairie, Y. T., & Laube, K. A. (2008). Sediment organic carbon burial in agriculturally eutrophic impoundments over the last century. *Global Biogeochemical Cycles 22*(1).

Graf, W.L. (1999). Dam nation: a geographic census of American dams and their large-scale hydrologic impacts. *Water Resources 35*, 1305–1311.

Juracek, K. E. & Zeigler, A. C. (2007). Estimation of sediment sources using selected chemical tracers in the Perry Lake and Lake Wabaunsee Basins, northeast Kansas. *USGS Scientific Investigations Report 2007-5020*.

Kastens, J. H., Baker, D. S., Peterson, D. L. & Huggins, D. G. (2016) Wetland Program Development Grant (WPDG) FFY 2013 – Playa Mapping and Assessment. *KBS Report 186*.

Langbein W.B. & Schumm, S. (1958). Yield of sediment in relation to mean annual 546 precipitation. *Transactions, American Geophysical Union 39*, 1076-1084.

Leonard, P. B., Baldwin, R. F., Homyack, J. A., & Wigley, T. B. (2012). Remote detection of small wetlands in the Atlantic coastal plain of North America: Local relief models, ground validation, and high-throughput computing. *Forest Ecology and Management 284*, 107-115.

Martinko, E., deNoyelles, F., Bosnak, K., Jakubauskas, M., Huggins, D., Kastens, J., Shreders, A., Baker, D., Blackwood, A., Campbell, S., & Rogers, C. (2014). *Atlas of Kansas Lakes: A resource for communities, policy makers and planners.*

Meade, R.H., Yuzyk T.R., & Day T.J. (1990). Movement and storage of sediment in rivers of the United States and Canada. *Surface Water Hydrology. Geology of North America, Boulder, Colorado. 1990*, 255–280.

Mulholland, P.J. & Elwood, J.W. (1982). The role of lake and reservoir sediments as sinks in the perturbed global carbon cycle. *Tellus (34)*, 490-499.

NHD. (2016). USGS National Hydrography Dataset. URL [http://nhd.usgs.gov/index. html]. Date accessed [June 2016].

Rahmani, V., Kastens, J., deNoyelles, F., Jakubauskus, M., Martinko, E., Huggins, D., Gnau, C., Liechti, P., Campbell, S., Callihan, R., Blackwood, A. (2017). Examining storage loss and sedimentation rate of large reservoirs in the U. S. Great Plains. Unpublished article.

Renwick, W. H., Smith, S. V., Bartley, J. D., & Buddemeier, R. W. (2005). The role of impoundments in the sediment budget of the conterminous United States. *Geomorphology 71*(1), 99-111.

Smith S.V., Renwick W.H., Buddemeier R.W., & Crossland C.J. (2001) Budgets of soil erosion and deposition for sediments and sedimentary organic carbon across the conterminous United States. *Global Biogeochemical Cycles 15(3),* 697–707.

Smith, S. V., Renwick, W. H., Bartley, J. D., & Buddemeier, R. W. (2002) Distribution and significance of small, artificial water bodies across the United States landscape. *Science of the Total Environment 299*(1): 21-36.

Stallard, R.F. (1998) Terrestrial sedimentation and the carbon cycle: coupling weathering and erosion to carbon burial. *Global Biochemical Cycles 12,* 231–257.

Trimble S.W. & Bube K.P. (1990) Improved reservoir trap efficiency prediction. *ENVIRON. PROFESS.,12(3),* 255–272.

USGS, (2009). National Hydrology Dataset Feature Catalog. URL [http://nhd.usgs.gov/]. Data accessed [October 2016]

U.S. Census Bureau. (2015). Population Estimates: Population and Housing Unit Estimates 2015. URL [https://www.census.gov/popest/]

Vörösmarty, C. J., Green, P., Salisbury, J., & Lammers, R. B. (2000). Global water resources: vulnerability from climate change and population growth. *Science 289*(5477), 284-288.

Wu, Q., Lane, C., & Liu, H. (2014). An effective method for detecting potential woodland vernal pools using high resolution LiDAR data and aerial imagery. *Remote Sensing 6*(11); 11444-11467.

Chapter II

Approaches in Identifying New Water Bodies and Improving Geometries Relative to the NHD

Introduction

Small impoundments demonstrate significant anthropogenic alteration of landscape systems and processes. The effects of these fluvial modifications range in nature, including hydrological, geochemical, and ecological impacts. While there is abundant literature investigating the various effects of impoundments, popular water datasets vary in the extent of their spatial resolution and inclusion of water bodies, which is a central limitation in water body-related research. For this study focused in eastern Kansas, novel high resolution data and methodologies offer an opportunity to improve on the National Hydrography Dataset (NHD) by means of adding recently constructed impoundments and revising feature geometries via high-resolution topographic data. The methodology demonstrated in this chapter and the resulting datasets provide new tools in improving regional knowledge of water body distribution, which can be applied to the continued study of impoundment effects and watershed management.

Hydrological, Sedimentation, and Geochemical Effects of Impoundments

Hydrological effects of impoundments

While there are numerous hydrological consequences of impounding lentic systems, certain effects may be keenly felt in Kansas due to its high density of small impoundments and

precipitation trends that are characterized by periods of drought, intermittent heavy rainfall, and flash flooding. Chief among the impacts of impoundments are increased evaporation rates, altered groundwater recharge, and decreased downstream flow. The prolific impoundment practices of the agricultural Midwest reflect local landowner attempts to counteract natural water loss by storing water on the surface. While impoundments may result in water being more readily available locally, the larger-scale cumulative effect is an increase in water loss due to evaporation, which occurs more rapidly in a densely impounded landscape than one permitting natural downstream flow and percolation (Smith et al., 2002). Furthermore, shallow systems, such as smaller impoundments, experience higher summer heating, resulting in greater evaporation than large water bodies (Harbeck, 1962; Smith et al., 2002). An additional consequence of impoundments is altered recharge incidence. The retention of water in upland areas by impoundments increases residence time and local groundwater recharge. In turn, downstream areas experience less discharge, percolation, and groundwater recharge (Smith et al., 2002). Additionally, stream flow becomes more homogenized with a reduction in peak flows and greater occurrence of low flow periods (Moore, 1969; Gordon et al., 1992). Abatement of peak flow events reduces flushing of accumulated sediments and organic matter in streams, and in turn accumulated sediments covering coarse substrates may reduce seepage and subsurface flow (Mammoliti, 2002). To investigate these various impacts on a regional scale, individual impoundment effects can be aggregated, and accurately assessing these effects may benefit from a complete and geometrically accurate water body dataset.

Sedimentation effects of impoundments

Small impoundments' cumulative effects on sediment retention have been studied on a national scale (Smith et al., 2002; Renwick et al., 2005; Downing et al., 2008), but on a regional

scale, more precise size and spatial distribution data is needed to address trap efficiency, or the percentage of sediment retained by a water body relative to the inflowing sediment load, and cumulative yield. Two thirds of annual total erosion in the conterminous United States is estimated to be deposited in lentic systems (Smith et al., 2002). Of this portion, the amount estimated to settle into "small" water bodies (< 4 ha) equals the combined total of all larger lakes and reservoirs (Smith et al., 2002). Renwick et al. (2005) used three separate models to estimate small impoundment sediment yield for the continental United States, and resulting total sediment rates ranged from 0.43 – 1.78 x $10^9 m^3 yr^{-1}$, which potentially matches or exceeds estimated total reservoir accumulation of 1.67 x $10^9 m^3 yr^{-1}$ and supports the conclusions of Smith and collaborators. However, there is a wide sediment yield range in this study, which reflects the difficulty of accurately estimating cumulative small impoundment yield on a large scale with coarse data. In turn, reducing the scale and extrapolating these findings to a specific region, such as the Midwest, would likely be impractical. Additionally, these landmark studies in small impoundment sedimentation omit any consideration of trap efficiency in their models, a result of scale, the sheer number of water features, and lack of data on various parameters involved in trap efficiency prediction.

Trap efficiency may be dependent on a variety of parameters, but all models require either surface area or volume as indicators of capacity, which is fundamental to yield trapping estimations. Two other factors, capacity and residence time, are partially dependent on water body geometry (Verstraeten & Poesen, 2000). Thus, attempts at assessing trap efficiencies on a regional scale benefit from datasets with accurate feature geometries. In addition to individual water body geometries, distribution of impoundments plays a part in cumulative and individual sediment collection. Local high impoundment density typically results in high local yields

(Smith et al., 2002). However, sediment originating from an upstream impoundment will be finer, and the downstream impoundment will have a lower trap efficiency should other parameters hold constant (Churchill, 1948). In Kansas, discharge and velocity may be high during the flood events characteristic of the region. These events may result in greater scouring, higher sediment loads, and reduced discharge residence times. In these cases, it may take multiple impoundments within a lotic system to effectively slow velocity and induce deposition. If efforts are to be made to account for small impoundment trap efficiencies on a regional scale, such as a Kansas reservoir drainage, geometric accuracy of water bodies is necessary. Trap efficiency modeling would benefit from comprehensive impoundment inventories with precise geometries to assess densities, connectivity, and capacities.

Geochemical effects of impoundments

Given that sediment is itself a sink for nutrients, impoundments also serve as nutrient sinks, reducing riverine nutrient transport. A spatial modeling study (Bosch, 2008) of two Michigan watersheds investigated impoundment size and positioning in relation to total phosphorous (TP) and total nitrogen transport (TN). Results showed TP and TN transport doubling when impoundments were removed from the model. As expected, impoundments were most effective at reducing TP and TN transport when positioned near the mouth of the river or in nitrogen and phosphorous source areas (Bosch, 2008). Finally, multiple smaller impoundments caused a greater cumulative reduction in transport than a single large reservoir (Bosch, 2008). The trend of small impoundments trapping more combined nutrients can be credited to faster vertical accretion and the tendency of smaller impoundments to occur adjacent to agricultural and human sources of nutrient loading (Smith et al. 2002). Given the high density of small impoundments in Kansas and the current issues surrounding reservoir filling and eutrophication

occurrences, the results from Bosch raise the question: How are small impoundments reducing the likelihood of eutrophication in downstream reservoirs by serving as nutrient sinks? If farm ponds are in fact catchments for high nitrogen and phosphorous source areas (i.e., fertilized crop land), the reduction in nutrient transport could provide a significant service in managing downstream reservoir water quality.

An additional service often overlooked in small impoundment valuation is the burial of organic carbon (OC). This process may be considered more significant in reducing atmospheric carbon dioxide levels than regulating downstream water quality. Downing and colleagues (2008) assessed OC burial in 40 impoundments in an intensively farmed region of Iowa. Results indicated that impoundments buried a higher concentration of OC than natural lakes due to heavier sedimentation and sediment aggregate transport, and OC burial proportions were significantly higher in small impoundments (Downing et al., 2008). As in the case of nitrogen and phosphorus, this effect can be attributed to the tendency for rapid vertical accretion by small impoundments. Additionally, rapid accretion in farm ponds can result in altered decomposition rates than larger water bodies. Optimal microbial activity occurs at or near the maximum amount of water a soil can hold against gravity, and as soil becomes waterlogged, decomposition slows (Rice, 2002). Artificial ponds create a permanently saturated environment for rapidly accumulating organic carbon. This results in altered redox rates which may be further hindered by suboxic or anoxic conditions following eutrophication. These nutrient and geochemical effects of impoundments can be tied with sediment transport and trapping, which suggests that improving the quality of water body data available to model sediment catchment may offer new opportunities to study other impoundment sink effects on a regional scale.

It should be noted that impoundments are not exclusively sinks or reducers of downstream sediment and nutrients yields. There is relatively little research on how and when a small impoundment turns from a sediment sink to a sediment source, but an argument could be made that impoundments are infilling at similar rates to nearby reservoirs due to similarities in landscape factors. Conversely, the typically low capacity to catchment area ratio of small impoundments (Verstraeten & Poesen, 2000) suggests that their life as sinks is much shorter than for large reservoirs. Should a shift from sediment sink to source occur, the re-release of contents into a stream system would likely disturb the lotic reach and contribute an abundance of sediment, nutrients, and organic matter to the downstream lentic body. This deleterious effect on water quality and increased sediment transport would reflect a reverse in the sediment sink services of small impoundments. Additionally, impoundments can indirectly increase downstream erosion and sediment yield through flow alteration. Dams reduce out of bank flows but extend bank-full flows (Wetter, 1980). Protracted periods of bank-full flows can accelerate bed and bank erosion, and the resulting additional sediment may then be deposited in downstream lentic systems.

Ecological Effects of Impoundments

The abundance of artificial water bodies found in Kansas reflects a dramatic anthropogenic shift in ecological impacts. Regional consequences dependent on impoundment distribution include providing corridors for invasion, species assemblage gradation, and habitat fragmentation. Research resulting in improved and current impoundment distribution data may prove beneficial in research and management surrounding these effects.

Dispersal sources and corridors for aquatic invasives

Constructing a network of impoundments in the Midwestern United States has resulted in corridors for migration for many species associated with lentic systems. The classic case is migratory waterfowl. These species use impoundments as "stepping stones" during temporal migrations, and in effect, this service provided by impoundments is valued by hunters and nature enthusiasts alike. However, impoundments also create new ecosystems, which lack resilience and favor generalists. In turn, impoundment networks facilitate invasion and act as corridors for exotic species.

An argument could be made that natural lentic systems, such as lakes or pools, could seemingly facilitate invasion in a similar manner as impoundments. In a study conducted in the Great Lakes region of the United States, Johnson and collaborators (2008) sought to investigate this notion by investigating how impoundments and natural lakes enable the establishment of five aquatic invaders of differing taxa. For each invader, impoundments were found 2.5-7.8 times more likely to be invaded than natural lakes, and impoundments more often housed multiple invaders (Johnson et al., 2008). In addition, these proportions are likely an underestimate, as inaccessible natural lakes, which are far less affected by human activity, were omitted from the study. Reasons for successful establishment of invasive species in impoundments stem primarily from the young age of impoundments. The oldest impoundment included in the study was 161 years old, while the oldest glacial lake was approximately 10,000 years old (Johnson et al., 2008). The young age of impounded systems results in increased niche availability, a simplified trophic structure, and lower biotic resistance. A high disturbance regime with fluctuations in water levels, temperature, fish stocking, and nutrient content could also

increase invasiblility (Johnson et al., 2008). Furthermore, invasive species may have adapted to impoundments in their previous ranges, which could increase their establishment success.

In terms of small impoundments such as those characteristic of Kansas, change in water quality is likely an additional facilitator of invasive species success and native species loss. Shallow water bodies experience greater summer heating (Smith et al., 2002), which results in reduced dissolved oxygen (DO) concentration. Reduction of peak flow due to upstream damming can reduce streambed flushing (DeCoursey, 1975; Zale et al., 1989), which may increase stream turbidity. Additionally, nutrient enrichment, algal blooms, and eutrophication in farm ponds decreases DO concentration and increases stream turbidity (KDHE, 1981). These changes in water quality in small impounded features may favor hardy generalists and limit success of sensitive endemics and sight-feeders (Mammoliti, 2004).

Following impoundment of a lotic system in Kansas, it is standard practice to introduce sport fish, such as the largemouth bass, *Micropterus salmoides* (Mammoliti, 2002). As an introduced piscivorous population grows, there is an increase in the number of individuals dispersing upstream or being washed downstream. This increases predation pressures on obligate stream species. Predation by game species, such as *M. salmoides*, has been documented as a significant influence on the reduction or extirpation of native stream species in Kansas such as cyprinids (Mammoliti, 2002). Although native stream species of Kansas have historically occurred with other piscivorous fishes (*Lepomis cyanellus, Ameiurus melas,* and *Micropterus punctulatus*), most are considered facultative piscivores and rely less on fishes in their diet (Mammoliti, 2002). In effect, impoundments in Kansas serve as sources for exotic obligate piscivores, which increase predation pressure and alternative fish assemblages.

Assemblage gradients caused by impoundments

Common traits of impoundments support the conception that impoundments are a form of disturbance. Altered flow is chief among these traits. While many terrestrial disturbance studies rely on a temporal scale in recovery assessment, a few studies have focused on impoundments as agents of disturbance in aquatic systems use a spatial scale to assess recovery. Findings indicate proximity both downstream and upstream of the disturbance to influence the degree of recovery.

A study conducted on the Cahaba and Tallapoosa Rivers of the Alabama River Basin assessed fish assemblage recovery on a flow regulation gradient. Results showed obligate fluvial species increased in richness and abundance in a gradient moving downstream and away from a hydroelectric dam (Kinsolving & Bain, 1993). Contrarily, microhabitat generalists demonstrated no significant assemblage gradient in the dammed or control rivers, reflecting that the taxa were relatively unaffected by flow fluctuations (Kinsolving & Bain, 1993). Obligate stream natives are thus more affected by the disturbance of altered flow regimes than generalists.

In addition to fishes, other taxa assemblages exhibit a similar gradient to disturbance by impoundment. In the Little River of Oklahoma, Vaughn and Taylor (1999) observed an extinction gradient in mussels. Moving downstream from an impoundment, mussels showed greater richness and abundance, with relatively rare species furthest from the impoundments. However, upon reaching the confluence (inflow from a second reservoir), the same trends were observed, although weaker (Vaughn & Taylor, 1999). In conclusion, considerable lengths of streams unaffected by neighboring impoundments are necessary to overcome the effects of an impoundment on species assemblages.

Assemblage gradient trends due to impoundments have also been noted in Kansas. Faulke and Gido (2006) assessed fish assemblages moving upstream from 19 Kansas reservoirs. The authors found significant results indicating a decrease in reservoir species occurrence and an increase in assemblage variability and native species occurrence moving further upstream (Faulke & Gido, 2006). In effect, areas upstream of impoundments can also exhibit assemblage gradients.

Altering the flow regime and native assemblages results in a gradient of homogenization centered on impoundment proximity. As shown by Vaughn and Taylor (1999), this gradient resets once resubmitted to the effects of another impoundment. Given the high density of impoundments in Kansas, there are likely systems unable to escape the gradient cycling and eventually settle into a more homogenized steady-state. Identifying the thresholds for impoundment disturbance recovery could be useful in mitigating this homogenization and improving conservation management. Additionally, current impoundment distribution data noting recently constructed impoundments could be valuable to gradient modeling focused on recent disturbance.

Habitat fragmentation, homogenization, and loss

Harsh environmental conditions that select for high colonization rates make prairie stream fishes particularly vulnerable to the effects of fragmentation (Hudman & Gido, 2013), and it has long been established that impoundments serve as barriers for migration of aquatic species (Deacon, 1961). Given the ephemeral nature of many headwaters in prairies and the proliferation of impoundments in Kansas, impoundments preventing recolonization following local extirpation is a common occurrence. Furthermore, research has shown reduced migration

resulting from impoundments to erode genetic diversity and reduce population fitness. Finally, retention of water in upland areas can cause desiccation and loss of naturally occurring wetland systems downstream.

In the Midwest, there is a clear link between impoundments and native cyprinid extirpation. In the Cottonwood Creek of Oklahoma, Stearman and Lynch (2013) established a negative relationship between a fragmentation metric based on impoundment density and cyprinid abundance and richness. The authors concluded that fragmentation associated with impoundments can be especially harmful to small-bodied, mobile minnow species (Stearman and Lynch, 2013). In a similar study in the Flint Hills of Kansas (Schrank et al., 2002), various landscape and ecologic factors were incorporated in a stepwise regression to establish indicators of Topeka Shiner (*Notropis topeka*) extirpation. The regression found the most significant indicator of whether the threatened species occurred within watershed subsections to be impoundment density. Impoundment density alone correctly classified 83% of extant sites and 85% of extirpated sites (Schrank et al., 2002). There are many potentially deleterious effects of impoundments, but increased fragmentation and recolonization prevention from high impoundment density is particularly harmful for headwater species.

Recent literature on population fragmentation from impoundments has illuminated genetic consequences to population isolation. Hudman and Gido (2013) investigated impoundment effects on genetic structure of a native cyprinid, *Semotilus atromaculatus,* in the Kansas River basin. Results showed a high degree of spatial genetic structure, suggesting that catchments house sets of isolated genetic units, and sites within catchments are further subdivided into groups divided by intervening lentic habitat (Hudman & Gido, 2013). These barriers for dispersal among tributaries may reduce the opportunity for genetic rescue of

populations in tributaries draining into impoundments. However, their findings also indicated that reservoirs may be less genetically deleterious if a tributary houses a large enough population (Hudman & Gido, 2013). The historic environmental conditions and life histories of native cyprinids reflect a pattern of local extirpation, recolonization, migration and associated gene transfer that has been significantly disrupted by large-scale habitat fragmentation.

In addition to acting as barriers for stream species migration, impoundments reduce and homogenize stream flow and habitat. Should water levels within impoundments drop due to drought, an upstream impoundment may prevent flow downstream, causing the next impoundment to receive a reduced input and to lose volume. This domino effect can cause lotic stretches connecting impoundments to experience low flow, fed only by the sliver of watershed below the upstream impoundment. By reducing peak flow in streams, scouring is less intense, and there is a decline of structurally diverse pools and an increase in predation success by invasive generalists such as largemouth bass (Mammoliti, 2002). Studies have shown structurally complex environments to be favorable for native species by providing more refuge and reducing predator forage efficiencies of invasive generalists (Menge & Sutherland, 1976; Power et al, 1985).

While impoundments directly affect adjacent stream habitat, collective upland water retention by impoundments may cause lowland wetland habitat loss. Wetland loss in the conterminous United States exceeds 500,000 km^2 (Mitsch & Gosselink, 1993). While a connection between upstream impoundment and wetland loss has been suggested (Tiner, 1989; Smith, 2002; Callihan, 2013), the water retention impacts and ecological ramifications have been difficult to assess. Should there be substantial loss of wetlands via constructed water bodies, a decline in wetland endemics or their migration to potentially less favorable impounded habitats

seems likely. Efficient water feature identification and surface area measurement that can be applied on a drainage scale could be a useful tool in modeling water displacement and investigating wetland displacement.

Significance of water body data

The various ecological consequences of constructed water bodies reflect a major anthropogenic alteration of ecosystems. While the list of ecological effects of impoundments exceeds those discussed, invasion facilitation, species assemblage gradation, and habitat alteration are all concerns recognized in Kansas and should be studied and managed in a spatial context. Water feature size, proximity, connectivity, and density all influence the discussed ecological effects. If these effects are to be studied on a regional scale, a current, accurate characterization of water body distribution would be of great value.

Current water body inventories

Historically, digital water feature inventories have been created through manual digitizing from source data including topographic maps, land use raster data, and aerial imagery. The process and efficiency of digitization has often been dependent on data resolution and the resources required for manual geoprocessing. National water body inventories vary in purpose and source data, and as a result, differ widely in feature inclusion and representation, particularly in the case of small water bodies. The National Hydrography Dataset (NHD) was developed using topographic quadrangle digitization coupled with visual identification using orthoimagery, and since its upgrade in 2007, it can be considered the most comprehensive national water body dataset for the United States (McDonald et al., 2012; Callihan, 2013). Studies using previous

datasets, including the NHD, show Eastern Kansas as having a dense distribution of small impounded features due in part to its degree of agricultural land use and absence of abundant natural lentic bodies. However, the full extent of impoundments and the associated effects in the region are not fully understood, and with the number of impoundments continuing to increase in Kansas, automated identification techniques using recent high quality data may help in keeping inventories current.

Limitations of popular water body datasets and inventory approaches

Following the advent of GIS and related digital image processing software, features on aerial imagery and topographic maps could be digitized for cataloguing and analysis purposes. However, spatial resolution and resources available for manual geoprocessing limit the quality of the inventory. In effect, inclusion and accuracy of small water body features has historically been difficult in large area inventory efforts. A study by Smith et al. (2002) illustrated the differences in lentic feature inclusion among popular national inventories and general underestimation when compared to estimations derived from higher resolution data sources. Smith et al. (2002) compared water body data from the National Atlas, the Census Bureau's Tiger Database, and the National Inventory of Dams (NID) to water feature data derived from the National Land Cover Dataset (NLCD) and the United States Geological Survey (USGS) Digital Line Graph (DLG). Smith et al. (2002) first used the NLCD to vectorize 30-m pixels representative of water bodies to estimate impoundment abundance in the conterminous United States. This dataset resulted in an estimate of 2.6×10^6 water bodies with a lower surface area limit of 1000 m^2 (Smith et al., 2002). When using higher resolution data offered by the USGS Digital Line Graph (DLG) dataset and a feature resolution limit of 25 m^2, the researchers chose to sample and extrapolate due to the time and effort required to manually extract water features from the DLG. The

resulting number for total water bodies in the conterminous U.S. was estimated at 9×10^6 (Smith et al., 2002). While enhanced spatial resolution (i.e., USGS DLG) improved identification of finer water features, the resources required by manual geoprocessing forced researchers to extrapolate regional findings, resulting in reduced accuracy. The results of both approaches led researchers to conclude that small water bodies (<10,000 m^2) are overwhelmingly dominant across the U.S., and "available datasets differ widely in representing those features" (Smith et al., 2002). The more conservative estimate of water bodies taken from the NLCD data estimated 35, 60, and 500 times as many water bodies as the TIGER, NID, and National Atlas databases, respectively (Smith, et al., 2002). The trend among the national inventories is fairly accurate coverage for water bodies over 100,000 m^2 and an absence of the majority of features under 10,000 m^2, which can be attributed to limited data resolution at time of cataloguing, limited or inadequate geoprocessing resources, or prioritization of large water bodies in water resources management.

To date, the most comprehensive water body dataset for the United States may be the NHD, but there are inherent limitations to this inventory. The NHD is the product of digitized water features drawn from topographic maps and aerial imagery. Original NHD source topographic maps range from the 1950s to present, and validation of water body geometry during digitization (beginning in the 1990s) has been limited to the temporal and spatial resolution of the orthoimagery available at the time (USGS, 2009). In 2007, the NHD upgraded its inventory of lentic features using 1:12,000 USGS Digital Line Graphs (DLGs) supplemented by Digital Orthophoto Quarter Quadrangles (USGS, 2007). The result was a change in scale from 1:100,000 to 1:24,000, or 1:12,000 in certain areas, and an increased inclusion of smaller water features. Despite a marked improvement in the small water body inventory, the upgrade still

relied on imagery dating as far back as the 1980s for Kansas (Callihan, 2013), and relied on manual photointerpretation methods, which are subject to human error and inconsistencies (Carpenter et al., 2011). Additionally, the boundary geometries of impoundments are dynamic, whether due to sedimentary processes or landowner management, and impoundments appear to be continually increasing across the U.S. (Smith et al., 2002; Renwick et al., 2005). While the updated NHD includes many of the long-term impoundments that are "at least 100 feet in the shortest dimension" (USGS, 2009), introducing new methodologies and more recent data may allow the identification of more recently constructed water bodies and update previous geometries.

Water body characterization and recent inventories in Kansas

Kansas exemplifies the agricultural industry's tendency towards constructing small impoundments and a dependence on reservoir water services. Kansas alone boasts over 240,000 impoundments of under 40 hectares, which combined cover approximately 288 square miles and store an estimated 1,299,000 acre/feet of water (Callihan, 2013). The density gradient for small impoundments as estimated by Smith et al. (2002) ranges from less than 0.03 impoundments per km^2 in western portions of the state to an average of 1-3 water bodies per km^2 in the eastern third. Regarding large reservoirs, Kansas has over 200 reservoirs, mostly state or federally owned, with surface areas exceeding 20 hectares (deNoyelles & Kastens, 2016). Eighty of these provide primary or backup drinking water for 60% of the state's population and provide flood control services, which was the primary purpose for construction of the state's 24 federal reservoirs. While these larger reservoirs provide municipal, flood control, and recreational services, smaller impoundments provide a variety of services including livestock watering, irrigation, domestic water, and recreation (deNoyelles & Kastens, 2016). For a region with

natural lentic systems limited to ephemeral playas predominately in western Kansas and relatively few oxbow and sinkhole lakes statewide (Martinko et al., 2014), this extensive landscape modification has substantially altered hydrological and physical processes.

Studies of small water body inventories in Kansas have advanced awareness of source data restrictions and variations in perceived regional abundance. In 2004, Buddemeier assessed the accuracy of the Kansas Surface Water Database and the Surface Water Information System in regards to small water bodies. The results showed the KSWD and SWIMS only included 1% and 3% of water bodies less than 40 ha, respectively, and features derived from coarser resolution imagery resulted in exaggerated surface areas due to larger pixels and the inclusion of mixed water and land pixels at the boundaries of water features (Buddemeier, 2004). In effect, lower resolution imagery or raster source data results in misrepresentation of surface areas as well as fewer features identified. Following the increase in NHD resolution and feature incorporation, Callihan (2013) used the new dataset in conjunction with the National Wetlands Inventory and the 2005 Kansas Land Cover Patterns dataset to evaluate small water body abundance in Kansas. Merging datasets and including only impounded features under 40 ha resulted in 241,295 small impoundments with a combined surface area exceeding that of all state and federal reservoirs in Kansas (Callihan, 2013). To date, this is the most thorough inventory for the state. However, its results rely on the accuracy of the NHD, which has its aforementioned limitations. An approach using newer high-resolution elevation data would offer an alternative to the NHD's more traditional feature inventory method and could illuminate shortcomings in NHD accuracy and completeness.

Water body identification associated with LiDAR-derived data

LiDAR (light detection and ranging) datasets have produced unprecedented spatial resolution for elevation data for many regions of the U.S. In recent years, studies have used 1 and 2-m LiDAR-derived elevation data to identify water features through automated geoprocessing approaches. In doing so, resource limitations, consistency issues, and efficiency restrictions associated with manual water body digitization have been avoided. 2-m LiDAR-derived digital elevation models (DEMs) are now available for the entirety of Kansas, which for the first time allows elevation-based automated identification of the state's small water features. Should DEM-based water feature identification methods prove successful for Kansas, they may be adopted in other regions as the USGS and partners work to produce high resolution elevation data for the entire United States.

Overview of LiDAR and DEM generation

The USGS is currently facilitating nationwide high-resolution elevation mapping via LiDAR data collection, and USGS specifications require a level of hydro-flattening to all bare ground DEMs. In 2009, a $14.3 million allocation from the "America Recovery and Reinvestment Act" marked the undertaking of Quality Level 2 (1 meter horizontal resolution) LiDAR data and DEM production for the conterminous United States (Heidemann, 2014). LiDAR-based elevation data are collected via laser pulses dispersed from LiDAR-equipped aircraft. As the reflected pulses return to their source, the data are recorded as a raw point cloud composed of multiple pulses per square meter of land surface with the minimum required pulse number dependent on Quality Level, and elevation is calculated based on return time and data recorded in unison with a GPS sensor. The point cloud often contains voids in data due to light

refraction and absorption, and a common source of void occurrence is the absorption, refraction, or both by water. The USGS specified treatment of significant water-attributed voids is "hydro-flattening" (Heidemann, 2014). As mandated by the USGS, all water bodies equal to or greater than 8000 m^2 are to be converted to a flat surface of equal elevation values at or below the surrounding terrain, and all rivers with a width of 30 meters or greater are to be flattened in segments with elevation values interpolated from riparian values (Heidemann, 2014). In turn, high-resolution, hydro-flattened elevation data offer a new level of precision in hydrological modeling and unique representation of water features.

Water body research associated with LiDAR

Using LiDAR-derived elevation data, researchers have been able to automatically distinguish water bodies in largely consistent, efficient, and easily duplicated approaches. A popular approach was demonstrated by Leonard et al. (2012), which used neighborhood analysis to distinguish depressions. The study incorporated 2 meter LiDAR elevation data into custom relief models to identify localized concavity and potential wetland locations. Each raster cell value was divided by the mean of the adjacent cell values. Should the ratio be < 1.0, concavity was indicated. Results showed an 85.1% accuracy rate in the automated wetland identification, after field validation. Wu et al. (2014) further demonstrated the advantages of topographic depression analysis using LiDAR-based DEMs in identifying vernal pools. Wu et al. (2014) developed a semi-automated approach to extract surface depressions from a 1 meter resolution DEM. A major benefit of the approach was that boundaries of vernal pools identified using DEMs can be extracted as polygon features, automating characterization of geometric properties and alleviating inconsistencies inherent in previous manual inventory attempts (Wu et al., 2014).

In western Kansas, Kastens and researchers (2016) identified playas by extracting sinks meeting depth threshold criteria from LiDAR-derived DEMs, naming the model the Topographic Wetland Identification Process (TWIP). Researchers found that DEM preparation prior to running TWIP, including applying a median focal filter and burning interpolated elevation values into buffered road and railroad areas, resulted in fewer false positives and general noise in the model results. The TWIP first creates a sink depth map by subtracting a prepared DEM from a filled DEM and selects sink depth pixels with a value less than or equal to a given depth threshold. These pixels are vectorized into polygons representing water bodies, the elevation values inside the polygons "punched" from the DEM, and the process is repeated with new features appended to the dataset until no new features are identified. After suitable DEM preparation and applying various depth thresholds, researchers identified 37.3% of features present in the Playa Lakes Joint Venture (PLJV) dataset (Kastens et al., 2016). Given the broad study area, the ephemeral nature of playas, the extensive number of features not intersecting with the PLJV dataset, and purpose of the funding, exact determination of which additional features identified were undocumented playas and which were false positives was not carried out. However, the study demonstrated an automated approach to identifying subtle water features over a broad area of Kansas, and the steps involved have been scripted in Python and packaged as an ArcGIS tool for easy and consistent execution. Furthermore, researchers were able to delineate playa catchment areas via 2 meter DEMs, a task previously impossible to complete accurately for the smallest playas due to absence of high-resolution DEMs.

LiDAR data for the state of Kansas

The LiDAR Implementation Plan beginning in 2011 led to production of 2 meter LiDAR-derived DEM mosaics collectively covering the entirety of Kansas (completed in 2016). While

adhering to much of the USGS standards of LiDAR collection, processing, and DEM generation, the plan added an additional requirement that exceeded the standard for accuracy of water feature processing established by the USGS. The plan required vendors to hydro-flatten all water bodies "greater than ¾ of an acre and streams wider than 50 feet" (LiDAR Implementation Plan, 2011). In effect, all water features greater than ¾ of an acre should be identifiable through geoprocessing designed to delineate hydro-flattened features.

Project Summary

There is a range of consequences stemming from damming – including hydrological, geochemical, and ecological – and collectively they represent a major anthropogenic disturbance of natural processes. While the effects can be observed anywhere impoundments occur, Kansas offers a unique opportunity to investigate their effects due to its lack of natural lentic bodies and density of agricultural ponds. Many of the aforementioned consequences of impoundments can be seen as aggregative in effect or dependent on distribution. In turn, regional research and management related to impoundment effects will benefit from a precise dataset of impoundment attributes and distribution. However, national inventories and attempts specific to Kansas have historically been restricted by available data, which may be dated, inconsistent, or too coarse in resolution. A general characteristic of past inventories has been the bias of data sources towards identifying large water bodies and neglect of small water bodies. However, with the update of the NHD, recent inventories have shown a greater number of small impoundments in Kansas than previously known. Still, the NHD is imperfect since it originates from manual digitization and mixed-date source materials. As new impoundments are constructed and higher-resolution

elevation data become available, the question arises: “is it possible to improve further on the NHD through a novel and efficient elevation-based approach?”

Since the compilation of the NHD for the area covering Kansas, new imagery and elevation data have been developed. Recent studies have demonstrated success in water feature identification via automated depression or sink analysis using 1-m and 2-m DEMs (Leonard et al., 2012; Wu et al., 2014; Kastens et al., 2016). With LiDAR-derived DEMs now available for the majority of Kansas, there is an opportunity to apply similar geoprocessing methods focused on water feature identification and to recognize recently constructed water bodies absent in the NHD as well as to update preexisting feature geometries. Furthermore, an automated geoprocessing approach may offer a more efficient, consistent, and easily duplicated alternative to previous methods relying on photointerpretation and topographic map digitization. With LiDAR-derived elevation data emerging for new regions of the United States, efficient and easily duplicated elevation-based methods for creating water feature inventories may be applied in other regions to improve understanding of water body distribution and significance.

This research uses recent high-resolution elevation data to test automated water body identification in a region characterized by substantial impoundment abundance and significant anthropogenic disturbance. The primary objectives are: 1) Conduct two automated water feature identification approaches, the TWIP taken from Kastens et al. (2016) and the Zero Slope approach, and gauge their efficiencies using aerial imagery, the NHD, and an accuracy assessment index, 2) Update the water body data of the NHD for selected drainage regions by incorporating newly identified features and amending less accurate geometries. In doing so, the following questions are addressed: 1) Is there an efficient elevation-based alternative to manual

lentic body delineation? 2) Can elevation-based water feature identification and geometry characterization improve the accuracy of the NHD water bodies dataset?

Methods

Study Area & Data Sources

Reservoir drainages of eastern Kansas were chosen as study areas for the following reasons: 1) It seems unlikely that water features would straddle drainage boundaries, so complete geometries are assumed to be contained within processing extents, 2) lentic features identified can be assumed to be impoundments since playa abundance is minimal in eastern Kansas, 3) and the results of this chapter serve as a foundation for the next chapter, which focuses on reservoir drainage characterization in eastern Kansas. Reservoir drainages selected for this study include Perry, Clinton, Pomona, Council Grove, Melvern, John Redmond, Marion, El Dorado, Toronto, and Fall River (Figure 1). Drainages were delineated using 30-meter resolution DEMs, and drainage boundaries ended below the dam(s) of any upstream reservoir(s) (e.g., Figure 2). This delineation procedure was based on the estimated 90% trap efficiency held by the upstream reservoirs (deNoyelles & Jakubauskus, 2008) and methods demonstrated by Rahmani et al. (2017).

Reservoir catchments cover portions of the following 20 counties: Atchison, Butler, Brown, Chase, Coffey, Douglass, Elk, Greenwood, Harvey, Jackson, Jefferson, Lyon, Marion, McPherson, Morris, Nemaha, Osage, Shawnee, Wabaunsee, and Woodson. Perry and Clinton reside in the Lower Republican basin; Pomona & Melvern in the Marias Des Cygnes; Marion, John Redmond, and Council Grove in the Neosho; Fall River and Toronto in the Verdigris; and

El Dorado in the Walnut. Catchment area ranges from 535 sq. km (Marion) to 6645 sq. km (John Redmond) with a mean of 1736.4 sq. km (Table 1). With the exception of portions of the Toronto and Melvern catchments, all catchments have annual precipitation rates of 850-1000 mm (Rahmani et al., 2017).

Vector datasets were downloaded from the Kansas Data Access & Support Center (DASC) including: National Hydrography Dataset "water bodies" shapefile produced by the USGS, 2002 KDOT non-state road system shapefile produced by Kansas Department of Transportation, TIGER 2014 center-line roads shapefile produced by the U.S. Census Bureau, and TIGER 2010 railroads shapefile produced by the U.S. Census Bureau. Additionally, 30 meter DEM tiles from the USGS National Elevation Dataset (NED) were obtained through DASC. LiDAR-derived 2-meter DEMs were provided by faculty at the Kansas Biological Survey, a research center affiliated with the University of Kansas. DEM tiles were produced from 2010 – 2016 by separate vendors under the 2011 LiDAR Implementation Plan. The ArcGIS World Imagery Basemap provided 0.3-meter resolution aerial imagery collected in July of 2015. Geoprocessing was conducted using ESRI ArcGIS, scripting and tool creation were carried out in Python, and spreadsheet and statistical analysis was conducted in Microsoft Excel following importation of water feature attribute data from ArcMap.

Preliminary Processing

An overview of geoprocessing procedures is displayed in Figure 3, and the steps for elevation data extraction are shown in Figure 4. Ten reservoir polygons of interest were retrieved from the NHD water body dataset to provide pour points for catchment determination. 30-meter

DEMs taken from the NED provided the surface data for watershed geoprocessing. Resulting drainage areas of 10 representative watersheds were converted to polygons and merged to provide a mask for extracting 2-meter elevation data. Given time requirements and previously demonstrated reservoir drainage delineation methodology (i.e., Rahmani, 2016), using 30-meter resolution DEMs for drainage delineation was deemed more practical than directly extracting reservoir catchments with 2-meter elevation data. Individual mxd files in ArcMap were created for specific reservoir drainage analyses, and reservoir drainage polygons derived from 30-meter elevation data provided extents to extract drainage specific 2-meter DEMs. Mosaicking 2-meter DEM tiles prior to drainage area DEM extraction was necessary since tile boundaries did not adhere to drainage area geometries, and several drainages required elevation data pulled from multiple tiles.

NHD water bodies were extracted using reservoir drainage area masks to inventory NHD features for each drainage. After applying a 100 meter buffer to the focus reservoir, NHD features intersecting the reservoir or buffer were checked with aerial imagery for clear disconnectedness. The reservoir and any possibly connected water bodies were removed from each drainage dataset (Figure 5). For proceeding sections, any reference to NHD data for a drainage refers to the NHD data following exclusion of the reservoir and reservoir-connected features.

Following procedure by Kastens and others (2016), a 3x3 focal median filter was applied to the 2-meter DEM for each reservoir catchment to remove minor sinks and peaks, followed by road and railroad removal. Since the focal statistics tool in ArcGIS does not permit a median operation on a float type raster, the procedure was coded in Python (see Appendix). As shown in previous studies (Leonard et al., 2012; Kastens et al., 2016), roads and railroads can be sources

of false “dams” in elevation-based water body identification if unchecked. The procedure to remove roads and railroad followed that of Kastens et al. (2016) (Figure 6). Road and railroad data were acquired through KDOT non-state roads, TIGER roads, and TIGER railroads shapefiles. While Leonard and others (2012) applied a 15 meter buffer, both Kastens et al. (2016) and my preliminary results favored a 30 meter buffer to smooth roads, railroads, and adjacent ditches from DEMs and eliminate false dams.

Topographic Wetland Identification Process model (TWIP) and Zero Slope (ZS) Method

The Topographic Wetland Identification Process model (TWIP) developed by Kastens and others (2016) employs a sink depth map and depth threshold to identify potential water bodies (see Appendix 1). Initially, sinks are filled and a sink depth map calculated by subtracting the original DEM from the filled DEM. Using a mask composed of resulting sinks, a zonal maximum depth raster is generated for sink patches. Sinks with zonal maximums meeting or exceeding the designated depth threshold are then extracted to create a raster layer representing potential water bodies (Figure 7). After testing various depth thresholds, a depth of 0.3 meters was found to be best for maximizing feature identification without excessive false positives. The resulting raster is then converted to polygons and appended to a water body shapefile. Should the converted raster result in an empty shapefile, the process terminates, and the water body shapefile contains the total TWIP results. If not, an inverted sink depth raster is created with appended water body patches removed. The process then iterates using the inverted sink depth raster as the DEM.

As specified in the LiDAR Implementation Plan (2011), streams with widths exceeding 50 meters and lentic bodies exceeding ¾ of an acre necessitate hydro-flattening. The Zero Slope tool (ZS) exploits hydro-flattened patches by identifying cells with a slope value of zero and converting those patches to polygons representative of water bodies (see Appendix 1). First, a raster of cell slope values is calculated from the 2-meter DEM. Cell values equal to zero are extracted from the slope raster and converted to polygons. Since a cell's slope value is a function of the greatest difference in elevation between the focal cell and adjacent cells, the perimeter cells of the hydro-flattened area have a slope value greater than zero. This results in underestimation of the hydro-flattened patch's area. To compensate for this, a buffer with distance equal to the cell size (2 meters) was applied to all polygons (Figure 8).

Noise and false positive removal required manual processing and validation using aerial imagery. All resulting TWIP and ZS features with areas less than 250 m^2 were selected and deleted from respective datasets. This removed noise and any potential water bodies under 1/16 acre, which would be difficult to disseminate given the resolution of aerial imagery. As with NHD preparation, a 100 meter buffer was created around the reservoir to avoid designating connected segments as distinct water bodies. Any polygons intersecting with the reservoir or the 100 meter buffer were examined in the context of aerial imagery, and any water bodies not clearly disconnected from the reservoir were removed from the dataset. Remaining TWIP and ZS polygons were intersected with NHD data, and those not intersecting were checked with aerial imagery and identified as true water bodies or false positives. Any TWIP or ZS features intersecting with the NHD were assumed to be true water bodies. In turn, false positives were removed, leaving only features intersecting with the NHD or verified with aerial imagery.

Accuracy Assessment

In order to quantify the geometric accuracy of the NHD, TWIP, and ZS features, fifty water bodies from each dataset were compared with water bodies manually traced from aerial imagery (Figure 9). Ten samples were taken from five reservoir drainage areas: Marion, Melvern, El Dorado, Council Grove, and Pomona. These reservoirs were selected due to successful execution of the TWIP tool within their watersheds and considered representative of the entire dataset. The five population groups consisted only of features identified in the NHD, TWIP, and ZS and were identified by intersection. Ten features were sampled randomly from each TWIP drainage population (see Appendix 1), and the corresponding NHD and ZS water bodies were identified via intersection.

Polygons were manually drawn for the fifty water bodies using 2015 30-cm resolution imagery at a 1:1000 – 1:2000 scale and appended to a new feature class named "Verified." Area polygons for three categories – Verified and NHD overlap, Verified and TWIP overlap, and Verified and Zero Slope overlap – were calculated for all sample features. An equation was implemented to assign an accuracy index value ranging from 0 – 1.00 to all samples for the three datasets (Figure 9). After determining indices for the 50 sampled features, summary statistics for mean, standard deviation, minimum, and maximum were calculated (Table 6).

Combined Dataset

Features from TWIP results, ZS results, and the NHD were merged into a final dataset named "Combined". Based on accuracy assessment results, the merging prioritization was as follows: 1) the TWIP features form the foundation of the final dataset, 2) all ZS features that do

not intersect with the TWIP features, 3) and all NHD features that do not intersect with the merged TWIP and ZS features (Figure 10).

Results

NHD Results

NHD water feature count, cumulative surface area, and percentage unidentified by the TWIP or ZS approaches are shown in Table 1. Calculations exclude the reservoir itself and any connected features. Naturally, the number of NHD water bodies tends to increase with increasing drainage area with the exceptions of Melvern Reservoir and Fall River Reservoir. Water body densities, or average count per square kilometer, range from 1.09 Ct/km^2 (Marion) to 2.97 Ct/km^2 (Clinton), with a mean count per km^2 of 2.04. The percentage of NHD features unidentified by either of TWIP or ZS procedures ranges from 41.78 % (El Dorado) to 88.31 %, (Toronto) with a mean of 69.68%.

TWIP Results

Results of the TWIP approach are summarized in Table 2. The approach encountered scaling issues and was most successful in identifying greater numbers of NHD features in smaller drainages. Significant processing issues occurred for three large drainages, Clinton, Perry, and John Redmond, and these drainages are therefore omitted from Table 2. Partial results were obtained for Clinton Reservoir, with the script only identifying features in the southwest portion of the drainage. While these results are omitted from the TWIP summary table (Table 2), they were incorporated in generating the Combined dataset and are recognized in later tables.

The script failed to execute for Perry Reservoir, the second largest drainage area, and that drainage is excluded from the TWIP results. The required road and railroad removal procedure could not be completed for the largest drainage, John Redmond, as the number of points resulting from the buffered roads and railroads caused the extract-values-to-points tool of ArcGIS to fail. In turn, that drainage also is excluded from the TWIP results. The approach was most successful in identifying NHD features for the three smallest drainage areas: Marion – 32.71%; El Dorado – 55.87%; and Council Grove – 35.64%. The approach identified over 90% of all ZS features in Council Grove, El Dorado, Fall River, and Marion drainages. In all drainages where execution was successful, features absent in the NHD dataset were identified, with an average of new features comprising 1.75% of the NHD count on average. The scaling issues may reside in file sizes, feature numbers, and/or processing limitations of ArcGIS tools included in the script. However, based on successful execution in smaller drainages and lack of a clear remedy, the current results were deemed sufficient to draw conclusions for the purposes of this study.

ZS Results

Results of the Zero Slope approach are summarized in Table 3. Failure of TWIP execution for Perry and John Redmond drainages prevented comparison of ZS and TWIP for those drainages. Percentage of NHD features identified through ZS ranged from 11.69% (Toronto) to 58.22% (El Dorado) with a mean of 30.31%. Features absent in the NHD were identified in all drainages, ranging from 12 (Fall River & Toronto) to 246 (John Redmond). Identification of new features relative to the NHD resulted in an average increase of 2.09% in impoundment number across all drainages. The Zero Slope approach successfully identified 99% or greater of all TWIP features for all drainages.

Combined Data

The Combined datasets are summarized in Table 4. Merging the TWIP, ZS, and NHD data resulted in an increase in water features relative to the NHD data for all drainage areas. The percentage increase relative to NHD count ranged from 0.28% (Toronto) – 3.97% (Marion) with a mean of 2.10%. El Dorado is the only drainage where the NHD does not provide the majority of geometries for the final dataset (41.03%). NHD data comprise the highest percentages of the final dataset features for Toronto (88%) and Fall River (85.13%). The percentage of TWIP features in final datasets ranges from 0% for Perry and John Redmond to 55.28% for El Dorado with a mean of 19.57%. Since TWIP feature geometries were favored over ZS geometries in appending order, ZS features comprise a mean of 11.98% of features included in final datasets. ZS features make up the highest percentages for datasets where TWIP processing was unsuccessful: Perry (30.03%), John Redmond (36.23%), and Clinton (25.74%). Since TWIP and ZS geometries supplanted intersecting NHD geometries, certain water bodies represented as fragmented or continuous by the NHD were replaced by contiguous or divided geometries (e.g., Figure 11). The summed change in NHD count is noted in the NHD Div/Join column, with positive values indicating an overall increase attributed to division of features, and a negative value indicating an overall decrease in NHD count due to joining.

Surface Area Difference

Table 5 contains the cumulative NHD and Combined water body surface areas for each drainage. Eight of the reservoir drainages experienced an increase in cumulative drainage area due to additional features and altered geometries of the Combined data relative to the NHD. Fall River and Toronto were the exceptions, showing a decrease in cumulative feature surface area of

16.28% and 14.50%, respectively. The maximum increase in water feature surface area was 48.41% (Marion) and the mean 8.37%. Change in density, or count per km^2, relative to the NHD was marginal across all drainages and was therefore omitted.

Accuracy Assessment

Summary statistics are provided for the geometric accuracy indices in Table 6. NHD accuracy indices exhibit the greatest range and deviation of the three datasets, with a minimum of 0.3064, a maximum of 0.9677, and a standard deviation of 0.1544. The mean NHD index, 79.22, is the lowest of the three datasets. The TWIP and ZS accuracy results are closely similar on all summary statistics, exhibiting mean index values of 0.9119 (TWIP) and 0.9111 (ZS) with minimal standard deviation (0.0437 – TWIP; 0.459 – ZS). Disregarding overlap and positional accuracy, percentage of total Verified surface area (% Verified SA) was calculated from summing surface areas for each dataset. NHD features totaled to 82% of Verified surface area and TWIP and ZS features totaled to 94.90% and 94.14%, respectively.

Discussion

TWIP accuracy and limitations

TWIP-derived features held the greatest geometric and positional accuracy as determined by a mean index value of 0.9119 (Table 6). Additionally, it demonstrated the greatest consistency, with an index standard deviation of 0.0437, when compared to the NHD (0.1544) and ZS (0.0459). These results supported prioritization of TWIP-derived water features when merging the three datasets.

Noise removal was largely achieved through removal of all features less than 250 m^2, but manual validation of features not intersecting NHD data was required. Overall, the manual geoprocessing required to remove false positives was minimal. However, required execution time far exceeded that for the ZS tool. For example, the smallest drainage, Marion (535 km^2), took approximately 2 hours for the TWIP tool to finish, while the ZS tool completed water feature identification in under 3 minutes. The largest drainage area successfully completed, Toronto (1855 km^2), required over 10 hours to execute the TWIP tool. The substantial time required for execution is likely attributed to the iteration of multiple map algebra operations and sink filling, which can be particularly time-consuming with high resolution elevation data and a large processing extent.

The approach was most effective in smaller drainages. For drainage areas that the tool executed successfully, percentage of NHD features identified ranged from 10.37% for Toronto to 55.87% for El Dorado (Table 2). The greatest percentages of NHD features identified occurred in the smallest drainage areas: Marion (32.71%), El Dorado (55.87%), and Council Grove (35.64%). The percentage of ZS features identified through the TWIP exceeded 90% for the three smallest drainages as well as Fall River. In all drainage areas that TWIP completed, features absent in the NHD were identified. As drainage area increased, the TWIP feature count did not increase. In fact, feature number ranged from 391 to 440 for reservoirs exceeding the size of the three smallest without correlation to drainage size. This tendency to identify a limited number of features may be due to limitations of feature number or file size for certain geoprocessing steps in the TWIP process.

Running TWIP on the Clinton drainage area resulted in a unique outcome. Features were only identified for the southwest portion of the drainage area. While the TWIP tool ran

successfully for some larger drainage areas (i.e., Fall River and Toronto), Clinton has the highest density of water bodies of all areas analyzed (Table 1). Halting of TWIP identification may have been related to inherent ArcGIS tool limitations when processing such large files or feature numbers. This may also have been the cause of the tool's failure to complete processing for Perry. While the precise cause of error in the procedure is unknown, the issue in DEM preparation for John Redmond's drainage area is clear. When attempting to use the extract-values-to-points tool of the spatial analyst toolbox, the tool completed processing but assigned elevation values of zero to 29% of the points. The tool was assigned to extract elevation values to 8.9 million points, which proved to exceed the tool's limitations. There are inherent and often undocumented limitations to ArcGIS tools, which may be unknown to the user and seldom encountered. However, processing high resolution elevation data (i.e., LiDAR-derived DEMs) over a substantial area may illuminate these limitations, and drawing attention to specific cases such as this can help others to avoid these problems and encourage programmers to develop remedies. A simple solution to these issues would be dividing up drainage areas and performing TWIP water feature identification for the subdivided areas. However, determining an appropriate parcel area to maximize efficiency of TWIP would be necessary, and time constraints, the objectives of this study, and ZS tool success discouraged further investigation.

Zero slope effectiveness and efficiency

Accuracy assessment results showed ZS geometric and positional accuracy to be comparable, although slightly less favorable, to TWIP accuracy. The ZS approach resulted in a mean accuracy index of 0.9111, representing higher accuracy than NHD features (mean index = 0.7922), and coming close to TWIP's mean index of 0.9119 (Table 6). Even with the single cell buffer incorporated into the ZS process, surface areas were consistently smaller for ZS compared

to TWIP results. This is likely due to heterogeneous alignment on stretches of hydro-flattened patch perimeter cells, particularly around inlet areas (e.g., Figure 8), and a resulting greater loss of pixels through selection of 0 slope values than pixel gain from a uniform buffer. In turn, 49 of the 50 features sampled showed a greater TWIP surface area than ZS surface area, and TWIP features averaged a 1.38% increase in surface area compared to corresponding ZS features. In terms of index variance, ZS samples had a standard deviation of 0.0459, reflecting greater consistency than the NHD (0.1544) and slightly less than the TWIP (0.0437). Accuracy assessment results favored ZS features over NHD but not TWIP when merging the datasets.

Smaller false positives were removed through deletion of any features less than 250 m^2, as was done with the raw TWIP data. Hydro-flattened rivers produced the majority of larger false positives and were manually removed. While intersecting the ZS features with NHD stream data to identify hydro-flattened stream segments was considered, this could lead to removing impoundments intersecting streamlines, and the clustering tendencies of hydro-flattened stream polygons allowed efficient manual removal. Due to the required manual removal of hydro-flattened lotic features, manual geoprocessing took slightly more time than with the TWIP dataset. However, execution of the tool was markedly quicker than the TWIP, taking at most two hours for the largest drainage (John Redmond), which the TWIP tool was unable to process successfully. The more time-efficient character of the ZS tool is attributed to its single iteration process and absence of sink filling and multiple map algebra operations. Generating a slope raster is the most time-consuming aspect of the script, but it requires far less time than TWIP's sink fill. Furthermore, removal of roads and railroads is unnecessary for the ZS approach, as it is not subject to the false dams created by those features. In summary, the ZS approach is far less time-consuming in terms of pre-processing and execution than the TWIP method.

In all reservoir drainages analyzed, ZS identified more features than the TWIP and a greater percentage of NHD features. ZS identified 99% or more of all features identified through the TWIP method. ZS identified 11.69% (Toronto) to 58.22% (El Dorado) of NHD water bodies, with a mean of 30.31% (Table 3). The mean percentage of increase in water bodies due to ZS results relative to NHD data was 2.09%. In contrast to TWIP results, there was a general increase in numbers of features identified with increasing drainage area, with the exceptions of Council Grove, Fall River, and Toronto, which all produced fewer features than some smaller drainage areas. Also in contrast to the TWIP approach, the ZS tool was successfully applied to the largest drainage areas, Perry and John Redmond, identifying 28.22% and 34.48% of NHD features, respectively.

Summary and Significance of Combined Dataset

Based on results of the accuracy assessment, TWIP and ZS–derived features exhibit superior surface area accuracy to NHD data. While TWIP results were not collected for John Redmond and Perry, ZS accuracy was comparable to TWIP, and the successful execution of the ZS method in those drainages led to their inclusion in the Combined datasets despite having only NHD data and ZS results to draw from. Since the geometries of TWIP and ZS results have been shown to be more valid than NHD features and new water bodies were identified for all drainages, merged datasets may be considered more accurate and complete compared to inventory approaches relying solely on the NHD.

As a consequence of new geometries, many previously segmented or continuous NHD water bodies were joined or divided based on TWIP and ZS depictions (e.g., Figure 11). In turn, the count of Combined bodies may be different from the sum of the NHD and the

nonintersecting TWIP and ZS features. The overall change in NHD feature count due to division or joining is shown in Table 4 (“Div/Join”). Half of the drainages experienced reduced feature count due to conjoining of features (negative values) and half experienced an increase in feature count due to fragmenting (positive values) with a mean increase in 1.3 features. In turn, no trend of NHD representing exclusive features as fragmented or fragmented features as joined was observed. TWIP results occasionally joined fragmented ZS features into singular features, resulting in new feature counts of the Combined dataset being less than new feature counts of the ZS for Toronto, El Dorado, Pomona, and Melvern drainages (Figure 12). Additionally, the TWIP method identified two water bodies absent in the NHD and ZS results, one in El Dorado and one in Melvern. Conversely, ZS identified all other TWIP features absent in the NHD as well as 5 additional water bodies for Melvern, 10 for Pomona, 1 for Toronto, 176 for Perry, and 246 for John Redmond.

Findings indicate the NHD underestimates cumulative water body surface area due to missing features and imprecise geometries. Comparison of the Combined surface areas and NHD surface areas shows a mean increase of 8.37% in total surface area relative to the NHD (Table 5). Additionally, surface area increase would likely be greater for Clinton, John Redmond, and Perry if the TWIP tool had executed properly since TWIP features tend to have slightly greater surface areas than ZS features. Omitting surface area supplied by features absent in the NHD and positional accuracy, total surface area of NHD features used in the accuracy assessment only summed to 82% of the totaled Verified feature surface area. Even without the addition of new features to the NHD, the NHD should be regarded as an underrepresentation of regional standing water.

Two drainage areas stand out due to low percentages of NHD features identified through ZS and reduced surface areas resulting from the Combined dataset. Fall River and Toronto have drainage areas of 1,434 km^2 and 1,855 km^2, respectively. According to the NHD, Fall River has 2,828 water bodies and Toronto has 3,943, yet ZS analysis only identified 415 features for Fall River (intersecting 14.41% of NHD water bodies) and 479 features for Toronto (intersecting 11.69% of NHD water bodies). TWIP results were fewer still, and interestingly, replacing this percentage of NHD geometries with TWIP or ZS results and appending additional water bodies resulted in substantial decreases in cumulative surface areas for both drainages (Table 5). Fall River and Toronto are adjacent drainages with the majority of their drainage areas in Greenwood County, Kansas. Elevation data used in this study was mosaicked from elevation tiles developed by different vendors from 2010 – 2016. While it is possible this region's tile may have experienced less thorough hydro-flattening compared to tiles created by other vendors, the time the LiDAR data was collected may offer another explanation. While the DEM for the Greenwood County and other southeast counties was produced in 2013, the source LiDAR data was collected in the winter of 2012, towards the end of a severe two year drought. Water levels may have been low, and there may have been a disproportional number of desiccated ponds the year of data collection. In turn, there were likely greater returns and fewer voids in the point cloud. This would result in the reduction in the number of hydro-flattened features, smaller geometries for hydro-flattened features, and underestimation of surface areas by elevation-based water body identification. However, precise collection date and conditions are needed to verify this possibility.

Conclusions

ZS and TWIP approaches improved NHD geometries overall and identified features absent in the NHD using automated geoprocessing and hydro-flattened 2-m elevation data. TWIP and ZS demonstrated greater accuracy and consistency when features were recognized compared to the NHD. However, the NHD includes substantially more lentic features than the ZS or TWIP produced, and the approaches should not be treated as stand-alone methods of inventorying. While both approaches required some manual post-processing and false positive removal, the TWIP requires substantially greater pre-processing and execution time than the ZS. The TWIP approach produced the most favorable geometries but identified few features missed by the ZS. Overall, the ZS identified more features included and absent in the NHD than the TWIP.

The ZS approach proved more reliable in large drainages relative to the TWIP. ArcGIS tools included in the TWIP script likely have inherent limitations regarding file size or feature number, preventing identification of increasing numbers of features delineated with increasing drainage area and successful script execution altogether in certain drainages. In effect, the ZS should be favored in large extent processing. Subdividing large processing extents is one possibility to improve TWIP performance. LiDAR data collected during periods of drought may result in substantially fewer and smaller voids, which results in fewer and smaller hydro-flattened patches.

The NHD underestimates water feature surface area in the study region. While this may be attributed in part to the absence of water bodies constructed post-NHD, the geometries of the NHD dataset tend to underestimate actual water surface areas. Therefore, inventories using the

NHD, such as those of McDonald (2012) and Callihan (2013) may be conservative in estimates of cumulative surface area.

The methods applied in this study are aimed at improving accuracy of current water body inventories through efficient automated approaches. The hydrological, geochemical, and ecological ramifications of impoundments are significant anthropogenic alterations of natural processes, and constitute sufficient justification for surveying, research, and management for water resources and conservation purposes. With new impoundments continuing to be constructed, efficient methods of updating water body distribution data have value in impoundment research and management. The methods demonstrated and resulting datasets provide a novel example in updating and improving water body inventories for eastern Kansas.

References

Bosch, N. S. (2008). The influence of impoundments on riverine nutrient transport: An evaluation using the Soil and Water Assessment Tool. *Journal of Hydrology 355*(1), 131 147.

Buddemeier, R. W. (2004). Detection and characterization of small water bodies A Final Technical Report for the NASA-EPSCoR/KTech- funded project: Kansas Geological Survey.

Callihan, R. A. (2013). Distribution, proliferation and significance of small impoundments in Kansas. (M.S.), University of Kansas, Lawrence, KS.

Carpenter, L., Stone, J., & Griffin, C. (2011) Accuracy of aerial photography for locating seasonal (vernal) pools in Massachusetts. *Wetlands 31,* 573–581.

Churchill, M.A. 1948: Discussion of analyses and use of reservoir sedimentation data by L.C. Gottschalk. *Proceedings of the Federal Interagency Sedimentation Conference, Denver, Colorado*. US Geological Survey, 139–40.

Deacon, J. E. (1961). Fish populations, following drought, in the Neosho and Marais des Cygnes rivers of Kansas. *Univ. Kansas Mus. Nat. Hist., Publ. 13(9)*, 359-427.

DeCoursey, D. G. (1975). Implications of floodwater retarding structures. *Transactions of the American Society of Agricultural Engineers, 18(5*), 897–904.

deNoyelles, F. & Jakubauskus, M. (2008). Current state, trend, and spatial variability of sediment in Kansas reservoirs. *Sedimentation in Our Reservoirs: Causes and Solutions*, 9-23.

deNoyelles, F. & Kastens, J. H. (2016) Reservoir sedimentation challenges in Kansas. *Transactions of the Kansas Academy of Science, 119(1)*, 69-81.

Downing, J. A., Cole, J. J., Middleburg, J. J., Striegl, R. G., Duarte, C. M., Kortelainen, P., Prairie, Y. T., & Laube, K. A. (2008). Sediment organic carbon burial in agriculturally eutrophic impoundments over the last century. *Global Biogeochemical Cycles 22*(1).

Falke, J. A. & Gido, K. B. (2006). Spatial effects of reservoirs on fish assemblages in Great Plains streams in Kansas, USA. *River Research and Applications 22 (1)*, 55-68.

Gordon, N. D., McMahon, T. A., & Finlayson, B. L. (1992). *Stream Hydrology: an Introduction for Ecologists 1st Edition.*

Harbeck, G. E. (1962). A practical field technique for measuring reservoir evaporation utilizing mass-transfer theory. Professional Paper 272-E, US Geological Survey.

Heidemann, H. K. (2014). LiDAR Base Specification Version 1.2. *US Geological Survey Standards Book 11, Collection and Delineation of Spatial Data*.

Hudman, S. P. & Gido, K. B. (2013). Multi-scale effects of impoundments on genetic structure of creek chub (Semotilus atromaculatus) in the Kansas River basin. *Freshwater Biology 58(2)*, 441-453

Johnson, P. T., Olden, J. D., & Zanden, M. J. V. (2008). Dam invaders: impoundments facilitate biological invasions into freshwaters. *Frontiers in Ecology and the Environment 6(7)*, 357-363.

Kansas Department of Health and Environment (KDHE). (1981) The impact of floodwater retarding impoundments on the biota and water quality of ephemeral Kansas streams. *Soil Cons. Serv. and Kansas Dept. Health Environ. Cooperative Project, Final Report*.

Kastens, J. H., Baker, D. S., Peterson, D. L. & Huggins, D. G. (2016) Wetland Program Development Grant (WPDG) FFY 2013 – Playa Mapping and Assessment. *KBS Report 186*.

Kinsolving, A. D. & Bain. M. B. (1993). Fish assemblage recovery along a riverine disturbance gradient. *Ecological Applications 3(1)*, 531-544.

Leonard, P. B., Baldwin, R. F., Homyack, J. A., & Wigley, T. B. (2012). Remote detection of small wetlands in the Atlantic coastal plain of North America: Local relief models, ground validation, and high-throughput computing. *Forest Ecology and Management 284*, 107-115.

LiDAR Implementation Plan. (2011). State of Kansas GIS Policy Board.

Mammoliti, C. S. 2002. The effects of small watershed impoundments on native stream fishes: a focus on the Topeka shiner and hornyhead chub. *Transactions of the Kansas Academy of Science, 105(3*), 219-231.

Mammoliti, C. 2004. Recovery plan for the Topeka shiner (Notropis topeka) in Kansas. Kansas Department of Wildlife and Parks.

Martinko, E., deNoyelles, F., Bosnak, K., Jakubauskas, M., Huggins, D., Kastens, J., Shreders, A., Baker, D., Blackwood, A., Campbell, S., & Rogers, C. (2014). *Atlas of Kansas Lakes: A resource for communities, policy makers and planners.*

McDonald, C. P., Rover, J. A., Stets, E. G., & Striegel, R. G. (2012). The regional abundance and size distribution of lakes and reservoirs in the United States and implications for estimates of global lake extent. *Limnology and Oceanography, 57(2)*, 597-606.

Menge, B. A. & Sutherland, J. P. (1976). Species diversity gradients: synthesis of the roles of predation, competition, and temporal heterogeneity. *American Naturalist 110(973)*, 351–369.

Moore, C. M. (1969). Effects of small structures on peak flow. *Effects of watershed changes on streamflow*. Univ. Texas Press, Austin. 101-117.

Power, M. E., Matthews W. J., & Stewart, A. J. (1985) Grazing minnows, piscivorous bass, and stream algae: dynamics of a strong interaction. *Ecology 66(5*), 1448–1456.

Rahmani, V., Kastens, J., deNoyelles, F., Jakubauskus, M., Martinko, E., Huggins, D., Gnau, C., Liechti, P., Campbell, S., Callihan, R., Blackwood, A. (2017). Examining storage loss and sedimentation rate of large reservoirs in the U. S. Great Plains. Unpublished article.

Renwick, W. H., Smith, S. V., Bartley, J. D., & Buddemeier, R. W. (2005). The role of impoundments in the sediment budget of the conterminous United States. *Geomorphology 71(1)*, 99-111.

Rice, C. W. (2002). Storing carbon in soil: why and how? *Geotimes 47*, 14–17.

Schrank, S., Guy, C., Whiles, M., & Brock, B. (2001). Influence of instream and landscape-level factors on the distribution of Topeka shiners Notropis topeka in Kansas streams. *Copeia 2*, 413-421.

Smith, S. V., Renwick, W. H., Bartley, J. D., & Buddemeier, R. W. (2002) Distribution and significance of small, artificial water bodies across the United States landscape. *Science of the Total Environment 299(1),* 21-36.

Stearman, L. & Lynch, D. (2013). Patterns of assemblage change in prairie stream fishes in relation to urban stormwater impoundments. *Hydrobiologia 718(1)*, 221-235.

Tiner, R. (1989). Current status and recent trends in Pennsylvania's wetlands. In Majumdar, S.K., Brooks, R.P., Brenner, F.J. and R.W. Tiner eds. Wetlands Ecology and Conservation: Emphasis in Pennsylvania. The Pennsylvania Academy of Science, Easton, PA, 368-387.

USGS, (2009). National Hydrology Dataset Feature Catalog. URL [http://nhd.usgs.gov/]. Date accessed [October 2016]

Vaughn, C. C. & Taylor, C. M. (1999). Impoundments and the decline of freshwater mussels: a case study of an extinction gradient. *Conservation Biology 13(4),* 912-920.

Verstraeten, G. & Poesen, J. (2000) Estimating trap efficiency of small reservoirs and ponds: methods and implications for the assessment of sediment yield. *Progress in Physical Geography 24(2),* 219-251.

Wetter, L. H. (1980). The effects of small watershed dams on streamflow. *Transactions of the Kansas Academy of Science*, *83(4),* 237–238.

Wu, Q., Lane, C., & Liu, H. (2014). An effective method for detecting potential woodland vernal pools using high resolution LiDAR data and aerial imagery. *Remote Sensing 6(11),* 11444-11467.

Zale, A. V., Leslie, D. M., Fisher W. L., & Merrifield, S. G. (1989). The physicochemistry, flora, and fauna of intermittent prairie streams: a review of the literature. *United States Fish and Wildlife Service. Biological Report 89*, 51-44.

Figures

Figure 1: Reservoir Drainage Areas

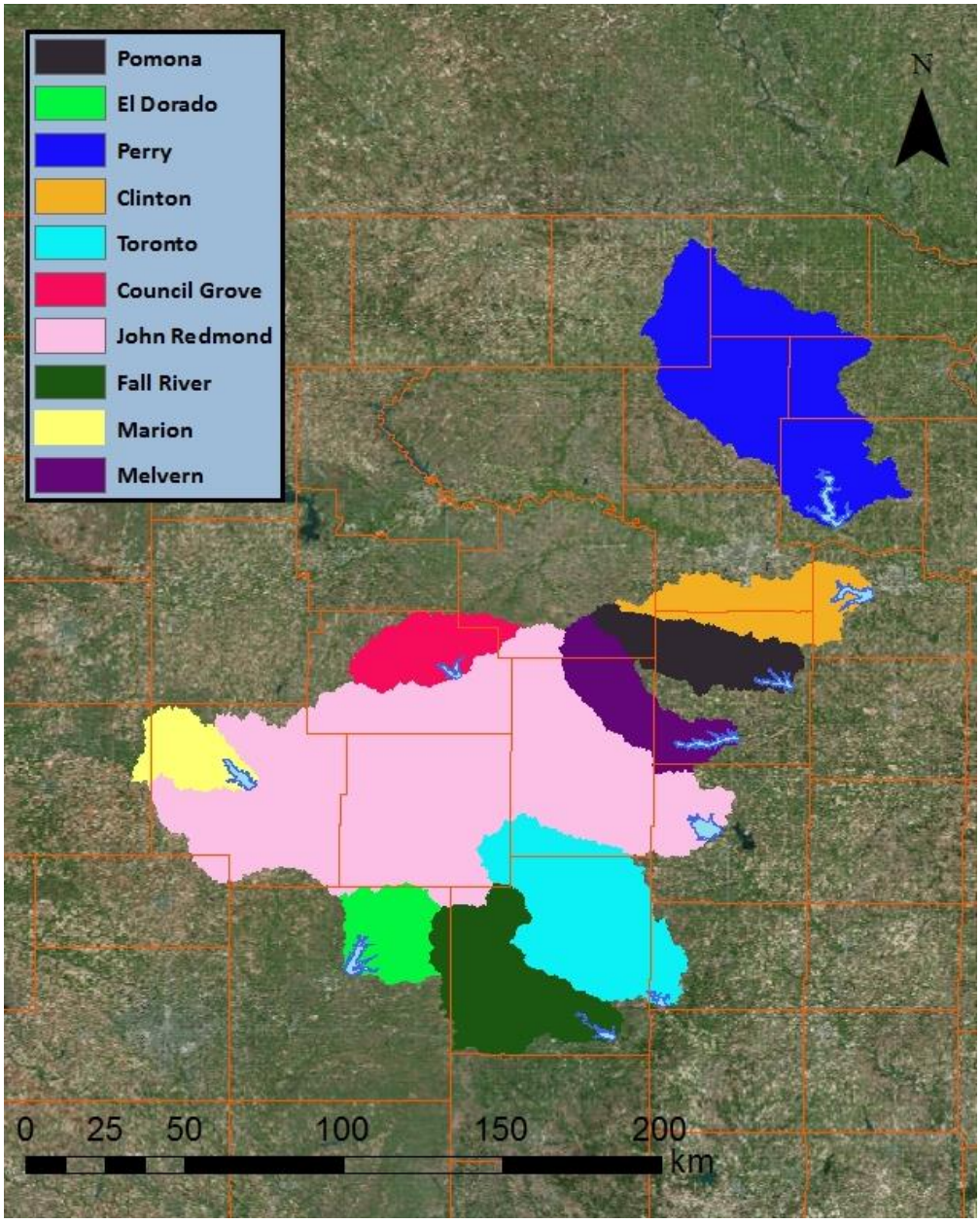

Figure 2: John Redmond Reservoir Drainage Boundary

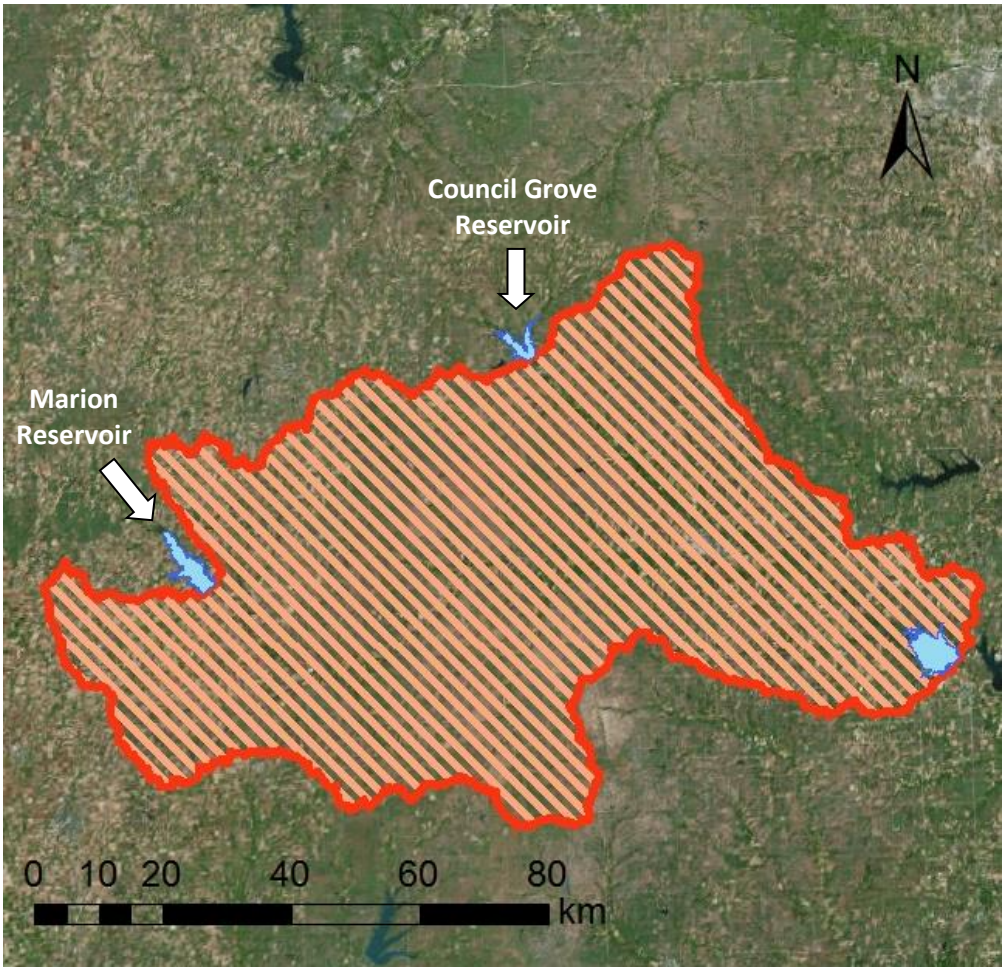

Boundaries of John Redmond's drainage end at the dams of Council Grove Reservoir and Marion Reservoir. This delineation is guided by the methodology of Rahmani et al. (2017).

Figure 3: Overview of Processing. Steps detailed in additional figures are marked (*). Parts A and B are shown below, and Part C along with a key are shown on the following page.

A) Drainage DEM preparation and drainage NHD data extraction. Reservoir polygons were extracted from the NHD and used as pour points for drainage delineation using 30-m resolution elevation data (NED). Resulting drainage polygons were used to clip NHD water body data and 2-m elevation data for each drainage. To conclude preliminary DEM processing, 2-m drainage DEMs were subjected to a median filter and road and railroad removal in accordance to methodologies of Kastens et al. (2016).

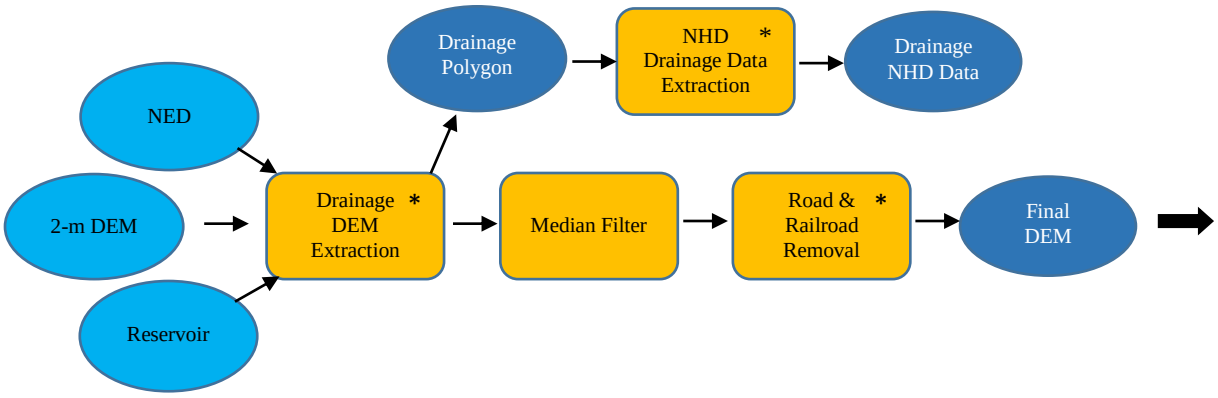

B) TWIP and ZS processing prior to comparison with drainage NHD data. TWIP and ZS methodologies were carried out, and resulting features under 250 m^2 were removed. Reservoirs and their potentially connected features were removed by identifying features intersecting the reservoir or its buffer, and aerial imagery was used to identify any of the intersecting features actually connecting to the reservoir.

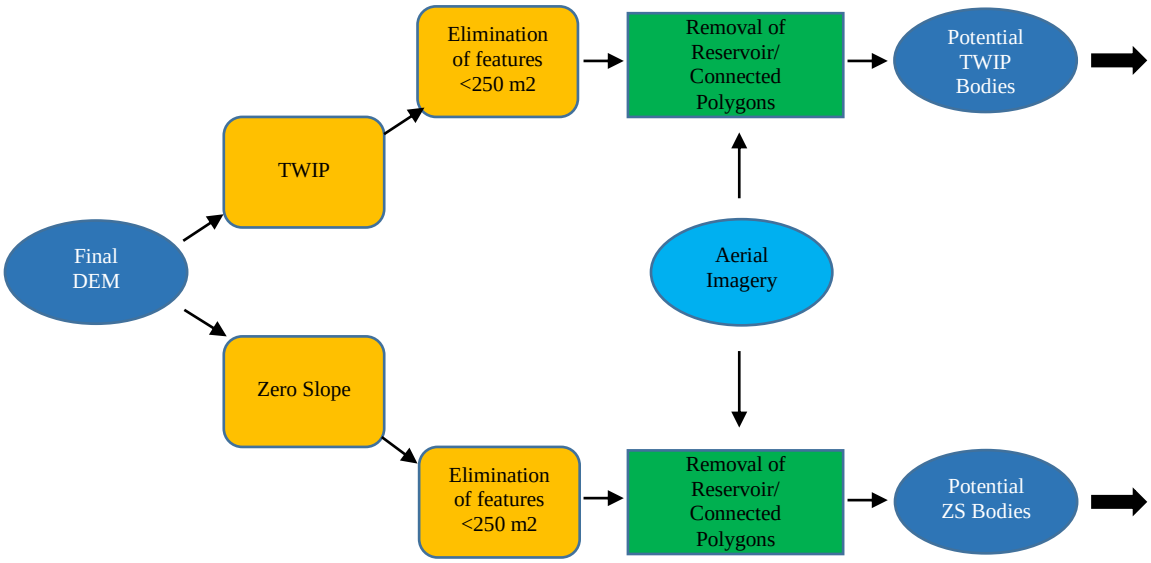

C) Validation of remaining features and merging into Combined dataset. Remaining features were validated via intersection with the NHD and manual review of nonintersecting features using aerial imagery. Finally, TWIP, ZS, and NHD results were compiled into the final dataset.

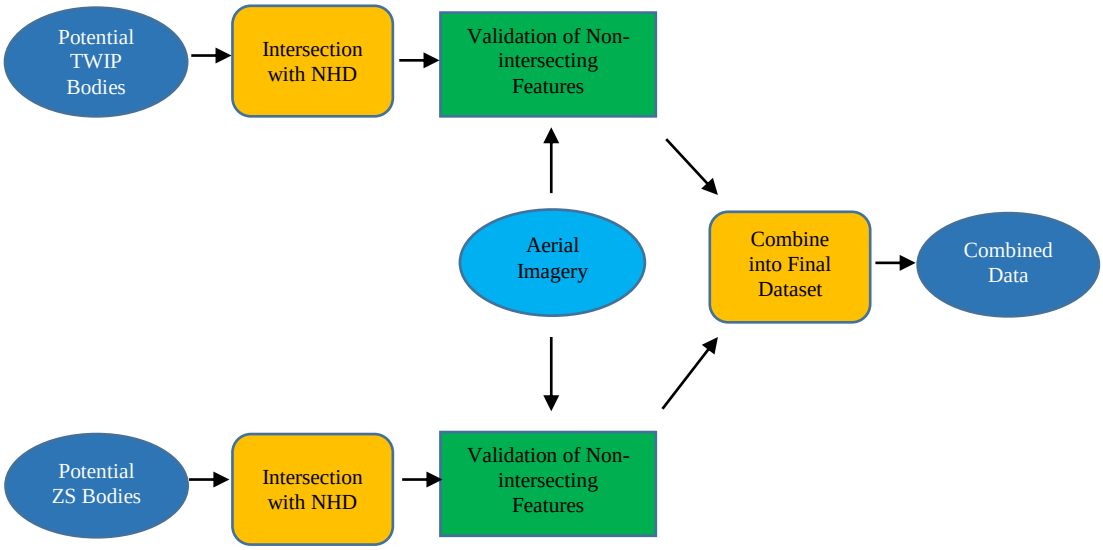

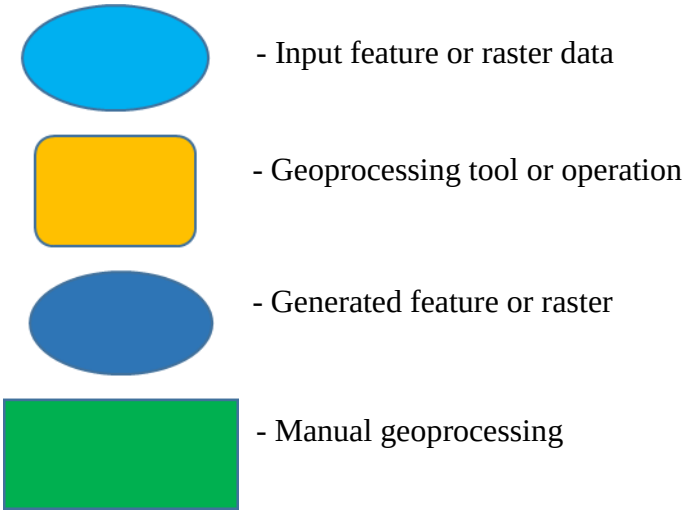

Figure 4: Drainage DEM Extraction

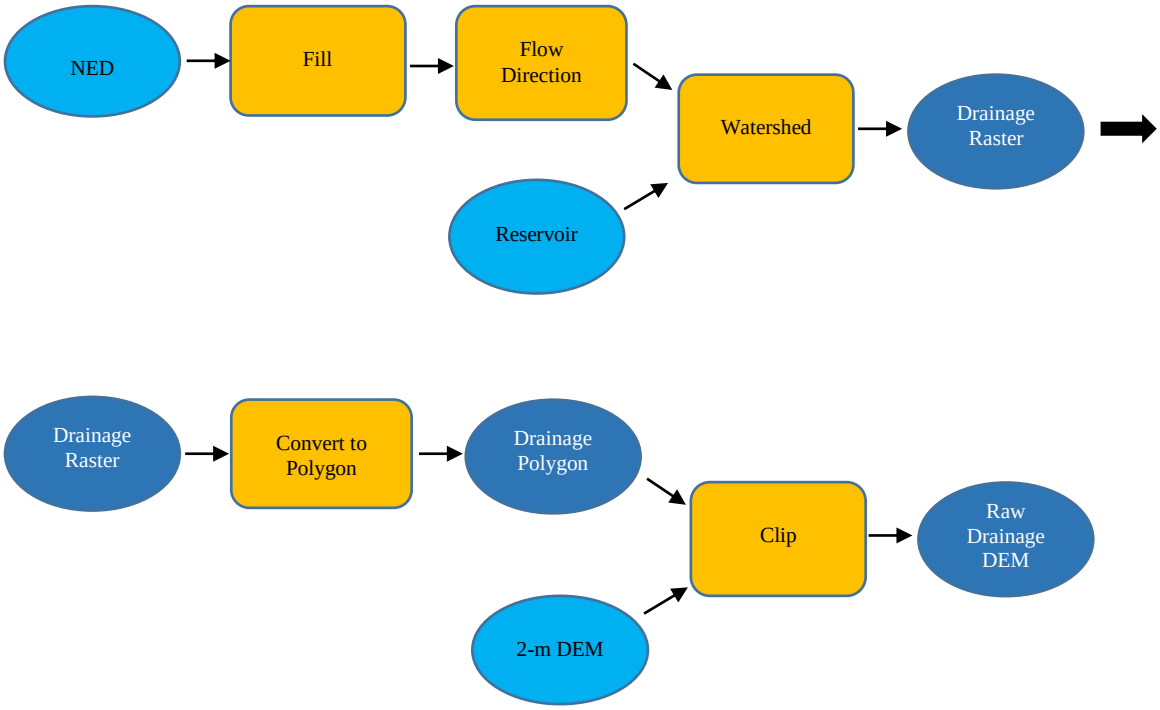

Figure 5: Extraction of NHD Data for Individual Reservoir Drainages

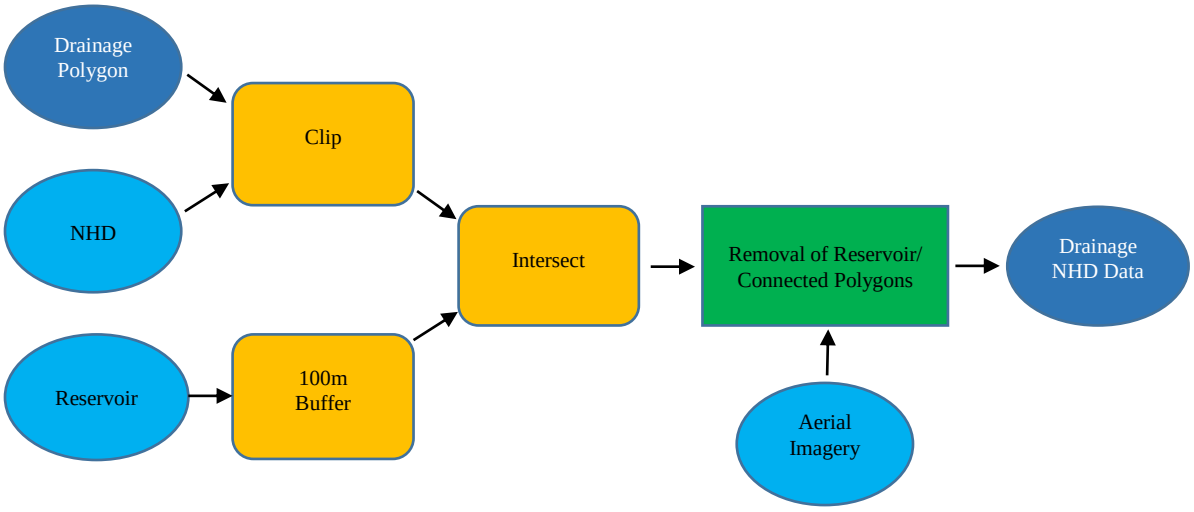

Figure 6: Road and Railroad Removal. TIGER roads, TIGER railroads, and K-DOT Non-state roads were first clipped, dissolved, and merged to create a single feature for removal from drainage DEMs. After various lengths were tested, a buffer radius of 30 meters was found sufficient for eliminating false dams caused by roads and railroads. A raster of the roads and railroads buffer was created for later application in raster calculator. The buffered feature was densified, and vertices converted to points, for which elevation values were extracted using the filtered 2-m DEM. Any points without elevation values (-9999) were removed, and a TIN was created from the remaining points. The TIN was then rasterized for use in raster calculator. With the raster calculator, values from the rasterized TIN were burned into the buffered road and railroad extent of the filtered DEM to produce the final drainage DEMs.

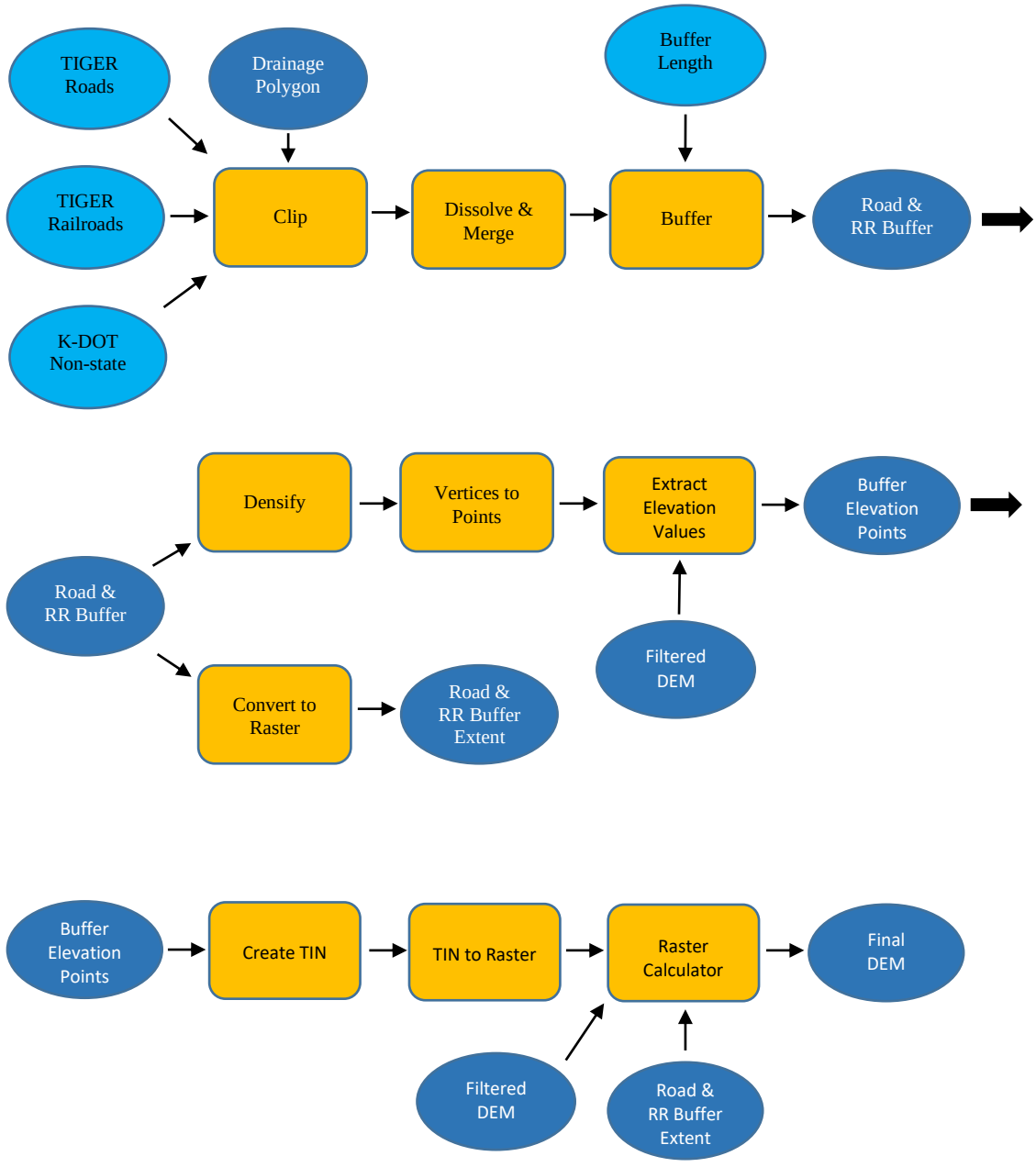

Figure 7: TWIP

A) Aerial imagery of an impoundment from Pomona drainage.

B) Sink depth map taken from subtracting the filled DEM from the original DEM.

C) TWIP feature resulting from a 0.3 meter depth threshold.

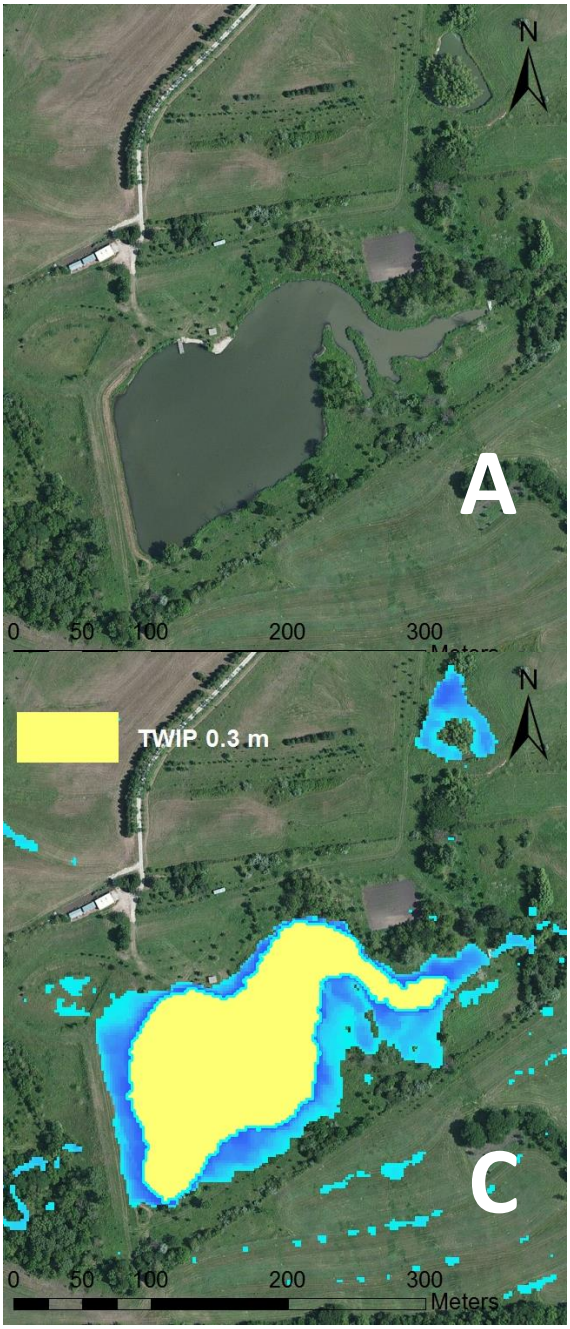

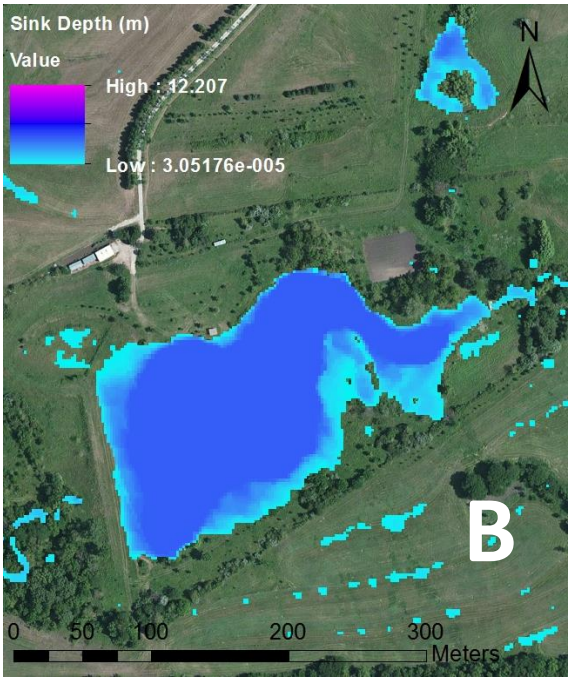

Figure 8: Effect of Zero Slope Buffer

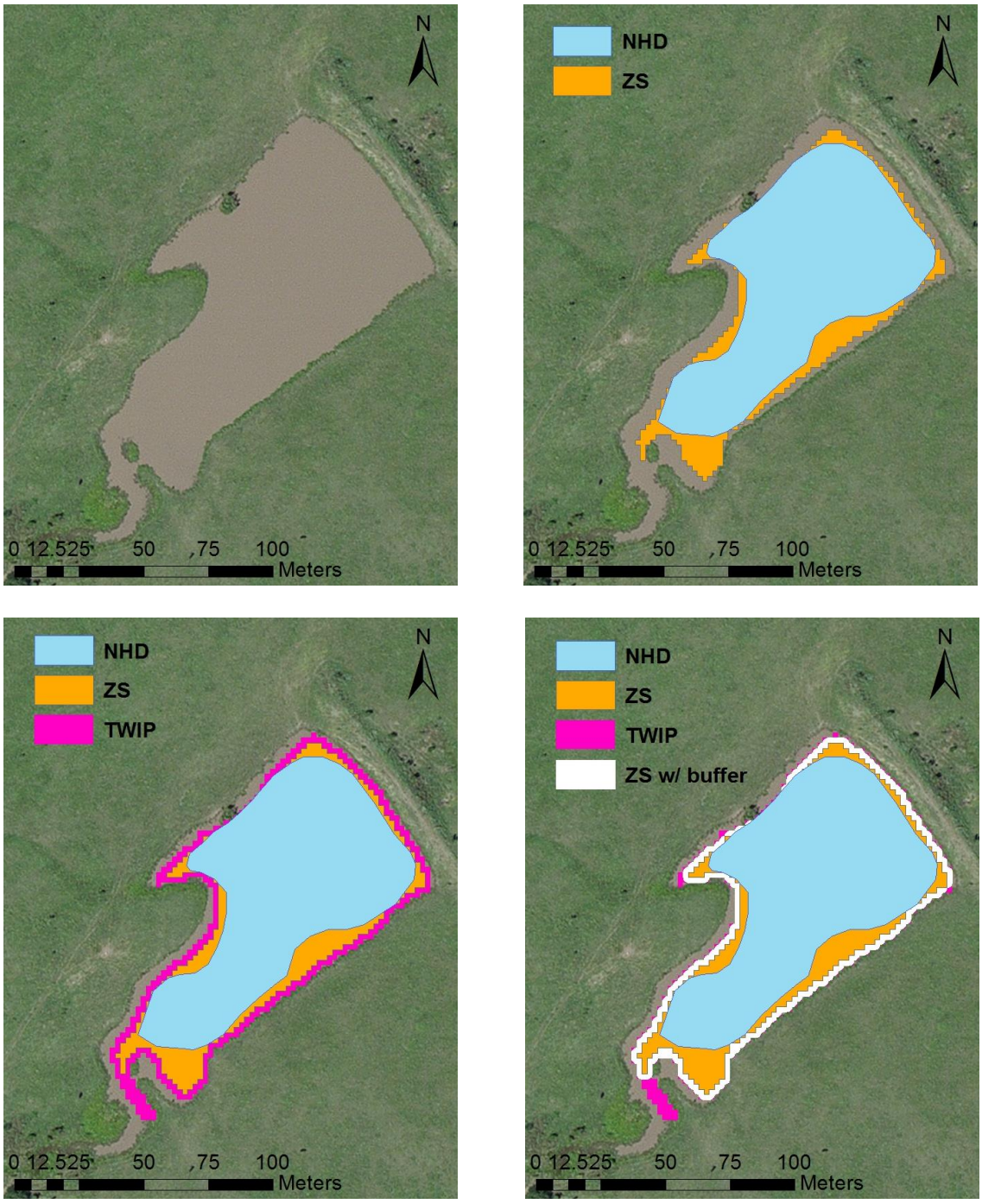

Figure 9: Accuracy Assessment for Zero Slope

Figure 10: Accuracy Assessment Equation.

$$\text{Accuracy Index} = \frac{2A}{(B + C)}$$

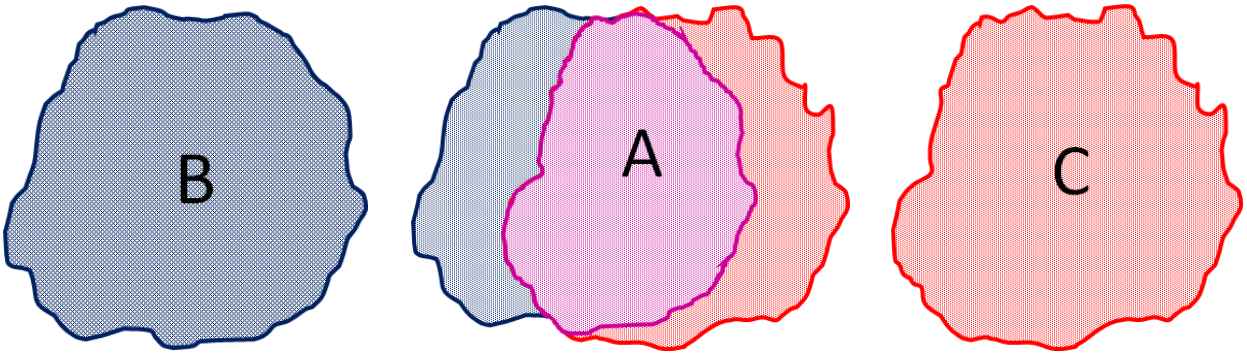

B represents the verified water body geometry; C represents the NHD, TWIP, or ZS geometry; A represents the overlap between B and C or the overlap between the verified surface area and the NHD, TWIP, or ZS surface area. Accuracy Index values range from 0 – 1.00. Values approaching 0 signify little geometric agreement, and values approaching 1.00 show strong geometric agreement.

Figure 11: Joining NHD Feature Fragments

A) Example of discontinuous water features of the NHD from El Dorado drainage.

B) Single water body represented as disjointed polygons by NHD

C) Features from the TWIP dataset resulting in the joining of NHD features

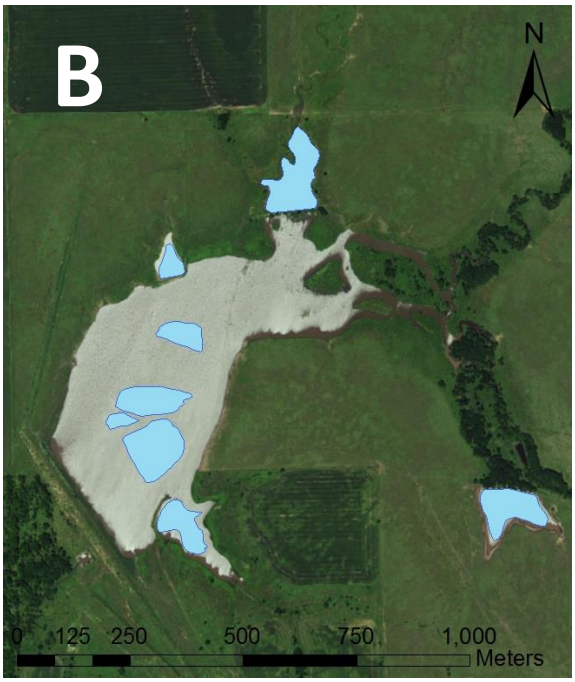

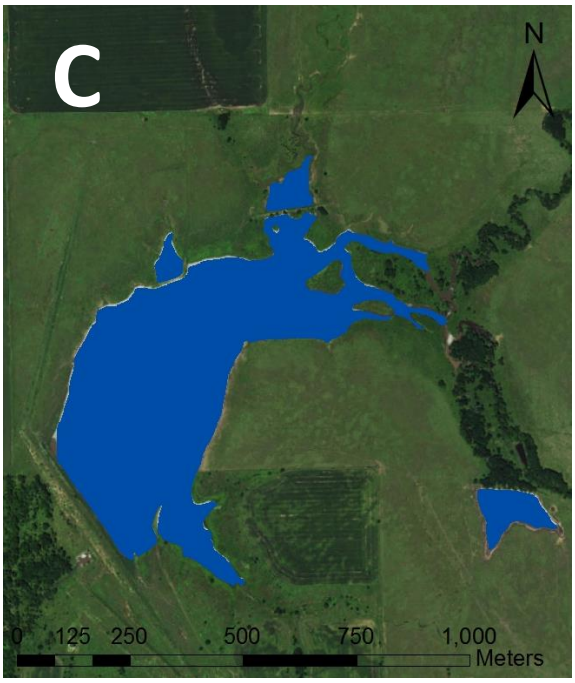

Figure 12: Fragmented Zero Slope Feature Joined by TWIP Procedure

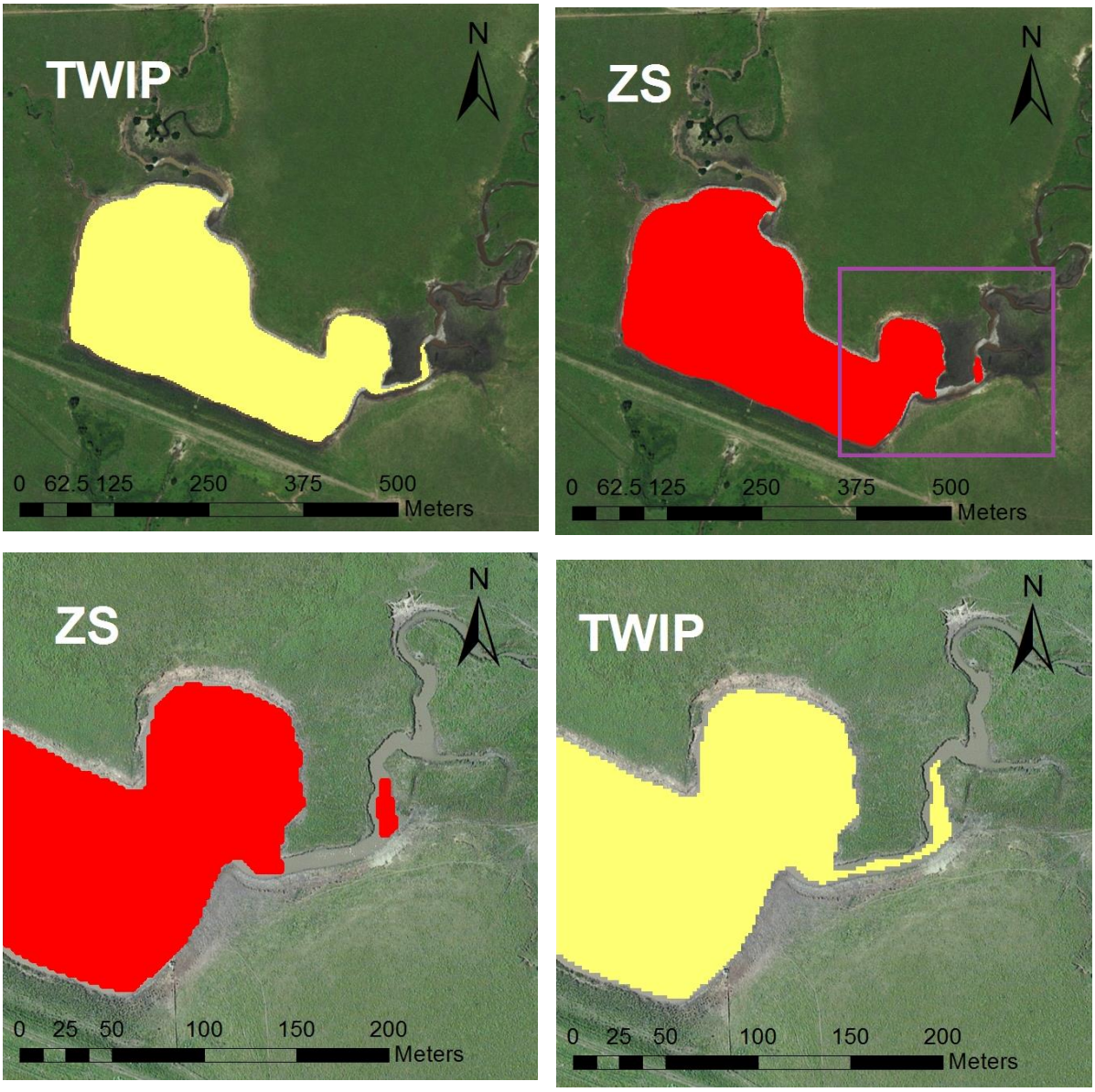

Narrow stretches of hydro-flattened cells connecting broader patches can lead to fragmentation in the ZS approach. In turn, intersecting TWIP features may result in more continuous geometries than the ZS approach.

Tables

Table 1: NHD Results

Reservoir	Area (km^2)	Ct	SA (km2)	NHD Only	% NHD Only	Ct/ km^2
Marion	535	584	1.4104	370	63.36	1.09
El Dorado	634	766	6.1141	320	41.78	1.21
Council Grove	677	1142	4.5877	728	63.75	1.69
Pomona	836	2290	5.7711	1730	75.55	2.74
Melvern	870	2048	6.6397	1423	69.48	2.35
Clinton	951	2828	10.2670	2039	72.10	2.97
Fall River	1434	2776	12.4129	2375	85.55	1.94
Toronto	1855	3943	16.0943	3482	88.31	2.13
Perry	2928	7694	31.1691	5523	71.78	2.63
John Redmond	6645	10861	37.5025	7073	65.12	1.63
Min	535	584	1.4104	320	41.78	1.09
Max	6645	10861	37.5025	7073	88.31	2.97
Mean	1736.5	3493.2	13.1969	2506.3	69.68	2.04

Includes drainage area sizes derived from 30 meter NED catchment delineation, NHD clipping, and intersecting results for ten selected reservoir drainages. Reservoirs and potentially connected water bodies were removed prior to calculations. Area represents drainage area in km^2; Ct is the number of NHD water body polygons with boundaries inside the drainage area; SA is the cumulative surface area of NHD features in km^2; NHD Only is the number of NHD features not intersecting TWIP or Zero Slope results; % NHD Only is the percentage of NHD features not intersecting TWIP or Zero Slope results; Ct/km^2 is the average count of NHD features per square kilometer drainage area.

Table 2: TWIP Results

Reservoir	Area (km^2)	Ct	Intrsct NHD	% NHD	Intrsct ZS	% ZS	New	% Inc NHD
Marion	535	210	187	32.71	210	90.60	23	3.94
El Dorado	634	439	414	55.87	438	94.19	25	3.26
Council Grove	677	417	401	35.64	416	97.88	16	1.40
Pomona	836	440	403	17.69	440	72.70	37	1.62
Melvern	870	420	393	19.29	419	63.69	27	1.32
Clinton	951	*	*	*	*	*	*	*
Fall River	1434	391	379	13.58	390	94.22	12	0.43
Toronto	1855	420	410	10.40	420	88.73	10	0.25
Perry	2928	**	**	**	**	**	**	**
John Redmond	6645	***	***	***	***	***	***	***
Min	535	210	187	10.40	210	63.69	10	0.25
Max	6645	440	414	55.87	440	97.88	37	3.94
Mean	1736.5	391	369.57	26.26	359	86.00	21.43	1.75

Table 2 shows the results of the TWIP procedure following removal of false positives, removal of the reservoir and potentially connected features, and results of intersection with the NHD and Zero Slope features. Area represents drainage area in km^2; Ct is the count of TWIP features produced for each drainage; Intrsct NHD is the number of TWIP features intersecting with NHD features; % NHD is the percentage of NHD features identified through the TWIP approach; Intrsct ZS is the number of TWIP features intersecting with ZS features; % ZS is the percentage of Zero Slope features identified through the TWIP approach; New is the number of TWIP features absent in the NHD data; % Inc NHD is the percentage of increase in NHD count should the New features be appended to the NHD.

*Execution of TWIP tool in the Clinton Reservoir drainage area resulted in water body identification for only the southwest portion.

**Data not obtained for Perry Reservoir due to failure of TWIP script.

***TWIP could not be carried out for John Redmond due to failure of required roads and railroads removal procedure.

Table 3: Zero Slope Results

Reservoir	Area (km^2)	Ct	Intrsct NHD	% NHD	Intrsct TWIP	% TWIP	New	% Inc NHD
Marion	535	234	211	36.64	212	100.00	23	3.94
El Dorado	634	465	439	58.22	444	99.77	26	3.39
Council Grove	677	425	409	36.16	416	99.76	16	1.40
Pomona	836	608	560	24.45	442	100.00	48	2.10
Melvern	870	661	627	30.52	421	99.76	34	1.66
Clinton	951	894	806	27.90	139	100.00	88	3.11
Fall River	1434	415	403	14.41	391	99.74	12	0.43
Toronto	1855	479	467	11.69	425	100.00	12	0.30
Perry	2928	2370	2194	28.22	*	*	176	2.29
John Redmond	6645	4019	3773	34.48	*	*	246	2.26
Min	535	234	211	11.69	139	99.74	12	0.30
Max	6645	4019	3773	58.22	444	100.00	246	3.94
Mean	1736.5	1057	988.9	30.31	361.25	99.88	68.1	2.09

Table 3 shows the results of the ZS procedure following removal of false positives, removal of the reservoir and potentially connected features, and results of intersection with the NHD and TWIP features. Area represents drainage area in km2; Ct is the count of ZS features produced for each drainage; Intrsct NHD is the number of ZS features intersecting with NHD features; % NHD is the percentage of NHD features identified through the ZS approach; Intrsct TWIP is the number of ZS features intersecting with TWIP features; % TWIP is the percentage of TWIP features identified through the ZS approach; New is the number of ZS features absent in the NHD data; % Inc NHD is the percentage of increase in NHD count should the New features be appended to the NHD.

* Data not obtained due to failure of TWIP script.

Table 4: Combined Dataset Results

Reservoir	Area (km^2)	Ct	New	% Inc NHD	% NHD	% TWIP	% ZS	NHD Div/Join
Marion	535	602	23	3.97	61.46	34.88	3.65	-5
El Dorado	634	780	27	3.56	41.03	56.28	2.96	-7
Council Grove	677	1152	16	1.41	63.19	36.20	0.61	-6
Pomona	836	2336	47	2.05	74.06	18.84	7.11	-1
Melvern	870	2083	33	1.61	68.31	20.16	11.52	2
Clinton	951	2930	88	3.09	69.59	4.74	25.67	17
Fall River	1434	2790	12	0.43	85.13	14.01	0.86	2
Toronto	1855	3957	11	0.28	88.00	10.61	1.39	3
Perry	2928	7893	176	2.29	69.97	0.00	30.03	23
John Redmond	6645	11092	246	2.27	63.77	0.00	36.23	-15
Min	535	602	11	0.28	41.03	0.00	0.61	-15
Max	6645	11092	246	3.97	88.00	56.28	36.23	23
Mean	1736.5	3561.5	67.9	2.10	68.45	19.57	11.98	1.3

Table 4 show the results of the final dataset. Area represents drainage area in km^2; Ct is the count of features; New is the number of features in the Combined dataset absent in the NHD; % Inc NHD is the percentage of increase in NHD count should the New features be appended to the NHD; % NHD is the percentage of the Combined count composed of NHD geometries; % TWIP is the percentage of Combined count composed of TWIP-derived geometries; % ZS is the percentage of Combined features composed of ZS-derived geometries; NHD Div/Join is the overall change in NHD count due to polygon division or joining resulting from TWIP or ZS geometries.

Table 5: Surface Area

Reservoir	Area (km^2)	Combined SA (km^2)	NHD SA (km^2)	Change in SA (km^2)	% Change in SA
Marion	535	2.0931	1.4104	0.6828	48.41
El Dorado	634	7.3882	6.1141	1.2741	20.84
Council Grove	677	5.0248	4.5877	0.4371	9.53
Pomona	836	6.1205	5.7711	0.3493	6.05
Melvern	870	7.3099	6.6397	0.6703	10.09
Clinton	951	10.7420	10.2670	0.4751	4.63
Fall River	1434	10.3923	12.4129	-2.0206	-16.28
Toronto	1855	13.7606	16.0943	-2.3337	-14.50
Perry	2928	35.1882	31.1691	4.0191	12.89
John Redmond	6645	38.2476	37.5025	0.7451	1.99
Minimum	535	2.0931	1.4104	-2.3337	-16.28
Maximum	6645	38.2476	37.5025	4.0191	48.41
Mean	1736.5	13.6267	13.1969	0.4298	8.37

Table 5 compares cumulative surface area between NHD datasets and Combined datasets. Area represents drainage area in km^2; Combined SA is the cumulative surface area of features included in the Combined dataset in km^2; NHD SA is the cumulative surface area of features included in the NHD dataset in km^2; Change in SA is the difference in cumulative surface area in km^2 after subtracting NHD SA from Combined SA; % Change in NHD SA is the increase or decrease in surface area of the Combined datasets relative to the NHD datasets ((Merged SA – NHD SA)/NHD SA)

Table 6: Accuracy Assessment Results

Statistics	NHD	TWIP	ZS
Index Mean	0.7922	0.9119	0.9111
Index Min	0.3064	0.7136	0.7084
Index Max	0.9677	0.9736	0.9742
Index Std dev	0.1544	0.0437	0.0459
Total SA (km^2)	556007	643478	638364
%Total Verified SA	82.00	94.90	94.14

Table 6 shows summary statistics for NHD, TWIP, and Zero Slope accuracy indices ranging from 0 – 1 and total surface area comparison with total Verified surface area. An index value approaching 0 indicates poor geometric and/or positional accuracy. An index approaching 1 indicates strong geometric and/or positional accuracy. Total SA presents cumulative surface area of sampled features in m^2; % Total Verified SA presents the percentage of cumulative Verified surface area resulting from the sum of sampled feature areas

Chapter III

Comparing Impoundment Abundance, Distribution, and Catchment Traits among Eastern Kansas Reservoir Drainages

Introduction

The decline of water resources is a global concern, with region-specific issues reflecting local geography and history of land use practices. Eastern Kansas is largely dependent on reservoirs for water services, reservoirs which are approaching the end of their usable lives as they infill with sediment. Current management strategies for imminent reservoir restoration focus dredging, which will require considerable costs and treats a symptom but fails to address the causes of reservoir sedimentation. Lack of natural lentic features and widespread agricultural land use have led to an abundance of artificial water bodies, which are also infilling and in the process potentially reducing rates of sedimentation in downstream reservoirs. Precise measurement of impoundment sediment sink effects and resulting reduction in downstream sediment load is challenging, particularly on the scale of a federal reservoir drainage in Kansas, but it is accepted that impoundments have the potential to serve as significant sinks of sediment. Using new high-resolution elevation data for the region, this study delineates catchments of upstream water bodies within infilling reservoir drainages of eastern Kansas. Additionally, erosion-related traits are characterized for subcatchment and unimpeded runoff areas to better describe potential sink services of upstream impoundments in connection with Kansas reservoir

sedimentation. The methods and results of this study provide an example of exploratory research into the relationship between upstream impoundments and reservoir sediment yields and provide a new resource for decision-making related to reservoir drainage management in Kansas.

Reservoir Fill Concerns in Kansas

As is this case with other declining resources, population growth and climate change have been identified as stressors in water resources loss, and Kansas is vulnerable to these effects due to the regional geography. Kansas has experienced a population increase of 164,000 people between 2000 and 2010 (U.S. Census Bureau, 2015), which represents an increased demand of nearly 1.8 Mm^3 of drinking water per year (Rahmani et al., 2017). Additionally, the region is dominated by cropland (43% statewide) with 47% of the land use within federal reservoir drainages constituting cropland (Homer et al., 2015). Cropland is considered a source of higher erosion potential and sediment runoff relative to other common land cover types such as woodland and grassland (Bedient et al., 2013). In terms of climate change, a significant consequence is increased weather extremes such as drought and flooding (Hurd et al., 1999; Miley et al., 2005; Rahmani et al., 2015). For regions where flooding and drought are inherent in weather patterns (i.e., the United States Midwest), more severe flooding and drought may lead to greater sedimentation in reservoirs and increased surface area evaporation, respectively. With the exception of playas and relatively few natural lakes, Kansas demonstrates a water resources infrastructure partially dependent on man-made reservoirs (Martinko et al., 2014), which experience disproportionately high amounts of infill during high flow events brought about by intense storms (Meade & Parker, 1985). With prolific agricultural land use, an increasing local

and global population, and a regional climate prone to drought and flooding events, Kansas may experience increased agricultural and municipal demand for water within a water resources infrastructure susceptible to climate-induced stress.

Much of Kansas relies on aging reservoirs for flood control and drinking water services, and as these water bodies reach the end of their usable lifetimes, restoration through dredging will require significant costs. Kansas has over 200 reservoirs, mostly state or federally owned, with surface areas exceeding 20 hectares (deNoyelles & Kastens, 2016; NHD, 2014). Eighty of these provide primary or backup drinking water for 60% of the state's population and provide flood control services, which was the primary purpose for construction of the state's 24 federal reservoirs (deNoyelles & Jakubauskas, 2008). The 24 federal reservoirs were constructed from 1948 to 1981, are estimated to hold more water than all the other state's water bodies combined, and were constructed with a usable life expectancy of 50 years (deNoyelles & Kastens, 2016). As these reservoirs approach the end of their usable lives, they lose storage capacity to sedimentation, shallow zones expand, and the relatively young and unstable biotic communities can shift towards excess cyanobacteria growth, which can be detrimental to water quality (deNoyelles & Jakubauskus, 2008). By 2030, the first three federal reservoirs in Kansas – Tuttle Creek, Toronto, and John Redmond – will reach 50% infilled, the approximate percentage at which functionalities are expected to be impaired, and will require restoration measures (deNoyelles & Kastens, 2016). If current fill rates remain constant, another 8 of the state's 24 federal reservoirs will be half in-filled by 2105, and 44% of the total storage will be lost for the combined 24 (deNoyelles & Kastens, 2016). As the state plans dredging action to recover reservoir capacity, projected costs are substantial. At a present-day cost of roughly $6 for removal of one cubic yard of sediment, restoring the 24 federal reservoirs to their original

volume by the end of the century would cost $13.8 billion (deNoyelles & Kastens, 2016). Furthermore, 1.4 million acres of one foot deep sediment would have to be disposed of, and costs and methods of disposal are difficult to ascertain (deNoyelles & Kastens, 2016). These estimates are based on current rates and costs, and they do not consider possible exacerbation induced by climate change. In turn, these projections can be considered conservative in terms of expenditures and fill rates.

Given the impending restoration costs to maintain the state's reservoir infrastructure, new management approaches and related research may be highly valuable if they help to prolong reservoir usability and reduce the need for restoration efforts. Dredging treats the symptom of reservoir sedimentation but is temporary, costly, and fails to address the source of the problem. Additionally, previous reservoir development has occurred in optimal locations for flood control and water supply, which makes choosing new sites in proximity challenging (Kondolf et al., 2014). Without constructing new reservoirs, constructional and operational modifications to increase storage or allow high sediment load bypass have been suggested (deNoyelles & Kastens, 2016). Redesigning reservoirs accordingly would likely extend usable lives of the reservoirs and has done so in the case of John Redmond (deNoyelles & Kastens, 2016) but does little to address the causes of sedimentation. Reservoir management may benefit from comprehensive characterization of reservoir drainages, which investigates the sources and processes of sedimentation. By better understanding contributing and mitigating factors of reservoir sediment yield on the scale of drainage area, management decisions may be better equipped to address causes of sedimentation instead of its consequences.

Kansas Landscape Factors Related to Erosion and Sedimentation

Erosion-related factors

Several landscape factors influence runoff and erosion potential, and in turn, can be determinate of sediment load. Streamflow is the main source of sediment for reservoirs, and higher rates of sedimentation correlate with drainage areas experiencing greater precipitation (Langbein & Schumm, 1958). Increased runoff results in greater discharge and sediment carrying capacity, and potential runoff and sediment load are largely dependent on drainage area, gradient, soil type and permeability, and land use (deNoyelles & Jakubauskus, 2008; Bedient et al., 2013). Bedient et al. (2013) describe the significance of these factors in runoff modeling: drainage area determines the volume of water generated by a precipitation event; watershed slope reflects the change in elevation with distance in an overland flow area and influences overland flow velocity; soil type determines infiltration rate and water-holding capacity of the landscape; and finally, land use and land cover have significant effects on watershed response by influencing overland flow velocity, infiltration, and susceptibility to erosion (Bedient et al., 2013). Under the "Rational Method" common in hydrological modeling, land cover types ranking from least to greatest runoff potential are as follows: woodland or forest, meadow or grassland, pasture or range land, cultivated land, and urban areas with increasing percent imperviousness (Bedient et al., 2013).

The landscape of Kansas reflects widespread land cover alteration and increased susceptibility to erosion relative to natural conditions due to agriculture. Euro-American settlement beginning 125 – 150 years ago spread intensive row crop production to the region, which accelerated erosion rates (deNoyelles & Kastens, 2016). Settlers found the nutrient rich

and highly erodible mollisols dominating the area highly favorable for crop production, and these soils have since provided the source material for overland eroded sediment. In recent decades, more conservative agricultural practices have been implemented in the Midwest (e.g., cropland terracing and no-till farming). However, erosion rates greater than pre-settlement conditions remain, and agriculture persists as the major land cover of Kansas. Presently, 43% of the land cover of Kansas is cropland, and of the non-agricultural land cover, warm season grasses compose the majority of the undeveloped land or 34.78% of the state, cool season grasses occupy 7.16%, Conservation Reserve Programs (primarily grasses) 5.38%, woodlands 4.07%, and urban areas cover 1.73% (Peterson et al., 2010).

Catchment areas for reservoirs in Kansas experience the greatest land cover variation in terms of grassland and agriculture. While Tuttle Creek's catchment area is composed of 24.4% grassland and 70.5% cropland, Fall River Reservoir's contains 86.5% grassland and 4.7% cropland (Martinko et al., 2014). Woodland cover ranges from 0.4% of the catchment area for Kanapolis Reservoir to 18.6% for Clinton Reservoir (Martinko et al., 2014). Urban land use is minimal in all reservoir catchments and shows the least variation among reservoirs included in the Kansas Atlas of Lakes (Martinko et al., 2014). Given that precipitation rates are highest in the eastern third of the state, it is unsurprising that surface runoff-derived erosion tends to be greatest in that region (Peterson et al., 2010). Considering the range of grassland and cropland coverage among reservoir catchment areas, erosion rates and sediment loads likely vary among eastern Kansas catchments in response to land use differences.

Human-engineered fluvial systems have further altered erosion processes. Prior to Euro-American settlement, Kansas watersheds were dominated by native grasslands, and riparian vegetation effectively stabilized soil and slowed runoff (deNoyelles & Kastens, 2016). Drainage

modifications have been implemented in the form of straightened stream channels and constructed bank levees. While the purpose for these modifications is founded on channel position stabilization and local flooding mitigation, the changes have resulted in "high water flows, reduced residence time, increased in-channel erosion, and increased sediment carrying capacity compared to pre-European settlement conditions" (deNoyelles & Kastens, 2016). Research has indicated that the majority of sediment currently infilling reservoirs originated from channel-bank sources (Juracek & Zeigler, 2007).

Impoundments as sinks

Small impoundments have been recognized as significant sinks for sediment and related particulates, but are not well understood in connection to large reservoir sedimentation reduction. Dams have been described as "significant features of every river and watershed of the nation" (Gaff, 1999). While the effects of sediment and particulate trapping in impounded rivers is well documented (Trimble and Bube, 1990; Meade, 1990), the effects of upstream sediment trapping by smaller impoundments have often been overlooked (Mulholland & Elwood, 1982; Stallard, 1998; Smith et al., 2001; Smith et al., 2002). Of the few studies estimating cumulative sediment yield of smaller impounded features (surface area < 1 ha) in the conterminous United States, water feature density-based modeling has suggested annual sediment yield of small impoundments to be comparable to large reservoirs (Smith et al., 2002; Renwick et al., 2005). Two thirds of annual sediment loads are believed to be deposited in lentic systems (Smith et al., 2001), and Smith et al. (2002) thought this accumulation to be split fairly evenly between small and large water bodies. In a similar study by Renwick et al. (2005), three separate density-based models were employed to compare sedimentation of small and large artificial lentic bodies in the United States. Findings from the study estimate 25% of total sheet and rill erosion settling in

small impoundments, capturing 21% of the total watershed areas for the subcontinental United States, and total sedimentation for small impoundments range from 0.43 – 1.78 x $10^9 m^3 yr^{-1}$, potentially matching or exceeding estimated total reservoir accumulation of 1.67 x $10^9 m^3 yr^{-1}$ (Renwick et al., 2005). This wide range in small impoundment sediment yield estimates is due to limitations in data resolution and processing resources inherent in a large area of interest with minute features as the focus. Due to these caveats, these studies rely on water body density without precise subcatchment delineations and largely omit landscape variables related to erosion potential.

At a smaller scale, impoundment size and positioning have been recognized as significant factors influencing downstream reservoir nutrient loads. Impoundments are considered most effective at reducing total phosphorus and nitrogen transport when positioned at the mouth of the river or in nutrient source areas, and multiple small impoundments may result in a greater reduction in suspended nutrient load than a single large reservoir (Bosch, 2008). Small impoundments have also been observed trapping disproportionate amounts of organic carbon within a drainage area (Downing et al., 2008). The high burial rates of nutrients and organic carbon occurring in small impoundments have been attributed to heavier sedimentation and sediment aggregate transport relative to large reservoirs, the tendency for rapid vertical accretion, and frequent adjacency to human and agricultural sources of nutrient loading (Downing et al., 2008; Smith et al., 2002; Bosch, 2008). In a region with widespread agriculture, a dependence on man-made reservoirs, and an abundance of farm ponds, small impoundments likely play a role in regulating reservoir infill and nutrient overloading occurrence.

Kansas exemplifies the agricultural industry's tendency towards constructing small impoundments. In the United States, portions of the Midwest have both the smallest mean

surface areas and highest densities of impoundments due to agricultural water supply purposes, and the eastern portion of the Great Plains exhibits the greatest water body abundance (Smith et al., 2002). Kansas alone boasts over 200,000 impoundments under 40 hectares, most with surface areas less than or equal to one acre, which combined cover approximately 288 square miles and store an estimated 1,299,000 acre/feet of water (NHD, 2016; Huggins et al., 2011; Callihan, 2013). The density gradient of small impoundments as estimated by Smith and others (2002) ranges from less than 0.03 impoundments per km^2 in western portions of the state to an average of 1-3 water bodies per km^2 in the eastern third. The greater occurrence of impoundments in eastern Kansas is owed to its higher precipitation and greater surface flows, while the semi-arid western part of the state relies largely on subsurface water (deNoyelles & Kastens, 2016). Research quantifying the sediment yields of Kansas's small impoundments is limited (e.g., Foster, 2011), but their abundance and ties to the agricultural industry suggest significant sediment trapping potential in eastern Kansas and favorable placement for intercepting agriculture-derived nutrients.

For a state with natural lentic systems limited to ephemeral playas predominately in western Kansas and relatively few oxbow and sinkhole lakes statewide (Martinko et al., 2014), extensive impoundment construction has substantially altered hydrological and physical processes. The majority of sediment currently depositing in Kansas reservoirs is believed to originate from channel-bank eroded material (Juracek & Zeigler, 2007). Impoundments, which are placed in the path of channel-bank eroded material, often proximal to agricultural sources of nutrient unloading, and densely distributed in eastern Kansas, are relatively understudied on a reservoir catchment scale and may be important mitigators of Kansas reservoir sedimentation and nutrient overloading. Furthermore, small impoundments have been increasing an average of

1-3% annually in Kansas since the 1930s (Callihan, 2013). As their abundance increases and they garner recognition as sinks of sediment and nutrients, better characterizing their influence on downstream reservoir infill could be valuable to reservoir and drainage management.

Obstacles to incorporating small water features into reservoir drainage modeling

Various erosion models have been applied to study areas comparable to reservoir drainages, but integration of small impoundment sink effects has been largely neglected. The Universal Soil Loss Equation (USLE) set the precedent in incorporating soil erodibility, slope length, slope steepness, cover management, and rainfall runoff erosivity into a relatively simple and widely used model to predict average annual soil runoff (Wischmeier & Smith, 1978). Many models employing similar parameters have been developed since (e.g., Renard et al., 1991; Flanagan & Nearing, 1995; Arnold et al., 1998; Morgan et al., 1998). However, these models target rill and interrill erosion and do not account for gulley and channel erosion (Lim et al., 2005). In turn, model emphasis on overland erosion has resulted in small impoundment sink effects being ignored in most regional sediment yield studies. This neglect may be partially attributed to data limitations and the potentially time-consuming geoprocessing required should sufficiently high resolution data be available to address small impoundment catchment. For example, studies using the revised USLE or similar models often use a flow accumulation algorithm or tool to calculate the slope length factor (Jain & Kothyari, 2000; Fernandez et al., 2003; Lim et al., 2005). Should the study extent remain constant but elevation data pixel size be reduced to accurately delineate small impoundment drainages, flow accumulation calculation time may substantially increase, and total geoprocessing time would be compounded if the model

were iterated for each water feature within the study area. Additionally, other parameter data would need to match the resolution of the elevation data, which may require resampling or conversion and in turn reduced accuracy. Furthermore, water body datasets have historically underestimated small features (e.g., Smith et al., 2002; Buddemeier, 2004; Renwick et al., 2005), which limits accuracy of total cumulative impoundment sediment trapping estimates.

Due to lack of data, insufficient resolution, or limited geoprocessing resources, studies of small impoundment sedimentation in the conterminous United States have opted for density-based sedimentation yield estimation of sub regions and extrapolation via simpler models (Smith et al., 2002; Renwick et al., 2005). When estimating annual small impoundment sediment yield for the conterminous United States, projections by Renwick and others (2005) varied from 0.43 – 1.78 x $10^9 m^3 yr^{-1}$, reflecting the difficulty of measuring large–scale accumulation with exactness.

Beyond data quality and geoprocessing, an additional encumbrance to measuring small impoundment sediment trapping on a regional scale lies in the complexity of trap efficiency models and their bias towards larger water features. Trap efficiency (TE) is the proportion of inflowing sediment that is deposited in a lentic feature (Verstraeten & Poesen, 2000). Various empirical models have been developed centering TE estimation around a capacity–to–watershed ratio, capacity–to–annual–inflow ratio, or a sedimentation index (Bowen, 1943; Churchill, 1948; Brune, 1953; Heinemann, 1981). These models differ in index values and source data, but all derive TE from characteristics of inflowing sediment and retention time, which are controlled by pond geometry and various runoff variables (Verstraeten & Poesen, 2000). Empirical TE models have been based on limited data for large reservoirs in select areas, and in turn, TE curves can be misleading if used for small features with runoff traits differing from those developed for large reservoirs (Chen, 1975; Verstraeten & Poesen, 2000). While theoretical models have been

suggested to be more applicable for TE modeling of small impoundments, they often require detailed data on water feature and runoff traits (e.g., in- and out-flowing discharge), which is often lacking (Verstraeten & Poesen, 2000). Additionally, estimating cumulative sediment trapping in multiply–impounded stretches is further complicated by dynamic sediment particle size distribution. Sediments having passed through an impoundment are finer and less likely to deposit in the next impoundment, resulting in reduced TE by downstream impoundments (Churchill, 1948).

Trap efficiency of small impoundments is more unstable and sensitive to deposition and discharge fluctuation than larger water features, adding further difficulty to small impoundment sedimentation modeling. Farm ponds are expected to infill more rapidly than large reservoirs due to lower capacity–to–catchment–area ratios (Verstraeten & Poesen, 2000). This results in shorter usable lives in small impoundments. While age and percentage infilled may be well known for large reservoirs in Kansas (e.g., Martinko et al., 2014), similar information for small impoundments is not as well understood for the region. Additionally, records of dredging or restoration efforts conducted by private landowners are absent in regional water body inventories. As impoundments infill, they lose capacity, trap efficiency lessens, and impoundments revert to "pass through" systems similar to pre-impoundment conditions (deNoyelles & Kastens, 2016). The 50% infill benchmark for large reservoirs is not as determinate of functionality loss for small impoundments, since small impoundment response to suspended sediment is more sensitive to variation in discharge. Just as yearly precipitation patterns are dynamic, small impoundments may oscillate among sediment trapping, pass through, and flushing based on discharge intensity and frequency. Foster (2011), for example, found storm intervals determinate of sediment deposition trends in small impoundments in Kansas.

Suspended sediment loads in Kansas are comprised mostly of silts and clays, which require longer suspension times for deposition, and in cases of short intervals between storm events, small impoundments can experience significant flushing due to residence times too brief for deposition (Foster, 2011). The varying response of impoundments to inflowing sediment and lack of current infill knowledge make quantifying their influence on downstream sediment yield tenuous, and pursuit of descriptive research regarding their relationship on reservoir sedimentation may be more practical than quantitative modeling.

Possibly the most conspicuous caveat surrounding small impoundment regional modeling, is that their gross abundance makes sedimentation modeling especially challenging. Field surveying and validation of water body and drainage details necessary for most erosion and TE models is currently unfeasible on the scale of major Kansas reservoir drainages and their associated small impoundments. While sampling and interpolation using simple models have been somewhat successful (e.g., Smith et al, 2002), accuracy is lost when applied at other regions or scales. Furthermore, newly constructed or infilled impoundments can alter the distribution yearly, making aggregative modeling even more haphazard.

Impoundments have been shown to be significant sinks of sediment within watersheds (e.g., Smith et al, 2002; Renwick et al., 2005; Foster, 2011), but accounting for their collective influence on downstream sediment yields is challenging due to their dynamic response to inflowing sediment, the complex and large reservoir-oriented nature of most models, and various data limitations. However, a few traits fundamental to erosion and trap efficiency modeling can be characterized for impoundments and corresponding drainages. Capacity–to–catchment–area measurement has been the center of most trap efficiency models, and using surface area to represent capacity has been done in the past (i.e., Camp, 1946). With high resolution elevation

data, comprehensive small water body data, and novel processing and analysis methods, capacity to catchment area can be characterized for small impoundments within reservoir drainages. Furthermore, erosion-related traits of land use, soil type, and gradient can be calculated for small impoundment catchment areas. Characterizing key erosive and trap efficiency traits within a selected Kansas reservoir drainage in the context of subcatchment versus "direct" runoff can provide insight into potential reservoir infill mitigation attributed to upstream impoundments and an exploratory example in small impoundment sedimentation research.

High Resolution Subcatchment Delineation and Data Availability for Kansas

Use of LiDAR-derived digital elevation data in drainage delineation has been shown to increase accuracy in minor water feature catchment delineation relative to traditional elevation data (Liu et al., 2005). Light detection and ranging (LiDAR) elevation is collected via laser pulses dispersed from LiDAR-equipped aircraft. As the reflected pulses return to their source, the data are collected in a raw point cloud composed of multiple pulses per square meter of land, and elevation data points are determined from return time and data recorded in unison with GPS data (Heidemann, 2014). Vendors then process the raw LiDAR data and convert it to digital elevation models (DEMs), an efficient means to represent ground surface and a useful tool from which to extract hydrologic features within a geographic information system (GIS). Common horizontal resolutions of LiDAR-derived DEMs include 1 and 2 meters. This enhanced spatial resolution allows a new precision for hydrological modeling and has initiated various hydrographic network studies (Liu et al., 2005 Colson et al., 2006; Jones et al., 2008; Li and Wong, 2010; Petroselli, 2012; Tang et al., 2014). Noteworthy among these, Liu et al. (2005)

demonstrated LiDAR-derived DEMs' superior accuracy in delineation and extraction of subcatchments relative to commonly used 20-meter resolution elevation data. While improved detail of small-scale features may be expected with the improved resolution offered by LiDAR, Petroselli (2012) also found LiDAR-derived elevation data to be preferable for hydrogeomorphic characterization on a basin scale, providing more detail than commonly used 20 – 30-meter DEMs. In western Kansas, Kastens et al. (2016) developed automated methods for playa identification and delineation of playa catchments using 2-meter resolution DEMs, tasks previously impossible without sufficiently high-resolution elevation data.

High resolution elevation data are now available for Kansas and can be applied towards subcatchment delineation of impoundments within reservoir drainages. The LiDAR Implementation Plan beginning in 2011 led to production of 2-meter LiDAR-derived DEM mosaics collectively covering the entirety of Kansas (completed 2016). By using these elevation data and applying methods such as those demonstrated by Kastens et al. (2016), subcatchments from small impoundments within infilling reservoir drainages can be delineated with adequate detail. As high-resolution elevation data have only become available for most reservoir drainages within the past few years, a major study characterizing and comparing subcatchment traits among reservoirs has yet to be conducted.

Project Summary

Reservoir sedimentation is an imminent concern for Kansas, with most federal reservoirs expected to reach or approach the end of their usable lives by the end of the century. Current management strategies are costly and address the symptoms but do little to address the causes of

infill. Most sediment yield modeling incorporates overland erosion-related factors such as land use, soil characteristics, and gradient, but fails to account for small impoundment sediment trapping, which has the potential to capture sediment from both overland and channel-bank sources. The landscape of Kansas is one of widespread agricultural land use and significant manipulation of hydrological systems reflected by an abundance of small impoundments. It is accepted that impoundments have the potential to be significant sinks for sediment, but their relationship with downstream reservoir sediment yield in Kansas is not well understood. While there are many issues in quantifying sediment yields of small impoundments on a regional or reservoir drainage scale, characterizing impoundment distribution and subcatchment traits tied to erosion potential may provide new insight into the influences of impoundments on downstream reservoir sedimentation in Kansas. LiDAR-derived DEMs offer the means to delineate small impoundment catchments and investigate a little studied dynamic of reservoir infill rates for the region. A detailed characterization of impoundment distribution, subcatchment traits, and possible influences on reservoir sediment yields will contribute to the body of research surrounding reservoir infill for the region and could provide useful information for reservoir and reservoir watershed management decisions.

This research uses high-resolution LiDAR-derived elevation data to delineate subcatchment areas attributed to upstream water bodies within 9 Kansas reservoir drainages and calculates fundamental traits related to erosion and sediment trapping within the context of subcatchment and direct runoff areas. The primary objectives of this chapter are to: 1) Summarize water body distribution, water body catchment areas, and surface–area–to–catchment–area ratios for select reservoir drainages, 2) Delineate and characterize subcatchment and unimpeded runoff areas in terms of land use, soil traits, and gradient for select reservoir

drainages, 3) Compare the results of objectives 1 and 2 among reservoir drainages to investigate potential influences of upstream water bodies on downstream reservoir sediment yield. In doing so, this project addresses the questions: "How might the potential sink services of impoundments be studied by delineating and characterizing impoundment catchments?" and "How might small impoundment sink effects differ among Kansas reservoirs in connection to downstream sediment yield?"

Methods

Study Area & Data Sources

Reservoir drainages selected for this study include Perry, Clinton, Pomona, Council Grove, Melvern, Marion, El Dorado, Toronto, and Fall River (Figure 1). Drainages were selected in part due to their common precipitation patterns, which reduces the likelihood of precipitation differences influencing sediment yield rates among drainages. With the exception of portions of the Perry, Melvern, and Toronto drainages, all drainages have annual precipitation rates of 850-1000 mm (Figure 2). Reservoir catchments cover portions of the following 20 counties: Atchison, Butler, Brown, Chase, Coffey, Douglass, Elk, Greenwood, Harvey, Jackson, Jefferson, Lyon, Marion, McPherson, Morris, Nemaha, Osage, Shawnee, Wabaunsee, and Woodson. Perry and Clinton reside in the Lower Republican basin; Pomona & Melvern in the Marias Des Cygnes basin; Marion and Council Grove in the Neosho basin; Fall River and Toronto in the Verdigris basin; and El Dorado in the Walnut River basin.

Reservoirs selection was conducted to purposefully form a sample group with a range of drainage sizes, capacities, and sedimentation rates. By doing so, findings may be relatable to

many regional reservoirs and not to select categories (e.g., reservoirs projected to infill rapidly or much more slowly). Reservoir drainage size, age, capacity, percentage infill, and specific sediment yield are displayed in Table 1. Drainages range from 535 km^2 (Marion) to 29,928 km^2 (Perry) and have a mean size of 1,191 km^2. Ages range from 69 years (Fall River) to 38 years (El Dorado), and the average age is 51 years. Original capacities range from 34 million m^3 (Toronto) to 300 million m^3 Perry, and percentage infill as of 2015 ranges from 3.6% (Melvern) to 43.4% (Toronto). Annual specific sediment yields, cubic meters of sediment per km^2 drainage area, range from 135 (Fall River) to 487 (Pomona) with an average of 306 $m^3km^2yr^{-1}$.

Drainage water body datasets were produced as described in Chapter 2 (Combined dataset). 30-year normals precipitation data was retrieved from the PRISM Climate Group of Oregon State University. Road and railroad datasets were retrieved from the Kansas Data Access & Support Center (DASC), including the 2002 KDOT non-state road system shapefile produced by the Kansas Department of Transportation, the TIGER 2014 center-line roads shapefile produced by the U.S. Census Bureau, and the TIGER 2010 railroads shapefile produced by the U.S. Census Bureau. Additionally, 30-meter DEM tiles from the USGS National Elevation Dataset (NED) were retrieved from DASC. LiDAR-derived 2-meter DEMs were provided by faculty at the Kansas Biological Survey, a research center affiliated with the University of Kansas. DEM tiles were produced from 2010 – 2016 by separate vendors under the 2011 LiDAR Implementation Plan. 30-m 2005 Land Cover Patterns data were obtained from the Kansas Applied Remote Sensing Program of the Kansas Biological Survey. Gridded Soil Survey Geographic Data were retrieved from the USDA NRCS. Geoprocessing was conducted using ESRI ArcGIS, scripting and tool packages were coded in Python, and spreadsheet and statistical analysis was conducted in Microsoft Excel.

Preliminary Processing

Drainage delineation methods, drainage elevation data extraction, and 2-m DEM preliminary processing are detailed in Chapter 2. Road and railroad removal has been found necessary for accurate catchment delineation of minor water bodies by previous studies (Poppenga et al., 2010; Kastens et al., 2016). Poppenga et al. (2010), for example, found that without removing roads from high resolution DEMs, "the filling of depressions to create continuous surface flow can cause the flow to spill over an obstruction in the wrong direction." To avoid such occurrences, roads and railroads were removed following procedures in Kastens et al. (2016), which are detailed in Chapter 2.

Water Body Size Distribution and Catchment Calculations

Water features from the Combined dataset of Chapter 2 were grouped according to size and counted for each drainage. Size categories include less than 0.05 ha, 0.05 – 0.2 ha, 0.2 – 0.5 ha, 0.5 – 1 ha, and greater than 1 ha. Percentages for each size class were determined based on count, and summary statistics were calculated for impoundment size distribution comparison among reservoirs.

Water bodies from the Combined datasets served as pour points for subcatchment delineation in reservoir drainages (Figure 3). Water body catchments were converted to polygons for area calculation. Converting catchment raster data to polygon format can result in fragmentation (Figure 7). To account for this, water feature catchment area was calculated by summing all catchment polygons generated from the same raster value (water body FID number). These catchment size measurements were added as a new attribute in the water body

dataset and titled “CA”. Water body surface–area–to–catchment–area ratios were then calculated using CA values. The CA and surface–area–to–catchment–area ratios ratio calculations tool is documented in the Appendix.

Erosion-related Landscape Traits

Land use and soil data were extracted for subcatchment area and unimpeded flow area through similar procedures (Figures 4 & 5). 30-meter land use raster data from KARS and 10-meter SSURGO data were clipped to drainage extent and resampled to match the cell size of the DEM used for subcatchment delineation (2 meters). Catchments were dissolved into a single feature to extract erosion-related traits for cumulative drainage subcatchment. Land use and soil data were extracted using subcatchment area masks, and the raster calculator was used to extract data for drainage area not included in the subcatchment (direct runoff area). Land use attribute tables for subcatchment, direct runoff area, and the entire reservoir drainage were imported into Excel for percentage calculations and comparison among drainages. Soil erosion class and runoff information were incorporated into soil attribute tables by joining the component table from SSURGO. Soil attribute information for subcatchment, direct runoff, and drainage areas was imported into Excel for percentage calculations and comparison among reservoir drainages.

The procedure for obtaining slope summary statistics is represented in Figure 6. Slope cell values were calculated from a filled DEM following road and railroad removal. To include only the overland gradient, all pixels with a slope value of zero (hydro-flattened) were removed. Zonal statistics were calculated using subcatchment, direct runoff area, and drainage area as

zones. Results for the three categories were imported into Excel for comparison among reservoir drainages.

Results

Individual drainage summaries

Results per reservoir drainage are summarized in Figures 8 – 16. Section A provides a visualization of subcatchment coverage, which is shaded in purple, and lists the percentage of drainage area covered by subcatchment as well as the number of impoundments inventoried. As percentage subcatchment increases, the portion of drainage runoff passing through impoundments increases. In turn, higher subcatchment percentages indicate higher percentages of runoff passing through impoundments and potentially releasing sediment.

Section B shows land use distribution in pie charts for the reservoir drainage, direct runoff area, and subcatchment. Percentage values are displayed within the figures for the most abundant land use types (typically grassland and cultivated cropland), and as urban, other, and occasionally woodland occurred in minute percentages, those percentages can be found above each chart. Land use resulting in least to greatest runoff potential are as follows: woodland, grassland, cultivated cropland, and urban (Bedient et al., 2013).

Section C includes drainage area, specific sediment yield, subcatchment area, and impoundment density information. Drainage area is provided in km^2. Sediment yield from Rahmani et al. (2017) is listed in cubic meters per km^2 per year. Subcatchment area ("Subcatch") is listed in km^2. Percentage subcatchment (%Subcatch) and number of impoundments (Ct) are

also listed, followed by impoundment density (Density), and number of impoundments per km^2 of drainage area.

Section D displays impoundment size distribution for the drainage by count and percentage. Size classes include less than 0.05 ha, 0.05 – 0.2 ha, 0.2 – 0.5 ha, 0.5 – 1 ha, and greater than 1 ha. Percentage is calculated from the total number (Ct) of impoundments in the drainage.

Section E summarizes impoundment catchment sizes and water body surface–area–to–catchment–area ratios. Catchment size results are listed in ha with a median value provided to represent central tendency. Average surface–area–to–catchment–area ratio is taken from the median ratio value.

Combined results

Water body surface area distributions, cumulative water surface areas, and impoundment density for select reservoir drainages are displayed in Table 2. 24,523 water bodies in total were included in the analysis. Of all surface areas analyzed, 15.24 % are under 1/20 ha, 60.27% under 1/5 ha, and 85.32 % under 1/2 ha. The greatest portion of features were within the 1/20 -1/5 ha size class (45.03%). 8.60% of features constituted the 1/2 – 1 ha group, and 6.09% of surface areas exceeded 1 ha. Densities ranged from 1.13 impoundments per km2 (Marion) to 3.08 per km^2 (Clinton), with an overall density of 2.29 per km^2.

Water body catchment summary statistics are shown in Table 3, water body surface–area–to–catchment–area ratio results are shown in Table 4, and percentage subcatchment is included in Table 5. Median catchment size for all catchments is 4.55 ha, and catchment sizes range from 0.005 ha – 11273 ha. The combined area of the catchments for all nine drainages is

394,846 ha or 3,948 km^2. Median surface–area–to–catchment–area ranged from 1:23.7 (Perry) to 1:43.3 (Marion), with an overall average of 1:26.3. Highest ratios were due to National Hydrography Dataset (NHD) source material. These water bodies were not derived from elevation data, so polygon contours do not adhere to the DEM cells comprising catchment areas, and pour points could be off center in the DEM. As a result, it was possible for surface–area–to–catchment–area ratio to exceed 1.00. Furthermore, water features may have filled in since NHD completion, which can result in the delineated catchment simply covering the area of the false water body (Figure 17). All ratios exceeding 0.90 were produced from NHD source data with the single exception of a Zero Slope-derived water body. In terms of cumulative catchment, drainage subcatchment coverage ranged from 26.22% (Council Grove) to 58.72% (El Dorado), with combined subcatchments covering 36.83% of the total study area.

Land use percentages for drainages, subcatchments, and direct runoff areas are provided in Table 6. Water coverage was excluded in percentage calculations. Urban, cultivated cropland, grassland, woodland, and "other" (bare rock, sand and gravel pits, and sandbars) land use classifications are included.

Soil erosion class and runoff category percentages for drainages, subcatchments, and direct runoff areas are provided in Tables 7 and 8. Soil erosion classes found in this study area include Class 1, Class 2, and areas of deposition. Class 1 are soils considered to have lost less than 25% of the original A and/or E horizons, Class 2 are soils considered to have lost 25 – 75% of the original A and/or E horizons, and deposition areas are areas where deposition currently exceeds erosion (SSURGO). Runoff is the loss of water from an area by overland flow. Runoff categories range from negligible to very high based on soil permeability and topography. Negligible runoff areas include concave areas, which are assumed not to produce runoff

(SSURGO). Data for both soil traits were unavailable for large portions of several drainages, and percentage area without soil data is included under “NoData”.

Slope summary statistics for drainages, subcatchments, and direct runoff areas are provided in Table 8. Values are listed in degrees. Mean slope for drainages ranges from 1.56° (El Dorado) to 4.01° (Perry). With the exception of Marion reservoir, where subcatchment and direct runoff slope averages are equal, all drainages have lower average slope in subcatchments than in direct runoff areas.

Discussion

Similarities and differences in erosion-related traits

The reservoirs and sedimentation index used in this study were purposefully selected to limit potential variables responsible for reservoir sedimentation differences. By selecting reservoir drainages with similar precipitation patterns (Figure 2), differences in precipitation can be relatively overlooked when considering the factors responsible for the contrasting sedimentation rates. Using a per unit drainage area sedimentation index – specific sediment yield – as opposed to other reservoir-specific measurements of sedimentation (e.g., percentage infilled), allowed this study to be drainage-oriented in its analysis of factors responsible for sedimentation and to avoid including reservoir specific traits. Specific sediment yield serves as a dependent variable that results entirely from drainage traits and is independent of reservoir traits (i.e., original capacity and age), which allowed for a more limited set of factors in the comparison of sedimentation variables.

Certain reservoir drainages with similar specific sediment yields are found to share common landscape traits. For example, the four reservoirs having the lowest yields – Fall River, Toronto, Melvern, and Marion – have the highest percentages of negligible soil runoff, and Fall River has both the lowest sediment yield (135 $m^3km^2yr^{-1}$) and highest negligible runoff percentage (41.36%). This indicates that these drainages have large portions of area where overland flow velocity slows or travels at a rate unconducive to topsoil erosion. Conversely, the two drainages with the highest sediment yields, Clinton and Pomona, contain large percentages of medium, high, and very high runoff areas, and each have less than 5% negligible runoff. Pomona, which has the highest specific sediment yield (487 $m^3km^2yr^{-1}$), also has the lowest percentage of water bodies over 1 ha (3.0%) and over 1/2 ha (8.9%). Clinton has the second lowest percentage of water bodies over 1/2 ha (11.7%). On the other hand, the Fall River drainage has the lowest percentage of water bodies under 1/20 ha (< 10%). Since trap efficiency is related to capacity, having lower percentages of large water bodies may reflect reduced occurrence of efficient sediment sinks, while an abundance of larger water bodies provides more opportunities to effectively trap sediment.

Land use in the Pomona and Clinton drainages is 27% cropland and 17.4% cropland, respectively, while the Fall River drainage has the lowest percentage of cropland (< 5%). Toronto, which has the second lowest sediment yield (140 $m^3km^2yr^{-1}$) also has a relatively low percentage of cropland in its drainage (7.5%). In turn, Fall River and Toronto receive less eroded material attributed to agriculture than Pomona and Clinton. Additionally, Fall River and Toronto both have high percentages of subcatchment, 41.4% and 39.5%, while Pomona has the third lowest at 28.4%. This indicates a greater proportion of drainage runoff passing through impoundments and potentially releasing sediment in the Fall River and Toronto drainages.

However, the highest percentage of subcatchment is in the El Dorado drainage (58.7%), which also has the third highest sediment yield (410 $m^3km^2yr^{-1}$). Furthermore, the El Dorado drainage is predominately grassland with less than 6% agriculture and has the highest percentage of large water bodies and lowest percentage of small water bodies of all drainages – more than 36% over 1/2 ha and less than 3% under 1/20 ha. When looking for potential causes for the drainage's high sediment yield, two traits draw attention. First, the El Dorado drainage has the lowest percentage of depositional area of all the drainages. This suggests that very little eroded material is settling in the landscape. Second, El Dorado has the second smallest drainage area and exhibits a relatively rounded shape. Larger, more elongated drainages tend to have a higher sediment delivery ratio, portion of the total erosion in a drainage making it to the reservoir (Walling, 1983). Essentially, if sediment has further to travel to reach the reservoir, it is more likely to deposit elsewhere before reaching the reservoir. For example, the Melvern drainage is 15.3% cropland and 27.5% subcatchment, yet is has the third lowest specific sediment yield (182 $m^3km^2yr^{-1}$). A reason for this low yield may be that the drainage shape is protracted, and sediment in certain areas would have to travel over 40 km to reach the reservoir. In effect, the El Dorado drainage has fewer areas suitable for deposition, a shorter distance for sediment to travel, and is likely experiencing a higher delivery ratio.

When looking at the remaining reservoir drainages and their sediment yields – Marion (243 $m^3km^2yr^{-1-}$), Council Grove (341 $m^3km^2yr^{-1-}$), and Perry (384 $m^3km^2yr^{-1-}$) – all three have lower than average subcatchment coverage and substantial cultivated agriculture. Marion has 34.5% subcatchment, Council Grove 26.2%t, and Perry 34.6%. The Perry drainage, which has the fourth highest sediment yield, is 32% cropland and has the highest percentage of water bodies under 1/20 ha (21.4%). This may indicate a large portion of sediment originating from

agricultural sources and an abundance of impoundments with small capacities and potentially low trap efficiencies. The Council Grove drainage is 28.2% cropland and has the lowest subcatchment coverage (26.2%), which suggests that there are fewer instances of runoff passing through impoundments and potentially depositing eroded material relative to all other drainages. Finally, the Marion drainage has the highest percentage of cropland (52.5%), relatively average subcatchment coverage, and lowest density of impoundments (1.13 per km^2), yet it has the fourth lowest sediment yield. Possible reasons for its lower than expected yield include its percentage deposition area and impoundment size distribution. 24.4% of its drainage is classified as depositional area, the second highest after Perry (40.7%). However, unlike Perry, fewer than 10% of impoundments in Marion's drainage are less than 1/20 ha and over 52% are greater than 1/5 ha. El Dorado is the only drainage with a greater percentage of large impoundments. In effect, the larger water bodies in Marion's drainage may be offsetting reservoir sediment yield through more effective sediment trapping relative to most other drainages.

Cumulative data, subcatchment, and direct runoff area trends

Of the 24,523 impoundments included in the analysis, over 60% are under 1/5 ha in surface area, and over 85% are under 1/2 ha. This size distribution highlights the region's tendency towards small impoundment construction. Drainage densities of 1.13 – 3.08 per km^2 support previous estimates (Smith et al., 2002) and represent some of the highest impoundment densities in the conterminous United States. Smith et al. (2002) estimated small impoundment catchments to be less than 1 km^2 on average for the region. This estimation can be considered conservative when compared to the median catchment area of 0.05 km^2 or mean catchment area of 0.16 km^2 resulting from the 24,523 catchments delineated in this study. By distinguishing catchment area of individual impoundments from larger reservoirs, small impoundment

catchments areas are much smaller on average than previously estimated by density-based calculations (i.e., Smith et al., 2002).

Soil trait differences between subcatchment and direct runoff area reflect impoundments' tendency to occur in higher reaches of a watershed. With the exception of Marion, areas classified as depositional comprise a greater percentage of direct runoff areas than do corresponding subcatchments, which suggests that impoundments are less likely to occur in lowland depositional areas. Furthermore, Class 1 soils, which have lost less than 25% of their topsoil, are more abundant in subcatchment areas for all drainages except Perry, which indicates that impoundments are more abundant in areas that have experienced less erosion, such as upland regions. Additionally, the exceptions of Marion and Perry can likely be discounted since the percentage difference in Class 1 between subcatchment and direct runoff area is less than 0.5% for Perry, and soil class data is unavailable for 22% of Marion's direct runoff area.

Land use differences in subcatchment and direct runoff area reflect the tendency of impoundments to occur in lower abundance where surface and ground water may be needed for agriculture. With the exception of the Clinton Reservoir drainage, cultivated cropland is consistently more abundant in direct runoff areas than subcatchments, and grassland is more abundant in subcatchment areas across all drainages. Given the higher percentage of grassland occurring in subcatchment areas and the tendency of impoundments to occur in upland areas, this underscores the connection between their placement in the landscape and their service in cattle watering, specifically in upland regions where water availability is otherwise periodic and the conditions unsuitable for crop production.

Contrary to other results, slope summary statistics do not suggest that impoundments tend to be more abundant in upland areas. In fact, all subcatchments have lower average slope values with the exception of the Marion Reservoir drainage, which has equivalent average slope values for subcatchment and direct runoff area. The reason behind this unexpected data trend likely lies in the methodology. Average slope was calculated for drainage, subcatchment, and direct runoff area after excluding hydro-flattened areas. However, streams and riparian areas were unaddressed and remained in the DEM. It is possible that riparian areas of larger order streams, which would be more likely to occur in proximity to reservoirs and in direct runoff areas, exhibited substantial slopes relative to overland areas. In turn, failing to exclude these riparian areas may have skewed average slope values for direct runoff areas, causing them to exceed average slope values for subcatchments.

Conclusions

Several trends in erosion-related traits were observed for drainages with similar specific sediment yields. Drainages with the highest percentages of negligible runoff area tend to have the lowest sediment yields, and drainages with low percentages of soils classified as depositional may be experiencing less overland deposition and more efficient sediment transport. Additionally, drainage geometry and size influences transport efficiency, and may be a significant cause for the high specific sediment yield exhibited by El Dorado Reservoir and lower specific sediment yield of Melvern Reservoir. Lower percentages of cultivated agriculture can be tied to lower drainage sediment yields, and two of the three lowest cropland percentages are found in the two lowest yield drainages (Fall River and Toronto). While percentage

subcatchment may be an influence on sediment yield, water body size distribution should be emphasized when considering potential sediment trapping by impoundments. The Fall River drainage, for example, has the lowest specific sediment yield and the lowest percentage of smaller impoundments (< 1/20 ha), while Clinton and Perry have the highest specific sediment yields and the lowest percentages of larger impoundments (< 1 ha).

While surface area to catchment area ratio results did not clearly appear connected to sedimentation trends, the concept should not be discarded. If further research were carried out, such as a quantifying the relationship between surface area and capacity through field sampling, a trap efficiency metric based on surface–area–to–catchment–area ratio could be developed. Interestingly, an unplanned result of the surface–area–to–catchment–area ratio tool suggests a unique application. If false water bodies are positioned on level topography, delineating their catchments can produce catchment areas similar in size to the water body surface areas (Figure 17). The resulting surface–area–to–catchment–area ratio will be close to 1.00. In effect, the script could be applied towards identifying erroneous water bodies in a dataset (e.g., NHD) by identifying disproportionate surface area to catchment area ratios.

Soil runoff, erosion, and land use trait differences between subcatchments and direct runoff areas indicate a greater abundance of impoundments in grassland headwater areas relative to agricultural areas and areas in closer proximity to reservoirs. Class 1 soils are more common in subcatchments, and depositional areas are more common in direct runoff areas, which indicates a tendency of impoundments to occur in higher reaches of the watershed where erosion is less severe and deposition less common. Additionally, direct runoff areas have greater percentages of cultivated agricultural land use, while subcatchments have greater percentages of grassland. As surface water is applied towards crop production, surface water storage in the form

of impoundments is less common. Furthermore, upland areas less suitable for crop production but suitable for grazing may promote impoundment construction for cattle watering where water availability would otherwise be periodic.

Reservoirs are a major component of infrastructure in Kansas, and many are approaching the end of their usable lives. As they approach 50% infill, dredging is required to restore reservoir capacity and services. Projected costs of dredging are substantial, and to avoid excessive costs of restoration, changes in management practices will be necessary to extend reservoir usable lives and delay restoration need. By applying new methodologies and enhanced data, better characterizations of the sources of reservoir sedimentation can be carried out. This study uses newly available high-resolution elevation data, novel analysis methods, and incorporates a significant potential mitigator of reservoir sedimentation, small impoundments, in an investigation into the causes of reservoir sediment yield. When exploring potential causes of difference in reservoir sedimentation, the various traits analyzed in this study should not be investigated in isolation, but instead should be studied in connection with each other. By better understanding not only the factors determinant of erosion but also the relationships among erosion-related factors, we can better understand the overall processes responsible for reservoir sedimentation rate. The factors addressed in this study are the primary determinants of reservoir sediment yield, and these are the factors that should guide reservoir drainage management decisions.

References

Arnold, J.G., Srinivasan, R., Muttiah, R.S., & Williams, J.R. (1998). Large area hydrologic modeling and assessment part I: model development. *Journal of American Water Resources Association 34(1*), 73–89.

Bedient, P. B., Huber, W. C., & Vieux, B. E. (2013). Chapter 2: Hydrologic analysis. *Hydrology and Floodplain Analysis 5th Edition*, 88-169.

Bosch, N. S. (2008). The influence of impoundments on riverine nutrient transport: An evaluation using the Soil and Water Assessment Tool. *Journal of Hydrology 355*(1), 131 147.

Brown, C.B. (1943). Discussion of Sedimentation in reservoirs by J. Witzig. *Proceedings of the American Society of Civil Engineers 69*, 1493–1500.

Brune, G.M. (1953). Trap efficiency of reservoirs. *Transactions of the American Geophysical Union 34(3)*, 407–418.

Buddemeier, R. W. (2004). Detection and characterization of small water bodies A Final Technical Report for the NASA-EPSCoR/KTech- funded project: Kansas Geological Survey.

Callihan, R. A. (2013). Distribution, proliferation and significance of small impoundments in Kansas. (M.A.), University of Kansas, Lawrence, KS.

Camp, T.R. 1946: Sedimentation and the design of settling tanks. *Transactions of the American Society of Civil Engineers 111(1),* 445–86.

Chen, C.N. (1975). Design of sediment retention basins. *Proceedings of the national symposium on urban hydrology and sediment control, July 28-31*, 285–98.

Churchill, M.A. 1948: Discussion of analyses and use of reservoir sedimentation data by L.C. Gottschalk. *Proceedings of the Federal Interagency Sedimentation Conference, Denver, Colorado*. US Geological Survey, 139–40.

Colson, T.P., Gregory, J.D., Mitasova, H., & Nelson, S.A. (2006). Comparison of stream extraction models using LIDAR DEMs. *Proceedings of the American Water Resources Association*.

deNoyelles, F. & Jakubauskus, M. (2008). Current state, trend, and spatial variability of sediment in Kansas reservoirs. *Sedimentation in Our Reservoirs: Causes and Solutions,* 9-23.

deNoyelles, F. & Kastens, J. H. (2016) Reservoir sedimentation challenges in Kansas. *Transactions of the Kansas Academy of Science, 119(1),* 69-81.

Downing, J.A., Prairie, Y. T., Cole, J. J., Duarte, C. M., Tranvik, L. J., Striegl, R. G., McDowell, W. H., Kortelainen, P., Caraco, N.F., Melack, J. M., & Middelburg, J. J. (2006). The global abundance and size distribution of lakes, ponds, and impoundments. *Limnology and Oceanography, 51*(5), 2388-2397.

Downing, J. A., Cole, J. J., Middleburg, J. J., Striegl, R. G., Duarte, C. M., Kortelainen, P., Prairie, Y. T., & Laube, K. A. (2008). Sediment organic carbon burial in agriculturally eutrophic impoundments over the last century. *Global Biogeochemical Cycles 22*(1).

Flanagan, D.C., & Nearing, M.A. (1995). USDA water erosion prediction project: hillslope profile and watershed model documentation. *NSERL Report No. 10.*

Fernandez, C., Wu, J. Q., McCool, D. K., & Stockle, C. O. (2003). Estimating water erosion and sediment yield with GIS, RUSLE, and SEDD. *Journal of Soil and Water Conservation 58(3*), 128-136.

Foster, G. M. (2011). Effects of Small Impoundments on Total Watershed Sediment Yield in Northeast Kansas, April through August 2011. (M.S.), University of Kansas, Lawrence, KS.

Graf, W.L. (1999). Dam nation: a geographic census of American dams and their large-scale hydrologic impacts. *Water Resources 35,* 1305–1311.

Heidemann, H. K. (2014). LiDAR Base Specification Version 1.2. *US Geological Survey Standards Book 11, Collection and Delineation of Spatial Data*.

Heinemann, H.G. (1981) A new sediment trap efficiency curve for small reservoirs. *Water Resources Bulletin 17(5),* 825–30.

Homer C.G., Dewitz J.A., Yang L., Jin S., Danielson P., Xian G., Coulston J., Herold N.D., Wickham J.D., & Megown K. (2015). Completion of the 2011 national land cover database for the conterminous United States-representing a decade of land cover change information. *Photogrammetric Engineering and Remote Sensing 81(*5), 345-354.

Huggins, D., Jakubauskas, M., & Kastens, J. (2011). Lakes & Wetlands of the Great Plains. *North American Lake Management Society 31(4),* 19-25.

Hurd B., Leary N., Jones R., & Smith J. (1999). Relative regional vulnerability of water resources to climate change. *Journal of the American Water Resources Association 512(35),* 1399-1409.

Jain, M. K. & Kothyari, U. C. (2000). Estimation of soil erosion and sediment yield using GIS. *Hydrological Sciences Journal 45(5*), 771-786.

Jones, K.L., Poole, G.C., O'Daniel, S.J., Mertes, L.A.K., & Stanford, J.A. (2008). Surface hydrology of low-relief landscapes: Assessing surface water flow impedance using lidar derived digital elevation models. *Remote Sensing of Environment 112(11),* 4148–4158.

Juracek, K. E. & Zeigler, A. C. (2007). Estimation of sediment sources using selected chemical tracers in the Perry Lake and Lake Wabaunsee Basins, northeast Kansas. *USGS Scientific Investigations Report 2007-5020*.

Kastens, J. H., Baker, D. S., Peterson, D. L. & Huggins, D. G. (2016) Wetland Program Development Grant (WPDG) FFY 2013 – Playa Mapping and Assessment. *KBS Report 186*.

Kondolf G.M., Gao Y., Annandale G.W., Morris G.L., Jiang E., Zhang J., Cao Y., Carling P., Fu K., & Guo Q. (2014). Sustainable sediment management in reservoirs and regulated rivers: experiences from five continents. *Earth's Future 2(5),* 256-280.

Langbein W.B. & Schumm, S. (1958). Yield of sediment in relation to mean annual 546 precipitation. *Transactions, American Geophysical Union 39,* 1076-1084.

Li, J., & Wong, D.W. (2010). Effects of DEM sources on hydrologic applications. *Computers, Environment and Urban Systems 34(3*), 251–261.

Lim, K. J., Sagong, M., Engel, B. A., Tang, Z., Choi, J., & Kim, K. (2005). GIS-based sediment assessment tool. *Catena 64*(1), 61-80.

Liu, X., Peterson, J., & Zhang, Z. (2005). High-resolution DEM generated from LiDAR data for water resource management. *Proceedings of the International Conference on Modeling and Simulation (MODSIM05),* 1402–1408.

Martinko, E., deNoyelles, F., Bosnak, K., Jakubauskas, M., Huggins, D., Kastens, J., Shreders, A., Baker, D., Blackwood, A., Campbell, S., & Rogers, C. (2014). *Atlas of Kansas Lakes: A resource for communities, policy makers and planners.*

Meade R.H. & Parker R.S. (1985). Sediment in rivers of the United States. *US Geological Survey Water-Supply Paper 2275,* 49-60.

Meade, R.H., Yuzyk T.R., & Day T.J. (1990). Movement and storage of sediment in rivers of the United States and Canada. *Surface Water Hydrology. Geology of North America, Boulder, Colorado. 1990,* 255–280.

Milly P.C., Dunne K., & Vecchia A.V. (2005). Global pattern of trends in streamflow and water availability in a changing climate. *Nature 438 (7066),* 347-350.

Morgan, R.P.C., Quinton, J.N., Smith, R.E., Govers, G., Poesen, J.W.A., Auerswald, K., Chisci, G., Torri, D., & Styczen, M.E. (1998). The European Soil Erosion Model (EUROSEM): a dynamic approach for predicting sediment transport from fields and small catchments. *Earth Surface Processes and Landforms 23(6),* 527–544.

Mulholland, P.J. & Elwood, J.W. (1982). The role of lake and reservoir sediments as sinks in the perturbed global carbon cycle. *Tellus (34),* 490-499.

Peterson, D. L., Whistler, J. L., Egbert, S. L., & Martinko, E. A. (2010). 2005 Kansas Land Cover Patters Phase II: Final Report KBS Report #167.

Petroselli, A. (2012). LIDAR data and hydrological applications at the basin scale. *GIScience and Remote Sensing 49(1),* 139–162.

Poppenga, S. K., Worstell, B. B., Stoker, J. M., & Greenlee, S. K. (2010). Using selective drainage methods to extract continuous surface flow from 1-meter lidar-derived digital elevation data. Scientific Investigations Report 5059. U.S. Geological Survey.

PRISM Climate Group. 2015. PRISM Climate Data 2015

Rahmani V., Hutchinson S. L., Harrington Jr. J. A., & Hutchinson J. M. (2015). Analysis of frequency and magnitude of extreme rainfall events with potential impacts on flooding; a case study from the central United States. *International Journal of Climatology*.

Rahmani, V., Kastens, J., deNoyelles, F., Jakubauskus, M., Martinko, E., Huggins, D., Gnau, C., Liechti, P., Campbell, S., Callihan, R., Blackwood, A. (2017). Examining storage loss and sedimentation rate of large reservoirs in the U. S. Great Plains. Unpublished article.

Renard, K. G., Foster, G. R., Weesies, G. A., & Porter, J. P. (1991). RUSLE: revised universal soil loss equation. *Journal of Soil and Water Conservation 46 (1),* 30–33.

Renwick, W. H., Smith, S. V., Bartley, J. D., & Buddemeier, R. W. (2005). The role of impoundments in the sediment budget of the conterminous United States. *Geomorphology 71*(1), 99-111.

Smith S.V., Renwick W.H., Buddemeier R.W., & Crossland C.J. (2001) Budgets of soil erosion and deposition for sediments and sedimentary organic carbon across the conterminous United States. *Global Biogeochemical Cycles 15(3),* 697–707.

Smith, S. V., Renwick, W. H., Bartley, J. D., & Buddemeier, R. W. (2002) Distribution and significance of small, artificial water bodies across the United States landscape. *Science of the Total Environment 299*(1): 21-36.

Tang, Z., Li, R., Li., X, Jaing, W., & Hirsh, W. (2014). Capturing LiDAR-derived hydrologic spatial parameters to evaluate playa wetlands. *Journal of the American Water Resources Association 50(1),* 234-245.

Trimble S.W. & Bube K.P. (1990) Improved reservoir trap efficiency prediction. *ENVIRON. PROFESS.,12(3),* 255–272.

U.S. Census Bureau. (2015). Population Estimates: Population and Housing Unit Estimates 2015. URL [https://www.census.gov/popest/]

Verstraeten, G. & Poesen, J. (2000) Estimating trap efficiency of small reservoirs and ponds: methods and implications for the assessment of sediment yield. *Progress in Physical Geography 24(2),* 219-251.

Vörösmarty, C. J., Green, P., Salisbury, J., & Lammers, R. B. (2000). Global water resources: vulnerability from climate change and population growth. *Science 289(5477),* 284-288.

Walling, D. E. (1983). "The sediment delivery problem. *Journal of Hydrology 65(1),* 209-237.

Wischmeier, W.H., & Smith, D.D. (1978). Predicting rainfall erosion losses. A guide to conservation planning. *The USDA Agricultural Handbook No. 537.*

Figures

Figure 1: Reservoir Drainage Areas

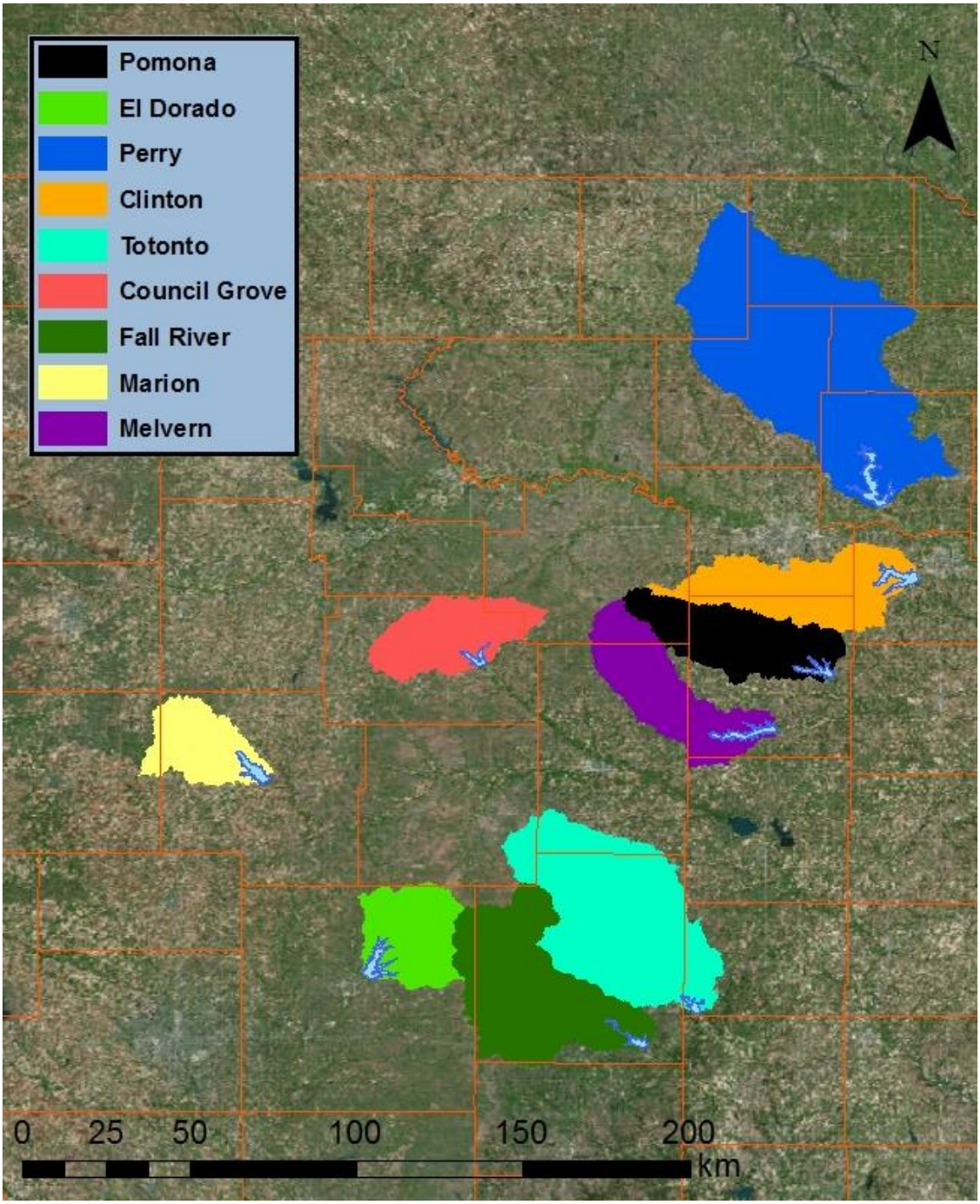

Figure 2: Annual Precipitation for Kansas. Reservoir drainages are outlined to show placement in precipitation gradient. Drainages of Perry(1), Melvern(2), and Toronto(3) extend just beyond the 850 – 1000 mm boundaries. The six other drainages are within the 850 – 1000 mm annual precipitation range.

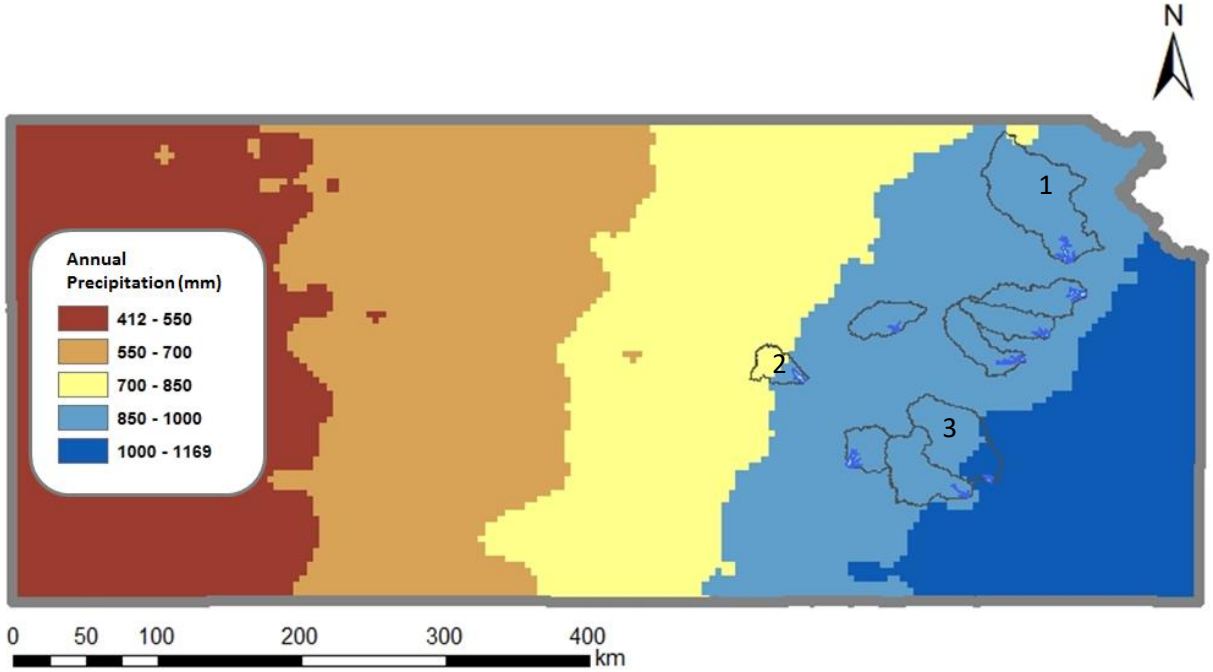

(PRISM Climate Group. 2015. PRISM Climate Data 2015

Figure 3: Catchment Delineation

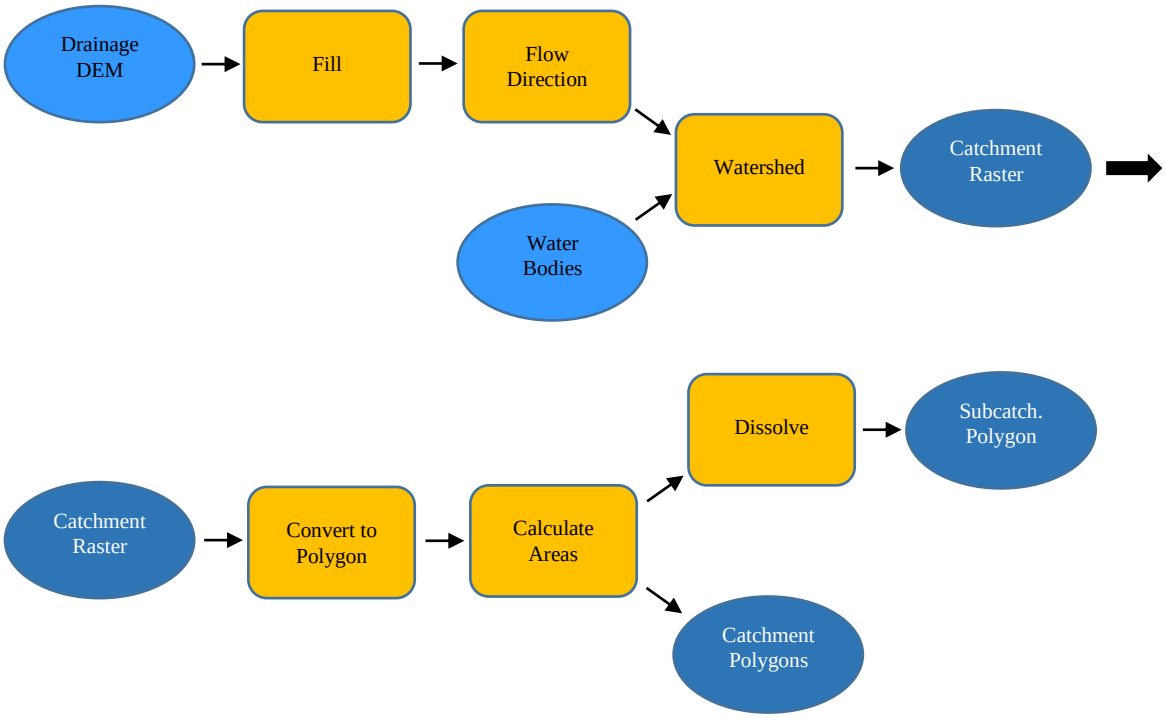

Figure 4: Land Use Extraction for Drainage, Subcatchment, and Direct Runoff Area.

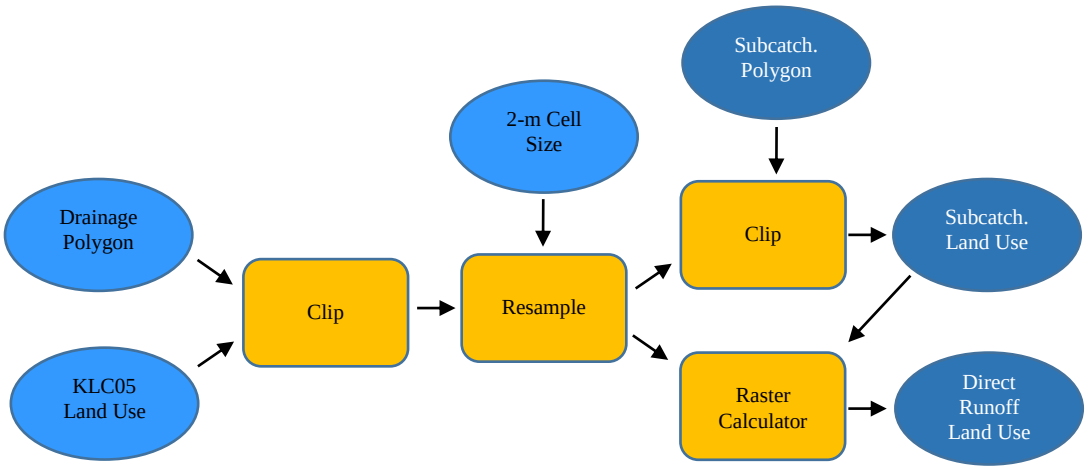

Figure 5: Soil Data Extraction for Drainage, Subcatchment, and Direct Runoff Area.

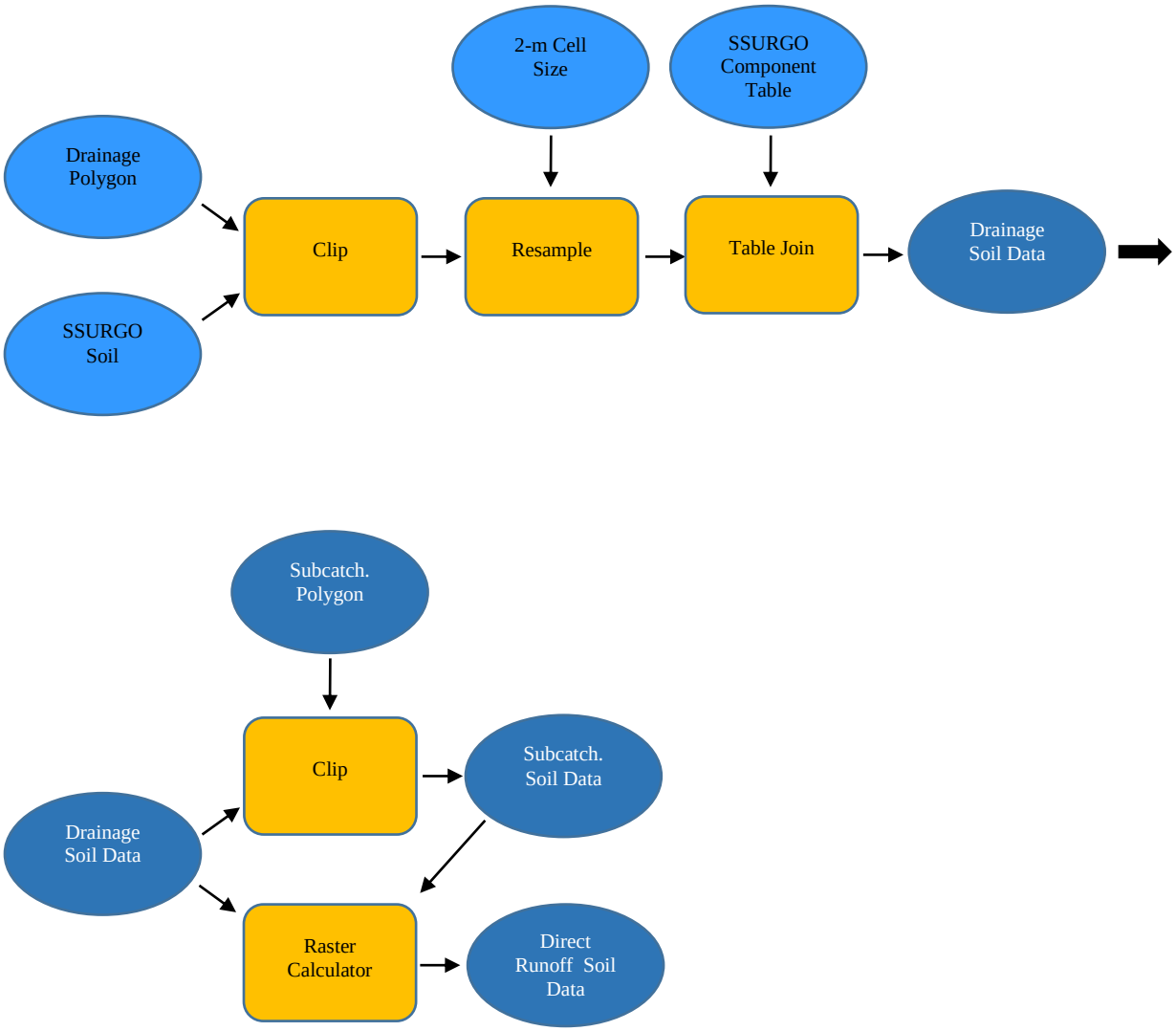

Figure 6: Slope Summary Statistics

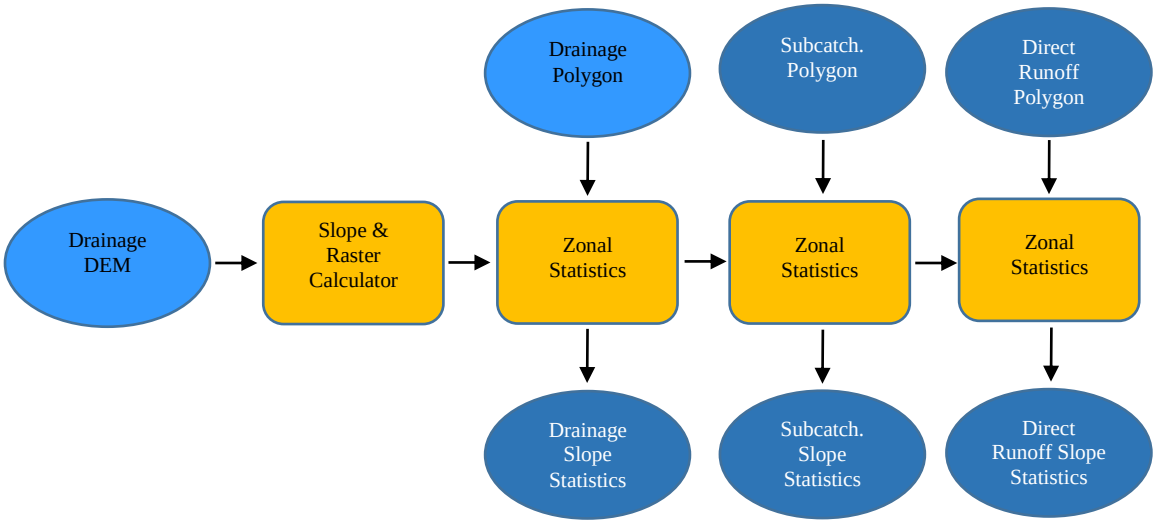

Figure 7: Catchment Fragmentation during Conversion from Raster to Polygon

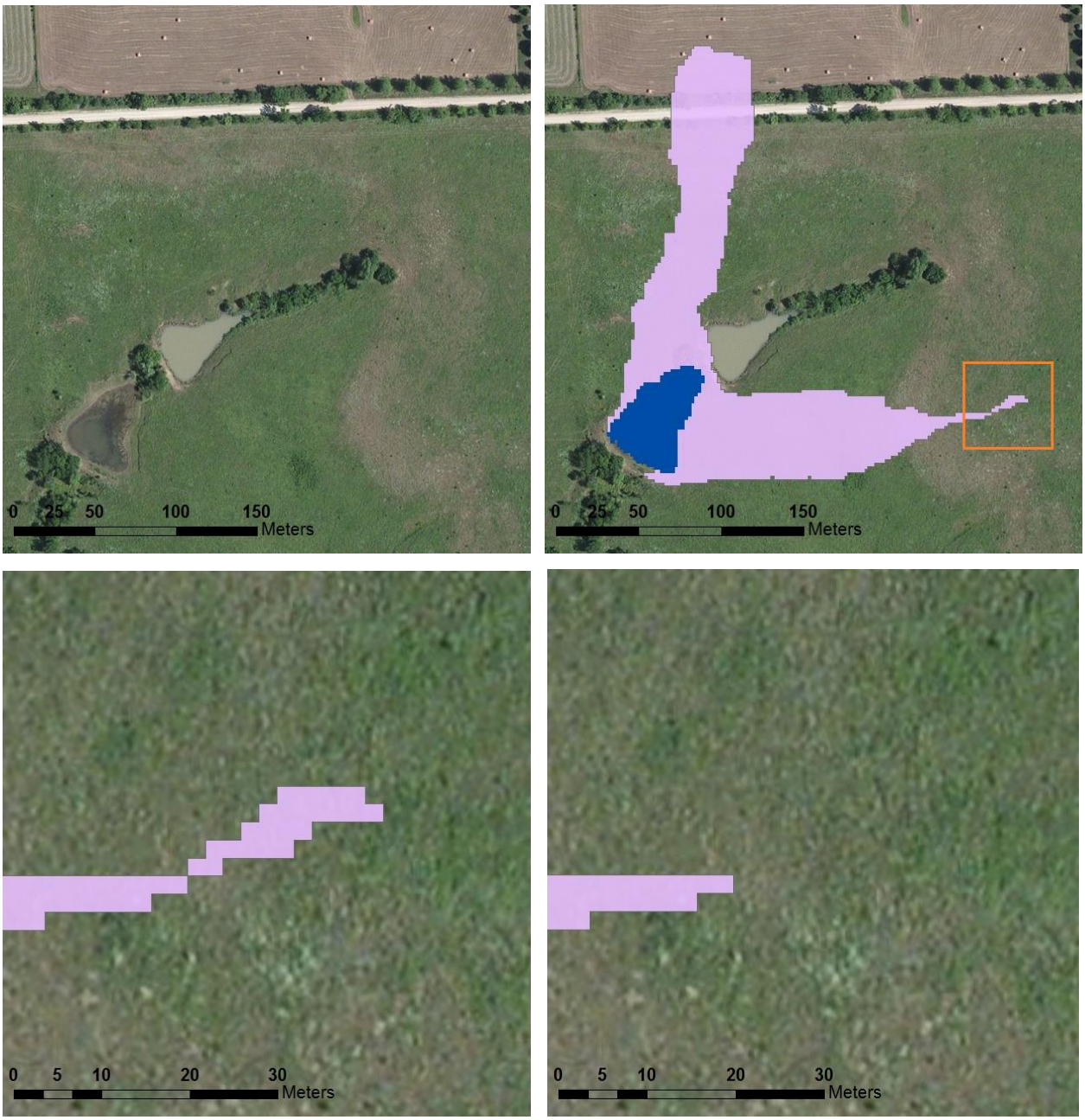

Following water body catchment delineation using the watershed tool in ArcGIS, catchments were converted to polygons for area calculation. Conversion leads to fragmenting of catchments if cells are connected at corners.

Figure 8: Results for Marion Reservoir Drainage

A) Subcatchment area (shown in purple).

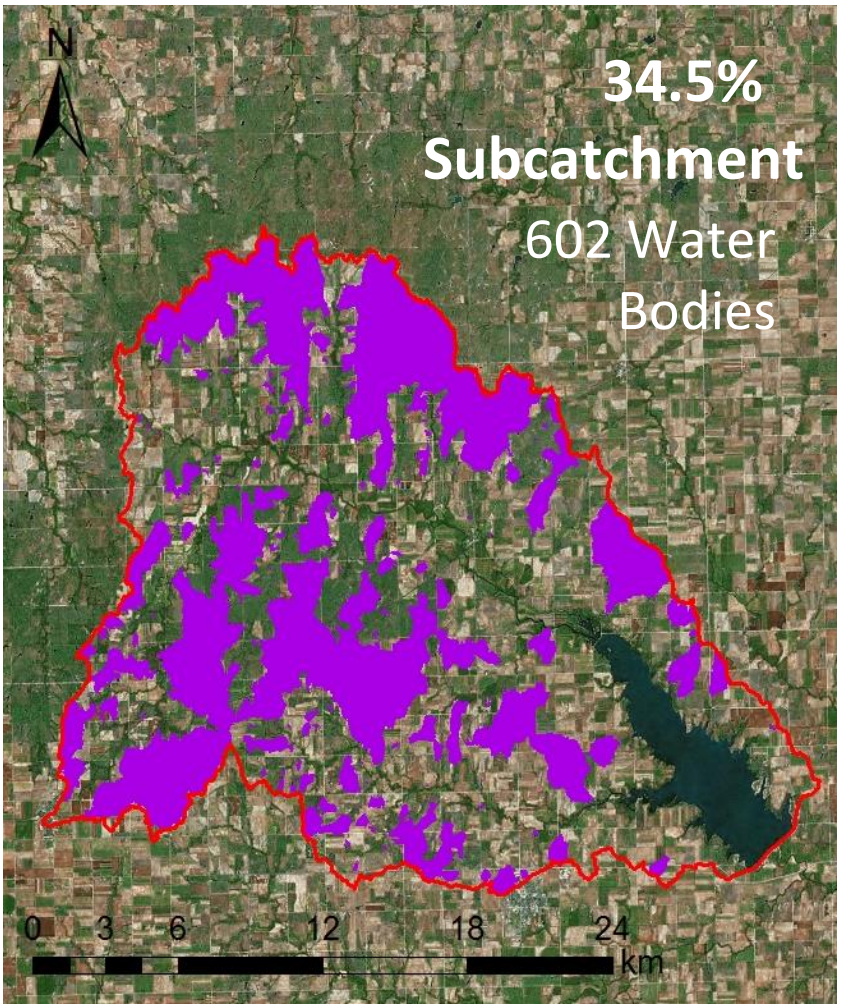

B) Land use distribution.

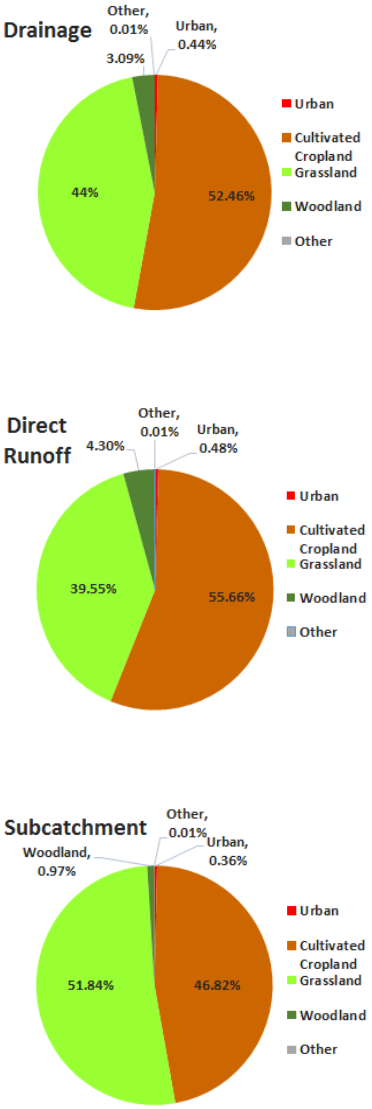

Area	Yield	Subcatch	%Subcatch	Ct	Density
535 km^2	243 m^3	184.5 km^2	34.49%	602	1.13 Ct/km^2

C) Drainage, yield, subcatchment, and water body density.

Water Bodies	< 1/20 ha	1/20 -1/5 ha	1/5 - 1/2 ha	1/2 - 1 ha	> 1 ha
Count	57	231	194	81	39
Percentage	9.47%	38.37%	32.23%	13.46%	6.48%

D) Water body surface area distribution.

Catchment Areas (ha)					Surface Area: Catchment Area			
Min	Q1	Median	Q3	Max	Min	Max	Median	Avg. Ratio
4.32E-02	2.99	11.14	30.50	958.59	1.08E-04	0.97	2.31E-02	1:43.3

E) Catchment size statistics and surface area to catchment area ratio summary.

Figure 9: Results for El Dorado Reservoir Drainage

A) Subcatchment area (shown in purple).

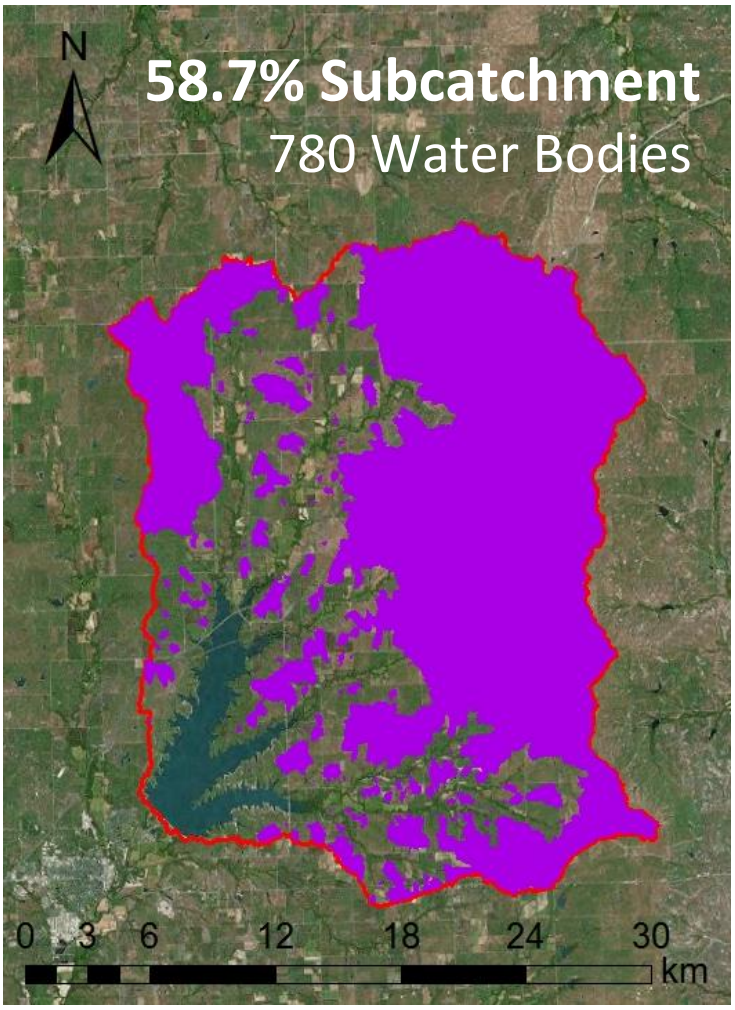

B) Land use distribution.

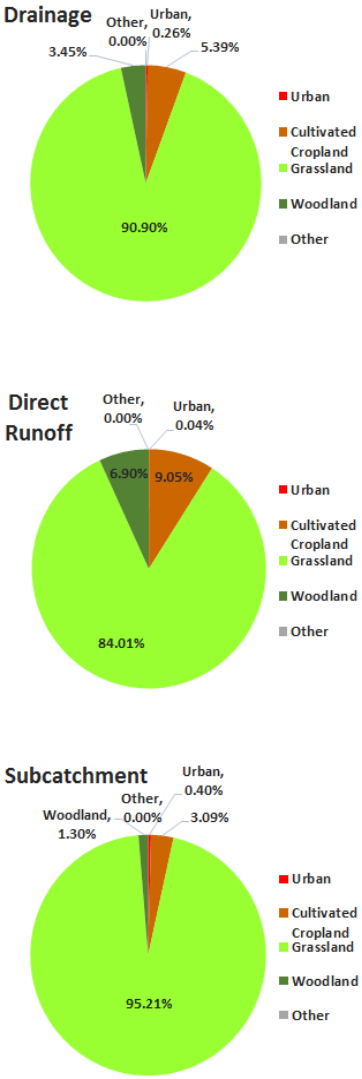

Area	Yield	Subcatch	%Subcatch	Ct	Density
634 km^2	410 m^3	372.3 km^2	58.72%	780	1.23 Ct/km^2

C) Drainage, yield, subcatchment, and water body density.

Water Bodies	< 1/20 ha	1/20 -1/5 ha	1/5 - 1/2 ha	1/2 - 1 ha	> 1 ha
Count	23	227	245	132	153
Percentage	2.95%	29.10%	31.41%	16.92%	19.62%

D) Water body surface area distribution.

Catchment Areas (ha)					Surface Area: Catchment Area			
Min	Q1	Median	Q3	Max	Min	Max	Median	Avg. Ratio
4.96E-02	4.73	13.46	33.38	2629.27	9.86E-05	0.83	3.16E-02	1:31.7

E) Catchment size statistics and surface area to catchment area ratio summary.

Figure 10: Results for Council Grove Reservoir Drainage

A) Subcatchment area (shown in purple).

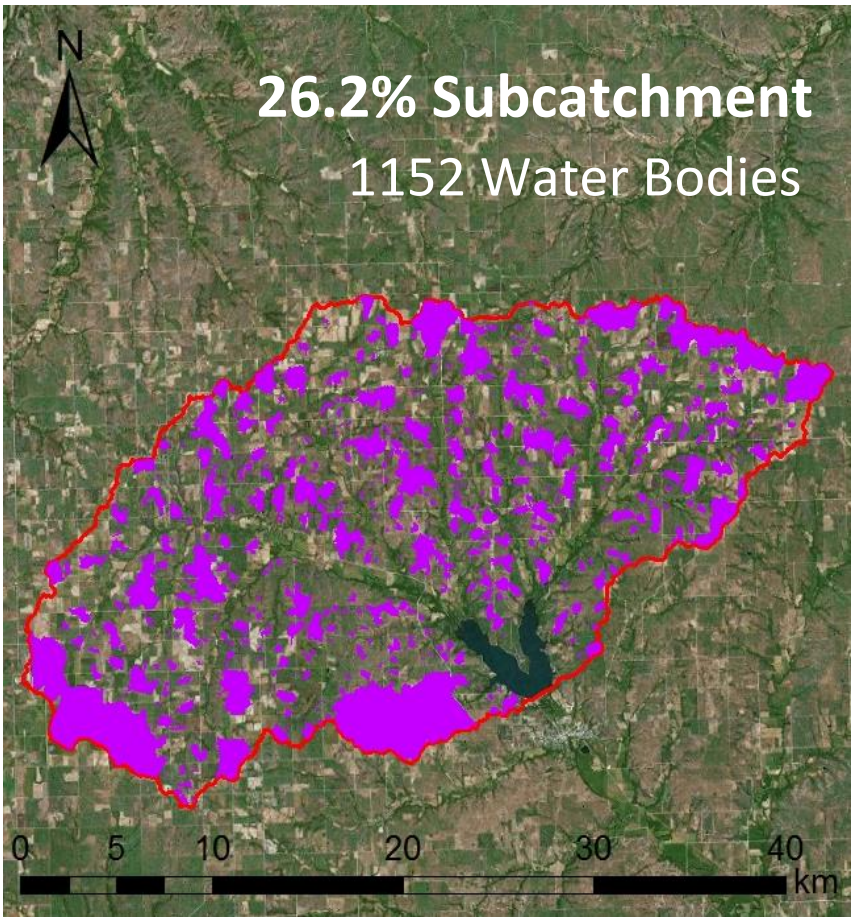

B) Land use distribution.

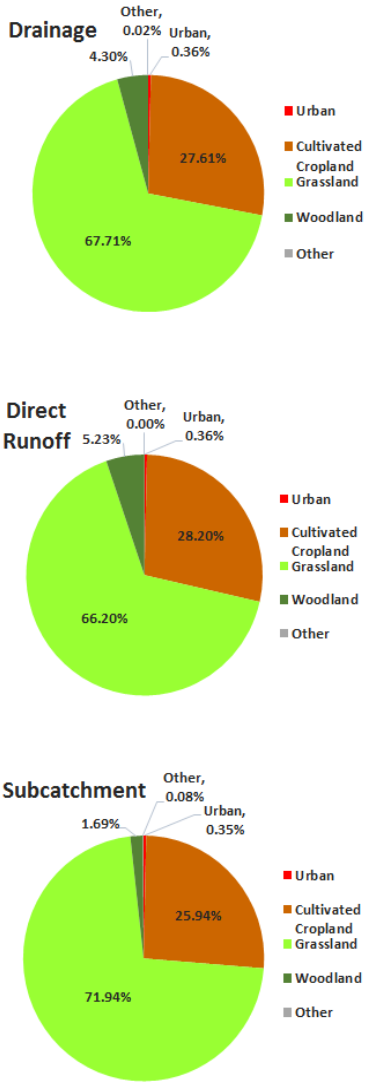

Area	Yield	Subcatch	%Subcatch	Ct	Density
677 km^2	341 m^3	177.5 km^2	26.22%	1152	1.70 Ct/km^2

C) Drainage, yield, subcatchment, and water body density.

Water Bodies	< 1/20 ha	1/20 -1/5 ha	1/5 - 1/2 ha	1/2 - 1 ha	> 1 ha
Count	126	516	343	121	46
Percentage	10.94%	44.79%	29.77%	10.50%	3.99%

D) Water body surface area distribution.

Catchment Areas (ha)					Surface Area: Catchment Area			
Min	Q1	Median	Q3	Max	Min	Max	Median	Avg. Ratio
1.59E-02	1.89	6.32	14.60	1779.96	4.68E-05	0.83	3.19E-02	1:31.4

E) Catchment size statistics and surface area to catchment area ratio summary.

Figure 11: Results for Pomona Reservoir Drainage

A) Subcatchment area.

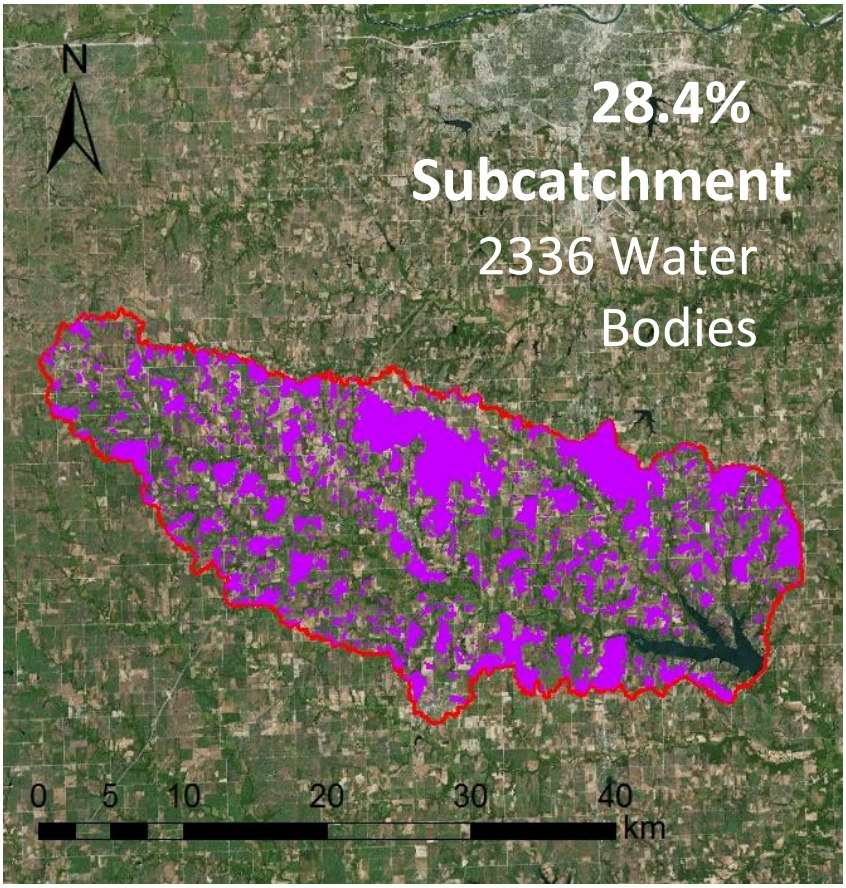

B) Land use distribution.

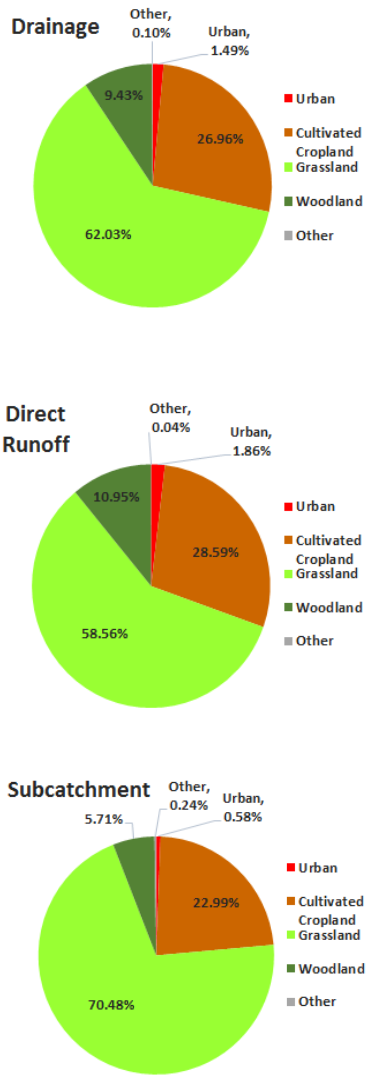

Area	Yield	Subcatch	%Subcatch	Ct	Density
836 km^2	487 m^3	237.6 km^2	28.42%	2336	2.79 Ct/km^2

C) Drainage, yield, subcatchment, and water body density.

Water Bodies	< 1/20 ha	1/20 -1/5 ha	1/5 - 1/2 ha	1/2 - 1 ha	> 1 ha
Count	338	1193	597	138	70
Percentage	14.47%	51.07%	25.56%	5.91%	3.00%

D) Water body surface area distribution.

Catchment Areas (ha)					Surface Area: Catchment Area			
Min	Q1	Median	Q3	Max	Min	Max	Median	Avg. Ratio
4.91E-03	1.22	4.05	10.12	873.08	4.83E-04	1.00	3.58E-02	1:27.9

E) Catchment size statistics and surface area to catchment area ratio summary.

Figure 12: Results for Melvern Reservoir Drainage

A) Subcatchment area.

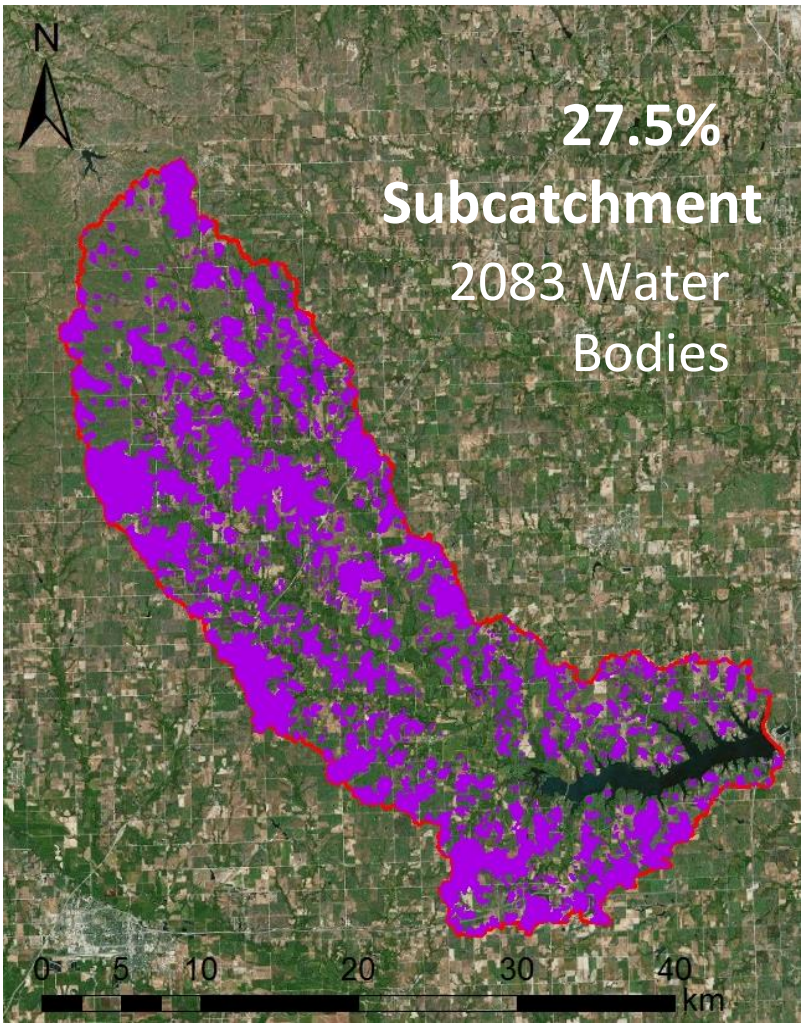

B) Land use distribution.

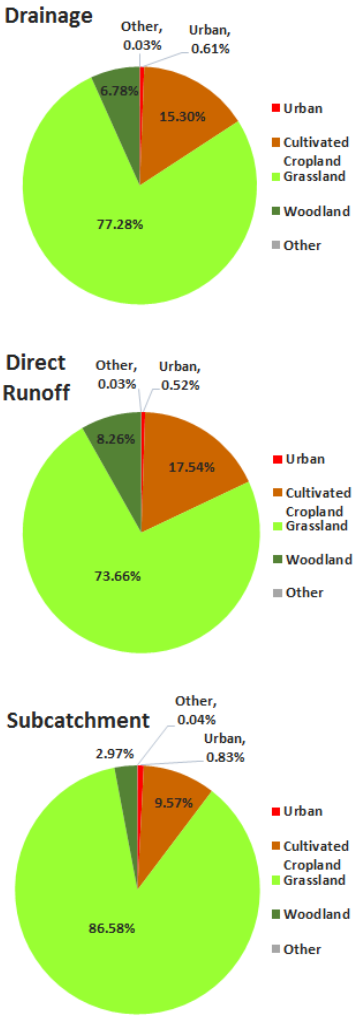

Area	Yield	Subcatch	%Subcatch	Ct	Density
870 km^2	182 m^3	238.9 km^2	27.46%	2083	2.39 Ct/km^2

C) Drainage, yield, subcatchment, and water body density.

Water Bodies	< 1/20 ha	1/20 -1/5 ha	1/5 - 1/2 ha	1/2 - 1 ha	> 1 ha
Count	263	969	546	198	107
Percentage	12.63%	46.52%	26.21%	9.51%	5.14%

D) Water body surface area distribution.

Catchment Areas (ha)					Surface Area: Catchment Area			
Min	Q1	Median	Q3	Max	Min	Max	Median	Avg. Ratio
1.38E-02	1.37	4.71	11.49	887.26	4.77E-04	1.00	4.09E-02	1:24.4

E) Catchment size statistics and surface area to catchment area ratio summary.

Figure 13: Results for Clinton Reservoir Drainage

A) Subcatchment area (shown in purple).

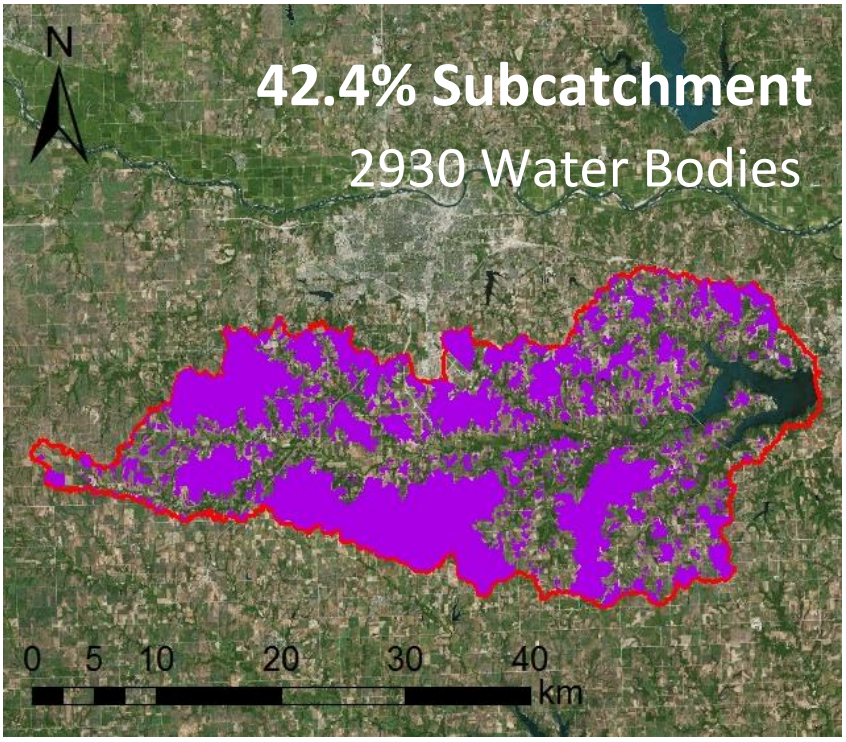

B) Land use distribution.

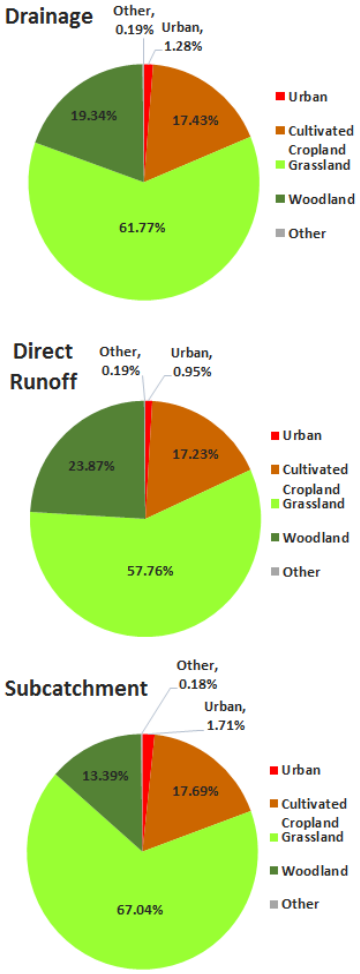

Area	Yield	Subcatch	%Subcatch	Ct	Density
951 km^2	432 m^3	401.0 km^2	42.16%	2930	3.08 Ct/km^2

C) Drainage, yield, subcatchment, and water body density.

Water Bodies	< 1/20 ha	1/20 -1/5 ha	1/5 - 1/2 ha	1/2 - 1 ha	> 1 ha
Count	459	1462	666	187	156
Percentage	15.67%	49.90%	22.73%	6.38%	5.32%

D) Water body surface area distribution.

Catchment Areas (ha)					Surface Area: Catchment Area			
Min	Q1	Median	Q3	Max	Min	Max	Median	Avg. Ratio
1.56E-02	1.20	4.14	10.90	1974.2	5.48E-05	1.00	3.62E-02	1:27.6

E) Catchment size statistics and surface area to catchment area ratio summary.

Figure 14: Results for Fall River Reservoir Drainage

A) Subcatchment area (shown in purple).

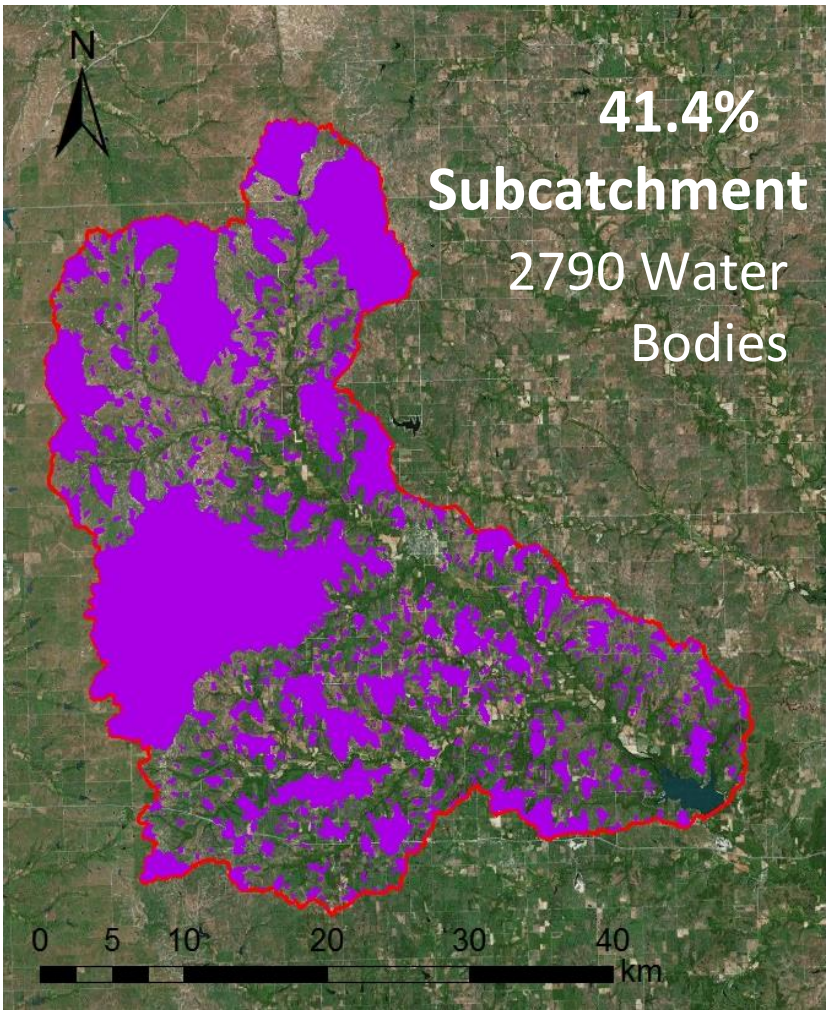

B) Land use distribution.

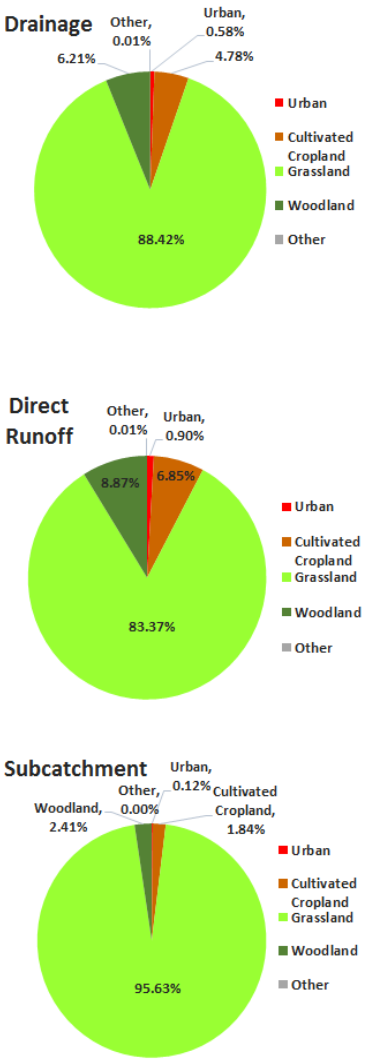

Area	Yield	Subcatch	%Subcatch	Ct	Density
1434 km^2	135 m^3	592.6 km^2	41.36%	2790	1.95 Ct/km^2

C) Drainage, yield, subcatchment, and water body density.

Water Bodies	< 1/20 ha	1/20 -1/5 ha	1/5 - 1/2 ha	1/2 - 1 ha	> 1 ha
Count	269	1294	881	235	111
Percentage	9.64%	46.38%	31.58%	8.42%	3.98%

D) Water body surface area distribution.

Catchment Areas (ha)					Surface Area: Catchment Area			
Min	Q1	Median	Q3	Max	Min	Max	Median	Avg. Ratio
1.38E-02	1.55	5.42	13.98	11273.0	1.06E-05	0.86	3.39E-02	1:29.5

E) Catchment size statistics and surface area to catchment area ratio summary.

Figure 15: Results for Toronto Reservoir Drainage

A) Subcatchment area (shown in purple).

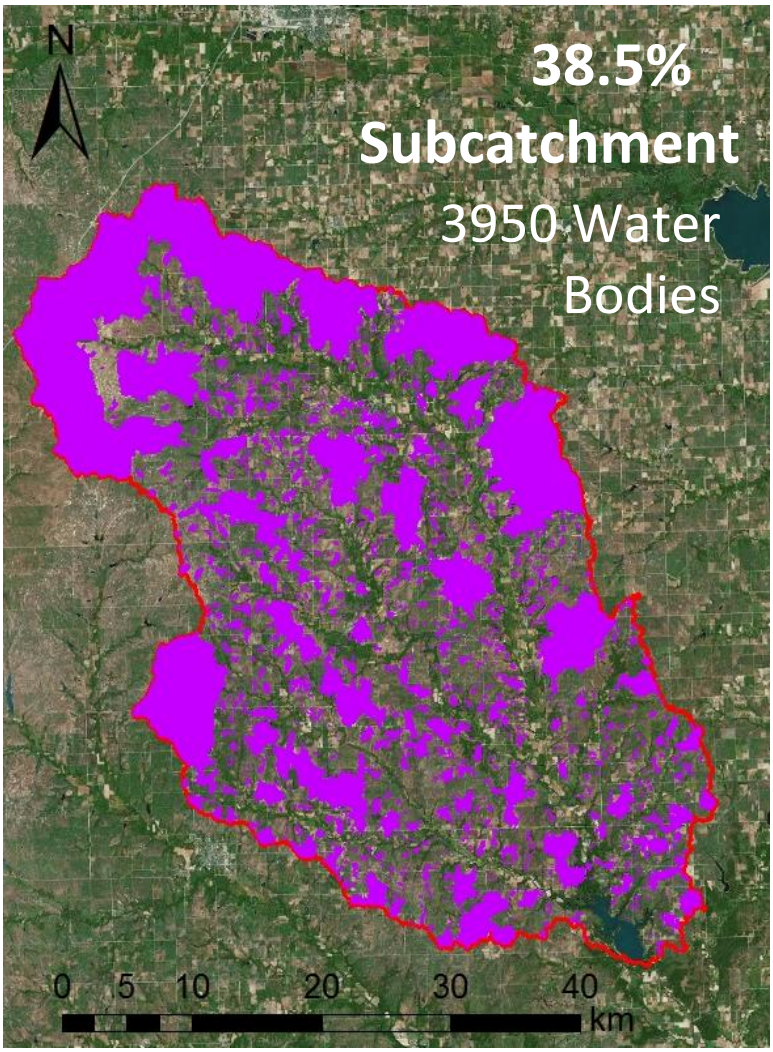

B) Land use distribution.

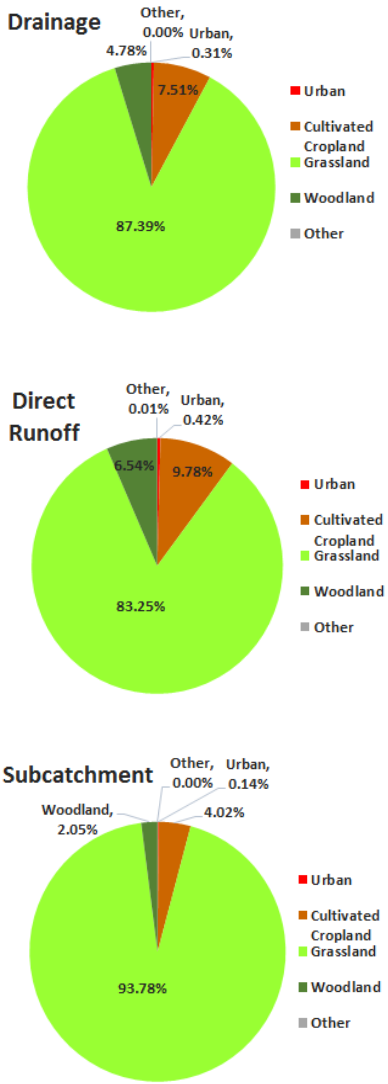

Area	Yield	Subcatch	%Subcatch	Ct	Density
1855 km^2	140 m^3	732.5 km^2	38.49%	3957	2.13 Ct/km^2

C) Drainage, yield, subcatchment, and water body density.

Water Bodies	< 1/20 ha	1/20 -1/5 ha	1/5 - 1/2 ha	1/2 - 1 ha	> 1 ha
Count	512	1855	1149	303	138
Percentage	12.94%	46.88%	29.04%	7.66%	3.49%

D) Water body surface area distribution.

Catchment Areas (ha)					Surface Area: Catchment Area			
Min	Q1	Median	Q3	Max	Min	Max	Median	Avg. Ratio
9.76E-03	1.26	4.03	10.53	4196.09	1.82E-04	0.92	4.02E-02	1:24.9

E) Catchment size statistics and surface area to catchment area ratio summary.

Figure 16: Results of Perry Reservoir Drainage

A) Subcatchment area (shown in purple).

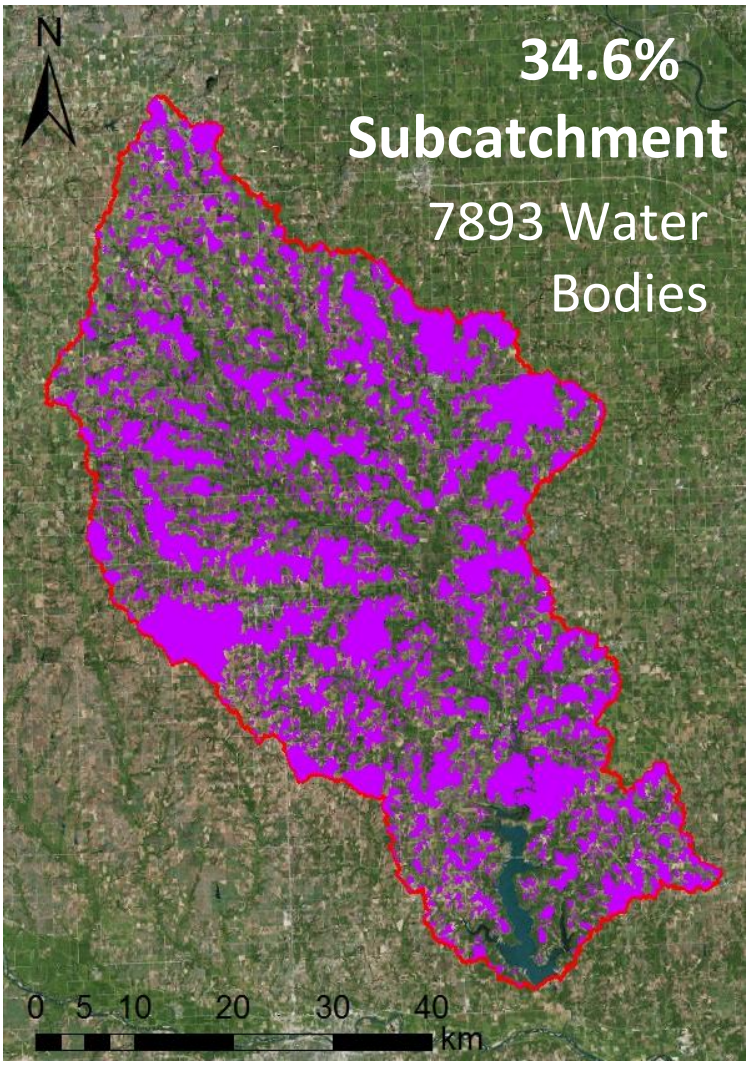

B) Land use distribution.

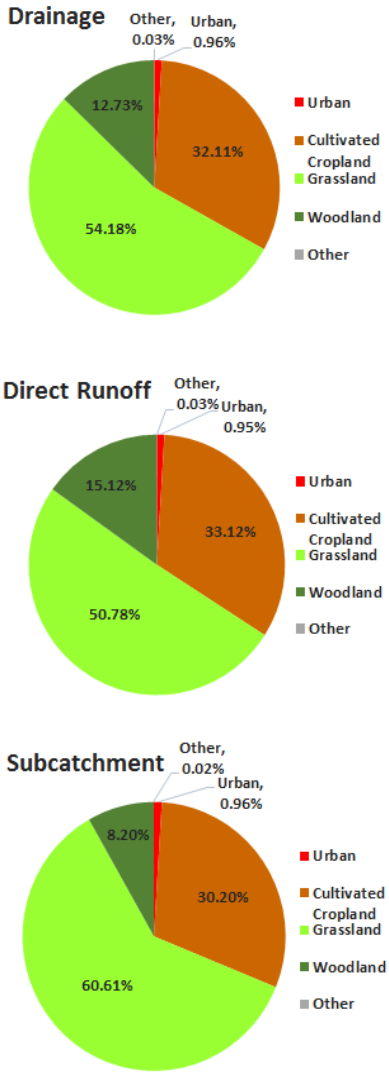

Area	Yield	Subcatch	%Subcatch	Ct	Density
2928 km^2	384 m^3	1011.6 km^2	34.55%	7893	2.70 Ct/km^2

C) Drainage, yield, subcatchment, and water body density.

Water Bodies	< 1/20 ha	1/20 -1/5 ha	1/5 - 1/2 ha	1/2 - 1 ha	> 1 ha
Count	1691	3295	1521	713	673
Percentage	21.42%	41.75%	19.27%	9.03%	8.53%

D) Water body surface area distribution.

Catchment Areas (ha)					Surface Area: Catchment Area			
Min	Q1	Median	Q3	Max	Min	Max	Median	Avg. Ratio
7.74E-03	1.02	3.95	11.21	3536.29	7.10E-05	1.03	4.22E-02	1:23.7

E) Catchment size statistics and surface area to catchment area ratio summary.

Figure 17: Surface–Area–to–Catchment–Area Ratio of Absent NHD Feature

A) Aerial imagery of a former pond.

B) Representation of the feature in the National Hydrography Dataset

C) Result of catchment delineation using NHD feature as pour point. Surface area to catchment area calculation resulted in a ratio of 1.03, which signaled an issue with this particular water body.

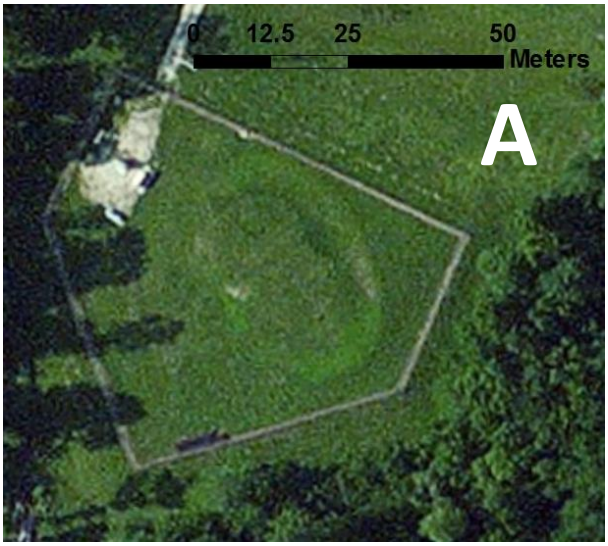

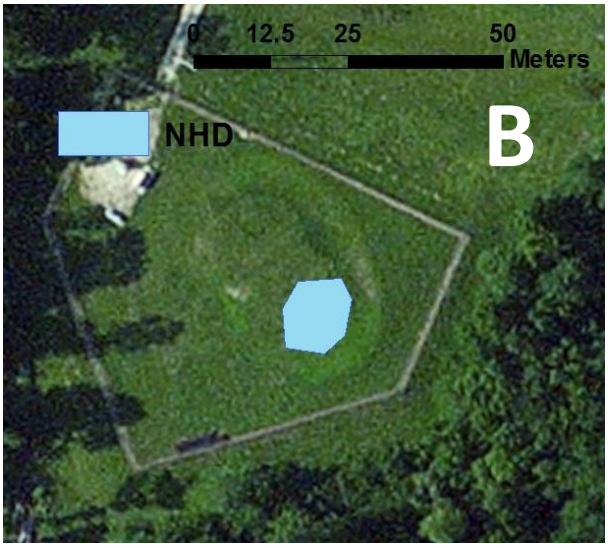

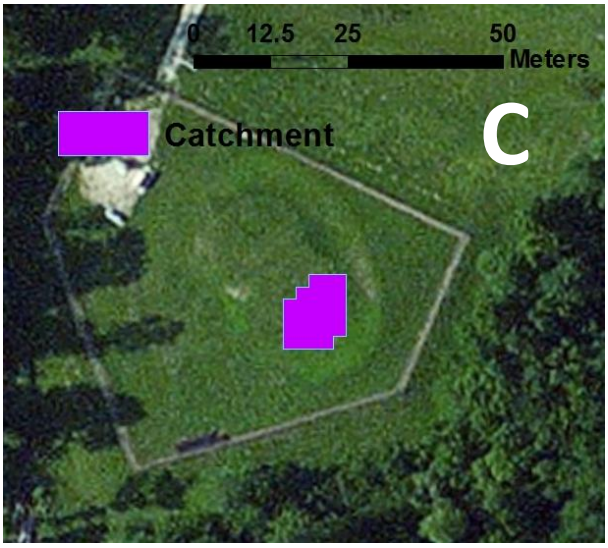

Tables

Table 1: Reservoir Sedimentation Summary

Reservoir	Drainage Area	Year-0	V-0 (Mm^3)	V-2015 (Mm^3)	Cap. Loss	SSY (m^3)
Marion	535	1967	105	99	5.9%	243
El Dorado	634	1979	202	193	4.6%	410
Council Grove	677	1963	65	53	18.5%	341
Pomona	836	1963	87	66	24.2%	487
Melvern	870	1972	190	184	3.6%	182
Clinton	951	1977	159	144	9.7%	432
Fall River	1434	1948	37	25	34.5%	135
Toronto	1855	1959	34	19	43.4%	140
Perry	2928	1962	300	240	20%	384
Min	535	1948	34	19	3.6%	135
Max	2928	1979	300	240	43.4%	487
Mean	1191	1966	131	114	18.3%	306

Drainage area, age, original capacity, capacity loss, and specific sediment yield for 9 reservoirs included in study. Data taken from Rahmani et al. (2017). Drainage area is given in square kilometers; Year-0 is the year reservoir operation began; V-0 is the original reservoir capacity in million cubic meters; V-2015 is the remaining reservoir capacity in the year 2015 in million cubic meters; Cap. Loss is the percentage capacity loss as of 2015; SSY is the annual sediment yield in cubic meters per square kilometer of drainage area.

Table 2: Water Body Surface Area Distribution

Reservoir	N	<1/20 ha	1/20 - 1/5 ha	1/5 - 1/2 ha	1/2 - 1 ha	> 1 ha	Ct/km2
Marion	602	57	231	194	81	39	1.13
El Dorado	780	23	227	245	132	153	1.23
Council Grove	1152	126	516	343	121	46	1.70
Pomona	2336	338	1193	597	138	70	2.79
Melvern	2083	263	969	546	198	107	2.39
Clinton	2930	459	1462	666	187	156	3.08
Fall River	2790	269	1294	881	235	111	1.95
Toronto	3957	512	1855	1149	303	138	2.13
Perry	7893	1691	3295	1521	713	673	2.70
TOTAL	24523	3738	11042	6142	2108	1493	2.29
	N	%	%	%	%	%	*SSY
Marion	602	9.47	38.37	32.23	13.46	6.48	243
El Dorado	780	2.95	29.10	31.41	16.92	19.62	410
Council Grove	1152	10.94	44.79	29.77	10.50	3.99	341
Pomona	2336	14.47	51.07	25.56	5.91	3.00	487
Melvern	2083	12.63	46.52	26.21	9.51	5.14	182
Clinton	2930	15.67	49.90	22.73	6.38	5.32	432
Fall River	2790	9.64	46.38	31.58	8.42	3.98	135
Toronto	3957	12.94	46.88	29.04	7.66	3.49	140
Perry	7893	21.42	41.75	19.27	9.03	8.53	384
TOTAL	24523	15.24	45.03	25.05	8.60	6.09	**306

*Specific sediment yield in cubic meters per square kilometer drainage per year taken from Rahmani et al., 2017.
**Mean specific sediment yield of nine reservoirs.

Table 3: Water Body Catchment Sizes Summary (in Hectares)

Reservoir	N	Min	Q1	Median	Q3	Max	Total
Marion	602	4.32E-02	2.99	11.14	30.50	958.59	18454
El Dorado	780	4.96E-02	4.73	13.46	33.38	2629.27	37230
Council Grove	1152	1.59E-02	1.89	6.32	14.60	1779.96	17749
Pomona	2336	4.91E-03	1.22	4.05	10.12	873.08	23755
Melvern	2083	1.38E-02	1.37	4.71	11.49	887.26	23892
Clinton	2930	1.56E-02	1.20	4.14	10.90	1974.17	40096
Fall River	2790	1.38E-02	1.55	5.42	13.98	11273.00	59256
Toronto	3957	9.76E-03	1.26	4.03	10.53	4196.09	73252
Perry	7893	7.74E-03	1.02	3.95	11.21	3536.29	101162
Total	24523	4.91E-03	1.30	4.55	12.19	11273.00	394846

Table 4: Surface–Area–to–Catchment–Area Ratios

Reservoir	Min	Max	Median	Avg Ratio
Marion	1.08E-04	0.97	2.31E-02	1:43.3
El Dorado	9.86E-05	0.83	3.16E-02	1:31.7
Council Grove	4.68E-05	0.83	3.19E-02	1:31.4
Pomona	4.83E-04	1.00	3.58E-02	1:27.9
Melvern	4.77E-04	1.00	4.09E-02	1:24.4
Clinton	5.48E-05	1.00	3.62E-02	1:27.6
Fall River	1.06E-05	0.86	3.39E-02	1:29.5
Toronto	1.82E-04	0.92	4.02E-02	1:24.9
Perry	7.10E-05	1.03	4.22E-02	1:23.7
Total	1.06E-05	1.03	3.81E-02	1:26.3

Table 5: Percentage Subcatchment

Reservoir	Drainage Area (km^2)	Subcatch Area (km^2)	% Subcatch	Avg Ratio	*SSY
Marion	535	184.5	34.49%	1:43.3	243
El Dorado	634	372.3	58.72%	1:31.7	410
Council Grove	677	177.5	26.22%	1:31.4	341
Pomona	837	237.6	28.42%	1:27.9	487
Melvern	870	238.9	27.46%	1:24.4	182
Clinton	951	401	42.16%	1:27.6	432
Fall River	1434	592.6	41.36%	1:29.5	135
Toronto	1855	732.5	39.49%	1:24.9	140
Perry	2928	1011.6	34.55%	1:23.7	384
Total	10720	3948.5	36.83%	1:26.3	**306

*Specific sediment yield in cubic meters per square kilometer drainage per year taken from Rahmani et al., 2017.
**Mean specific sediment yield of nine reservoirs.

Table 6: Land Use Distribution

Marion	Area	Urban	Cultivated Cropland	Grassland	Woodland	Other
	Drainage	0.44%	52.46%	44.00%	3.09%	0.01%
	Direct Runoff	0.48%	55.66%	39.55%	4.30%	0.01%
	Subcatchment	0.36%	46.82%	51.84%	0.97%	0.01%
El Dorado	**Area**	**Urban**	**Cultivated Cropland**	**Grassland**	**Woodland**	**Other**
	Drainage	0.26%	5.39%	90.90%	3.45%	0.00%
	Direct Runoff	0.04%	9.05%	84.01%	6.90%	0.00%
	Subcatchment	0.40%	3.09%	95.21%	1.30%	0.00%
Council Grove	**Area**	**Urban**	**Cultivated Cropland**	**Grassland**	**Woodland**	**Other**
	Drainage	0.36%	27.61%	67.71%	4.30%	0.02%
	Direct Runoff	0.36%	28.20%	66.20%	5.23%	0.00%
	Subcatchment	0.35%	25.94%	71.94%	1.69%	0.08%
Pomona	**Area**	**Urban**	**Cultivated Cropland**	**Grassland**	**Woodland**	**Other**
	Drainage	1.49%	26.96%	62.03%	9.43%	0.10%
	Direct Runoff	1.86%	28.59%	58.56%	10.95%	0.04%
	Subcatchment	0.58%	22.99%	70.48%	5.71%	0.24%
Melvern	**Area**	**Urban**	**Cultivated Cropland**	**Grassland**	**Woodland**	**Other**
	Drainage	0.61%	15.30%	77.28%	6.78%	0.03%
	Direct Runoff	0.52%	17.54%	73.66%	8.26%	0.03%
	Subcatchment	0.83%	9.57%	86.58%	2.97%	0.04%
Clinton	**Area**	**Urban**	**Cultivated Cropland**	**Grassland**	**Woodland**	**Other**
	Drainage	1.28%	17.43%	61.77%	19.34%	0.19%
	Direct Runoff	0.95%	17.23%	57.76%	23.87%	0.19%
	Subcatchment	1.71%	17.69%	67.04%	13.39%	0.18%
Fall River	**Area**	**Urban**	**Cultivated Cropland**	**Grassland**	**Woodland**	**Other**
	Drainage	0.58%	4.78%	88.42%	6.21%	0.01%
	Direct Runoff	0.90%	6.85%	83.37%	8.87%	0.01%
	Subcatchment	0.12%	1.84%	95.63%	2.41%	0.00%
Toronto	**Area**	**Urban**	**Cultivated Cropland**	**Grassland**	**Woodland**	**Other**
	Drainage	0.31%	7.51%	87.39%	4.78%	0.00%
	Direct Runoff	0.42%	9.78%	83.25%	6.54%	0.01%
	Subcatchment	0.14%	4.02%	93.78%	2.05%	0.00%
Perry	**Area**	**Urban**	**Cultivated Cropland**	**Grassland**	**Woodland**	**Other**
	Drainage	0.96%	32.11%	54.18%	12.73%	0.03%
	Direct Runoff	0.95%	33.12%	50.78%	15.12%	0.03%
	Subcatchment	0.96%	30.20%	60.61%	8.20%	0.02%

Table 7: Soil Erosion Class Distribution

Marion	Area	Deposition	Class 1	Class 2	NoData
	Drainage	24.23%	58.68%	0%	17.20%
	Direct Runoff	23.64%	54.33%	0%	22.02%
	Subcatchment	25.32%	66.91%	0%	7.77%
El Dorado	**Area**	**Deposition**	**Class 1**	**Class 2**	**NoData**
	Drainage	5.34%	74.23%	0.79%	19.64%
	Direct Runoff	9.21%	64.51%	1.06%	25.23%
	Subcatchment	3.17%	79.68%	0.64%	16.51%
Council Grove	**Area**	**Deposition**	**Class 1**	**Class 2**	**NoData**
	Drainage	9.76%	65.02%	18.00%	7.22%
	Direct Runoff	11.55%	63.70%	18.07%	6.68%
	Subcatchment	4.72%	68.74%	17.79%	8.75%
Pomona	**Area**	**Deposition**	**Class 1**	**Class 2**	**NoData**
	Drainage	11.36%	57.49%	0.31%	30.84%
	Direct Runoff	15.15%	55.15%	0.33%	29.36%
	Subcatchment	1.96%	63.28%	0.26%	34.50%
Melvern	**Area**	**Deposition**	**Class 1**	**Class 2**	**NoData**
	Drainage	10.04%	50.47%	3.53%	35.96%
	Direct Runoff	12.67%	47.98%	3.53%	35.82%
	Subcatchment	3.07%	57.05%	3.54%	36.33%
Clinton	**Area**	**Deposition**	**Class 1**	**Class 2**	**NoData**
	Drainage	9.11%	54.38%	5.81%	30.70%
	Direct Runoff	12.86%	51.44%	5.56%	30.14%
	Subcatchment	3.96%	58.42%	6.15%	31.47%
Fall River	**Area**	**Deposition**	**Class 1**	**Class 2**	**NoData**
	Drainage	14.76%	32.48%	0.19%	52.57%
	Direct Runoff	17.21%	31.57%	0.26%	50.96%
	Subcatchment	11.27%	33.77%	0.09%	54.86%
Toronto	**Area**	**Deposition**	**Class 1**	**Class 2**	**NoData**
	Drainage	12.76%	41.50%	0.76%	44.97%
	Direct Runoff	15.33%	38.22%	0.66%	45.79%
	Subcatchment	8.82%	46.55%	0.91%	43.73%
Perry	**Area**	**Deposition**	**Class 1**	**Class 2**	**NoData**
	Drainage	40.67%	19.24%	28.35%	11.75%
	Direct Runoff	42.04%	19.36%	24.36%	14.25%
	Subcatchment	38.07%	19.00%	35.90%	7.02%

Table 8: Soil Runoff Classification Distribution

Marion	Area	Negligible	Low	Medium	High	Very High	NoData
	Drainage	*33.42%	9.55%	2.65%	49.59%	0.00%	4.80%
	Direct Runoff	*35.47%	11.70%	2.86%	42.66%	0.00%	7.31%
	Subcatchment	*29.54%	5.48%	2.24%	62.70%	0.00%	0.04%
El Dorado	**Area**	**Negligible**	**Low**	**Medium**	**High**	**Very High**	**NoData**
	Drainage	8.19%	8.68%	48.56%	28.62%	0.26%	5.68%
	Direct Runoff	15.51%	14.66%	38.05%	30.71%	0.58%	0.49%
	Subcatchment	4.10%	5.33%	54.44%	27.45%	0.09%	8.59%
Council Grove	**Area**	**Negligible**	**Low**	**Medium**	**High**	**Very High**	**NoData**
	Drainage	3.87%	10.66%	35.44%	43.53%	4.30%	2.20%
	Direct Runoff	3.04%	13.75%	34.30%	42.73%	3.53%	2.65%
	Subcatchment	6.19%	1.97%	38.63%	45.78%	6.48%	0.94%
Pomona	**Area**	**Negligible**	**Low**	**Medium**	**High**	**Very High**	**NoData**
	Drainage	4.30%	1.95%	1.96%	24.41%	13.04%	54.34%
	Direct Runoff	4.42%	2.67%	1.97%	23.46%	12.16%	55.31%
	Subcatchment	3.99%	0.17%	1.94%	26.75%	15.19%	51.96%
Melvern	**Area**	**Negligible**	**Low**	**Medium**	**High**	**Very High**	**NoData**
	Drainage	12.78%	9.30%	2.99%	25.33%	11.15%	38.46%
	Direct Runoff	12.29%	11.26%	2.82%	25.08%	10.27%	38.27%
	Subcatchment	14.05%	4.13%	3.43%	25.98%	13.46%	38.96%
Clinton	**Area**	**Negligible**	**Low**	**Medium**	**High**	**Very High**	**NoData**
	Drainage	4.86%	4.60%	18.95%	37.56%	10.69%	23.34%
	Direct Runoff	3.34%	6.50%	22.18%	36.77%	8.87%	22.33%
	Subcatchment	6.96%	1.99%	14.52%	38.65%	13.17%	24.71%
Fall River	**Area**	**Negligible**	**Low**	**Medium**	**High**	**Very High**	**NoData**
	Drainage	43.20%	9.67%	17.30%	5.45%	11.49%	12.89%
	Direct Runoff	40.10%	13.27%	14.92%	4.97%	12.92%	13.82%
	Subcatchment	47.59%	4.57%	20.69%	6.13%	9.45%	11.57%
Toronto	**Area**	**Negligible**	**Low**	**Medium**	**High**	**Very High**	**NoData**
	Drainage	26.31%	9.41%	11.69%	8.61%	21.09%	22.88%
	Direct Runoff	25.04%	12.41%	10.79%	5.71%	22.76%	23.30%
	Subcatchment	28.26%	4.82%	13.08%	13.08%	18.53%	22.23%
Perry	**Area**	**Negligible**	**Low**	**Medium**	**High**	**Very High**	**NoData**
	Drainage	2.34%	8.88%	34.67%	9.36%	5.97%	38.79%
	Direct Runoff	2.09%	9.78%	32.60%	9.73%	6.90%	38.89%
	Subcatchment	2.08%	7.16%	38.60%	8.64%	4.21%	38.58%

*Marion was the only drainage which contained the “Very Low” soil runoff classification, and those areas were incorporated into the negligible category. Approximately 27% of negligible data is actually classified as Very Low.

Table 9: Slope Summary Statistics (Degrees)

Marion	Area	Min	Max	Range	Mean	STD
	Drainage	1.53E-4	59.16	59.16	1.95	2.19
	Direct Runoff	1.53E-4	59.16	59.16	1.95	2.34
	Subcatchment	1.53E-4	48.09	48.09	1.95	1.88
El Dorado	**Area**	**Min**	**Max**	**Range**	**Mean**	**STD**
	Drainage	1.53E-4	60.37	60.37	1.56	1.69
	Direct Runoff	1.53E-4	60.37	60.37	1.86	2.11
	Subcatchment	1.53E-4	53.83	53.83	1.35	1.25
Council Grove	**Area**	**Min**	**Max**	**Range**	**Mean**	**STD**
	Drainage	1.53E-4	66.30	66.30	2.60	3.10
	Direct Runoff	1.53E-4	66.30	66.30	2.74	3.32
	Subcatchment	1.53E-4	63.90	63.90	2.19	2.30
Pomona	**Area**	**Min**	**Max**	**Range**	**Mean**	**STD**
	Drainage	1	69.32	68.32	3.39	3.05
	Direct Runoff	1	69.32	68.32	3.52	3.27
	Subcatchment	1	54.32	53.32	3.03	2.31
Melvern	**Area**	**Min**	**Max**	**Range**	**Mean**	**STD**
	Drainage	1.53E-4	65.08	65.08	2.78	3.00
	Direct Runoff	1.53E-4	65.08	65.08	2.87	3.22
	Subcatchment	1.53E-4	60.61	60.61	2.50	2.22
Clinton	**Area**	**Min**	**Max**	**Range**	**Mean**	**STD**
	Drainage	1.53E-4	73.75	73.75	3.66	4.01
	Direct Runoff	1.53E-4	73.75	73.75	3.99	4.49
	Subcatchment	1.53E-4	67.68	67.68	3.21	3.19
Fall River	**Area**	**Min**	**Max**	**Range**	**Mean**	**STD**
	Drainage	1.53E-4	68.23	68.23	3.70	4.05
	Direct Runoff	1.53E-4	68.23	68.23	3.76	4.23
	Subcatchment	1.53E-4	64.61	64.61	3.58	3.71
Toronto	**Area**	**Min**	**Max**	**Range**	**Mean**	**STD**
	Drainage	1.53E-4	84.11	84.11	3.21	3.59
	Direct Runoff	1.53E-4	84.11	84.11	3.30	3.83
	Subcatchment	1.53E-4	79.96	79.96	3.07	3.09
Perry	**Area**	**Min**	**Max**	**Range**	**Mean**	**STD**
	Drainage	1.53E-4	72.08	72.08	4.01	3.96
	Direct Runoff	1.53E-4	72.08	72.08	4.21	4.36
	Subcatchment	1.53E-4	69.81	69.81	3.63	2.98

Chapter IV

Conclusions

Summary

Historically deficient of lentic features, eastern Kansas now exhibits one of the most densely impounded regions of the United States (Smith et al., 2002), which reflects major anthropogenic alteration of natural processes. A consequence of this alteration is the infilling of artificial water bodies, which Kansans are dependent on for agricultural and municipal services. Federal reservoirs are integral to the state's infrastructure, and many are approaching the end of their usable lives. With need for capacity restoration on the horizon, projected costs of dredging are substantial. In order to prolong usable lives and delay the need for restoration, alternative management practices for reservoirs are needed, and a better understanding of the causes of sedimentation in reservoir drainages could benefit management decision-making.

Given the dense distribution of small impoundments in eastern Kansas and the potential sink services they provide (Smith et al. 2002; Renwick et al., 2005), small impoundments are likely influencing federal reservoir sediment yields. With newly developed high-resolution elevation data, it is now possible to delineate and characterize impoundment catchment within reservoir drainages to better visualize and measure how impoundment distribution may be related to reservoir sediment yield. Additionally, current high-resolution elevation data can be used to identify recently constructed impoundments and potentially improve geometries of popular inventories, which may have inaccuracies due to dated source material and manual delineation methods. In effect, a more complete and accurate inventory of impoundments can be

generated and incorporated into an investigation of drainage traits responsible for reservoir sediment yields.

Chapter 2 tested and evaluated two automated elevation data-based methods of identifying and extracting water features in ten Kansas reservoir drainages. The primary goals were to identify newly constructed impoundments and improve geometries relative to the National Hydrography Dataset (NHD). Using 2-m LiDAR-derived digital elevation models (DEMs) created between 2011 – 2016, the Topographic Wetland Identification Process model (TWIP) from Kastens et al. (2016) and the Zero Slope approach (ZS) successfully identified new water bodies and improved geometric accuracies of duplicated features of the NHD. While geometric accuracy assessment results were comparable for both methods, the ZS was favorable for larger drainage processing due to its shorter processing time, greater number of features identified, lack of scaling issues, and ability to execute successfully without first removing roads and railroads from the DEM. The TWIP experienced scaling issues due to inherent processing limitations of certain ArcGIS tool(s) included in its script and only identified limited numbers of features or failed to run for larger drainages Therefore, the TWIP is not recommended for Kansas reservoir drainage scale processing of 2-m elevation data. The Combined dataset resulting from the TWIP, ZS, and NHD and the verified feature areas from the accuracy assessment indicated a tendency for the NHD to underrepresent cumulative surface area. This trend of underestimating water surface area should be noted in future regional inventories involving the NHD.

The study in Chapter 3 used high-resolution LiDAR-derived DEMs to delineate subcatchment areas of water body datasets produced in Chapter 2 for nine Kansas federal reservoir drainages and investigated potential sources of difference in reservoir sediment yield. This research calculated landscape traits related to erosion and sediment trapping for drainages,

subcatchments, and direct runoff areas. Specific sediment yield was used to compare drainage sediment delivery among reservoirs and omit drainage area as a causal variable for differences in sediment yield. Reservoir drainages included in the study were selected in part due to their similar precipitation patterns, which generally eliminated precipitation as a causal variable for sediment yield. The drainage traits analyzed in this study included: water body size distribution, water body catchment areas, water body surface area to catchment area ratios, percentage subcatchment, and land use, soil erosion class, soil runoff, and average slope for drainage area, subcatchment, and direct runoff area.

Trends were observed in erosion-related traits for drainages with similar specific sediment yields. Percentages of negligible runoff area were highest in the four drainages experiencing the lowest yields, suggesting a trend of less suitable sediment transport conditions relating to lower sediment yields. Additionally, lower percentages of cropland can be tied to lower drainage sediment yields, with two of the three lowest cropland percentages found in the drainages with the lowest sediment yields. Drainage geometry and size influences sediment transport efficiency, and smaller, more rounded watersheds may experience higher delivery ratios than larger, more elongated drainages (Walling, 1983). This could be the primary reason for the stark sediment yield differences between Melvern Reservoir and El Dorado Reservoir. The two drainages with the lowest percentages of large impoundments (> 1 ha) had the highest sediment yields, and the drainage having the lowest sediment yield also had the lowest percentage of small impoundments (< 1/20 ha). In effect, percentage subcatchment coverage alone may not be the most appropriate indicator of small impoundment sediment trapping effects. Water body size distribution should be emphasized in addition to subcatchment coverage when considering potential sediment trapping impacts. Comparison between subcatchments and

direct runoff areas suggested a trend of greater impoundment occurrence in upland grassland areas than lowland agricultural areas.

Further Research

The scripts demonstrated in Chapter 2 can be applied to any areas where high-resolution elevation data is available. For example, now that 2-m DEMs are available for all of Kansas, the ZS tool in conjunction with the NHD could be applied throughout the state to create a statewide enhanced water body dataset. Additionally, the ZS could be run for western Kansas and compared with the TWIP in playa identification suitability. Since LiDAR sampling occurs during winter months (Heidemann, 2014), water is more likely to have been present in playas during data collection, which could result in their hydro-flattening and recognition by the ZS tool.

Toronto and Fall River drainages were exceptions to the trend of increased cumulative water body surface area in the Combined dataset relative to the NHD. The Greenwood County elevation data, which both drainages partially cover, was produced in 2013 and collected over the 2012 – 2013 winter. Kansas experienced a severe drought from 2010 – 2012, but it is considered to have ended by 2013. If the sampling occurred before surface water conditions were restored, desiccated water bodies may have been represented as bare ground and the hydro-flattening may underrepresent typical surface water storage conditions. That may explain why fewer features and smaller surface areas were produced from both elevation data-based approaches. Pinpointing the dates of LiDAR collection and investigating surface water conditions at the time of sampling may provide insight into the cause of these inconsistent results.

Results of chapter 3 provide novel summaries of erosion-related drainage traits for Kansas reservoirs by incorporating upstream catchment. Analysis was conducted in a region with widespread agriculture exhibiting an exceptionally high density of small impoundments. It would be interesting to apply these same methodologies to summarize a drainage containing predominately natural lentic bodies. Would certain factors found to be important in connection to reservoir sediment yield in the heavily cropped study area also hold significance in drainages with contrasting land cover conditions? Given the trend of greater impoundment abundance in headwater areas due to surface water demand by agriculture in floodplains, how might a drainage with more naturally positioned water bodies compare in terms of subcatchment and erosion-related traits? Perhaps, comparison with contrasting drainages might provide additional insight into what causes sediment yields to be so high in the study region.

In this study impoundments were largely discussed under the assumption that they are acting as sinks. This may not always be the case. Foster (2011) found Kansas impoundments to revert to a pass–through system when intervals between precipitation events were minimal. Additionally, impoundments eventually infill and may shift to sources of sediment, which could increase downstream sediment load. More research is needed to understand how and when impoundments shift from sinks to sources in order to better understand their influence on downstream sediment load. While this study delineates catchments and measures surface areas, data on individual impoundment age could be useful in distinguishing their status as sinks or sources for sediment. Age data tell how long the impoundment has been infilling, and with catchment area delineated, the amount of sediment deposited could be roughly estimated. Should capacity data be available, such as in the form of a surface area to volume metric determined from field surveying, the percentage infilled could be estimated. With percentage infill, capacity,

and drainage area, we could begin to understand the trap efficiencies of small impoundments, and apply that knowledge towards better understanding small impoundment sink services in reservoir drainages.

An interesting observation discussed in Chapter 3 is the potential application of the surface area to catchment area ratio towards identifying false water bodies in a dataset. Should false water bodies, such as those that have infilled or were incorrectly added, occur in relatively flat topographic areas, the resulting catchment could approach or match the size of the water feature. In turn, the surface area to catchment area ratio may be disproportionately high. This tool could be used to search for erroneous water features in datasets according to high ratio values and remove them in an effort to improve the dataset.

To calculate slope summary statistics for drainages, subcatchments, and direct runoff areas, slope statistics were calculated after excluding hydro-flattened areas. However, streams and riparian areas were unaddressed and remained in the DEM. It is possible that riparian areas of larger order streams, which would be more likely to occur in proximity to reservoirs and in direct runoff areas, exhibited substantial slopes relative to overland areas. In turn, failing to exclude these riparian areas may have skewed average slope values for direct runoff areas, causing them to exceed average slope values for subcatchments. To remedy this, a buffer might be applied to stream data taken from the NHD, and cells removed from the slope raster according to buffer coverage. This might result in a more accurate representation of overland slope.

Significance

This project demonstrated automated methods which enhance the accuracy and completeness of the NHD with high-resolution elevation data. As LiDAR-derived DEMs become

increasingly common, projects such as this are especially useful since the water feature identification and extraction procedures are scripted and available for use in regions with newly available high-resolution elevation data. Furthermore, it demonstrates inaccuracies in the NHD while offering a means of improving the data, which encourages others to conduct more accurate inventories rather than rely solely on the NHD.

This project used newly available high-resolution elevation data and novel methods to focus on significant potential mitigator of reservoir sedimentation, impoundments, in an investigation into the causes of reservoir sediment yield. When exploring potential causes of difference in reservoir sedimentation, the various traits analyzed should not be investigated independently, but instead should be studied in connection. By better understanding not only the factors determinant of erosion but also the relationships among erosion-related factors, we can better understand the overall processes responsible for reservoir sedimentation rate.

References

Foster, G. M. (2011). Effects of Small Impoundments on Total Watershed Sediment Yield in Northeast Kansas, April through August 2011. (M.S.), University of Kansas, Lawrence, KS.

Heidemann, H. K. (2014). LiDAR Base Specification Version 1.2. *US Geological Survey Standards Book 11, Collection and Delineation of Spatial Data*.

Kastens, J. H., Baker, D. S., Peterson, D. L. & Huggins, D. G. (2016) Wetland Program Development Grant (WPDG) FFY 2013 – Playa Mapping and Assessment. *KBS Report 186*.

Renwick, W. H., Smith, S. V., Bartley, J. D., & Buddemeier, R. W. (2005). The role of impoundments in the sediment budget of the conterminous United States. *Geomorphology 71*(1), 99-111.

Smith, S. V., Renwick, W. H., Bartley, J. D., & Buddemeier, R. W. (2002) Distribution and significance of small, artificial water bodies across the United States landscape. *Science of the Total Environment 299*(1): 21-36.

Walling, D. E. (1983). "The sediment delivery problem. *Journal of Hydrology 65(1)*, 209-237.

Appendix 1

Script 1: Median Filter

```
#Median Filter Script

#Applies a 3X3 median filter to raw DEM to remove noise.
#This script works for elevation values measured to 1000th of a meter.
#(Hence, the raw data is multiplied by a thousand before conversion to integer)
#Conversion to integer is necessary to perform focal median analysis

#Parameters
#DEM - 2 meter raw DEM
   #Set as raster layer in tool properties
#Output DEM - Filtered DEM
   #Set as string in tool properties
#Workspace - workspace
   #Set as folder in tool properties

#Set workspace and processing extent
import arcpy
from arcpy.sa import *
from arcpy import env
arcpy.CheckOutExtension("Spatial")
env.overwriteOutput = True

#get input parameters from Arc toolbox
DEM = arcpy.GetParameterAsText(0)
Output_DEM = arcpy.GetParameterAsText(1)
Workspace = arcpy.GetParameterAsText(2)

def Median_Filter(DEM, Output_DEM, Workspace):
        env.workspace = Workspace
        env.overwriteOutput = True
        env.extent = Raster(DEM)
        env.snapRaster = Raster(DEM)

        Raw = Raster(DEM)
        Int_DEM = Int(Raw * 1000)
        Focal_DEM = FocalStatistics(Int_DEM, "", "MEDIAN","")
        Out_DEM = (Float(Focal_DEM)/1000)
        Out_DEM.save(str(Output_DEM))

#Execute Script
Median_Filter(DEM, Output_DEM, Workspace)
```

Script 2: Topographic Wetland Identification Process (TWIP)

Courtesy of Jude Kastens

```
# This script implements the Sinkhole Identification procedure. Original model by Jude Kastens. Interpreted in python by Ryan Callihan.
# Version 1.0.0
import arcpy, os
from arcpy import env
from arcpy.sa import *
arcpy.CheckOutExtension("Spatial")
arcpy.env.overwriteOutput = True
#get input parameters from Arc toolbox
DEM = arcpy.GetParameterAsText(0)
d = arcpy.GetParameterAsText(1)
HOLV = arcpy.GetParameterAsText(2)
workspace = arcpy.GetParameterAsText(3)

def sinkhole_indentifier(DEM, d, HOLV):
	global workspace

	arcpy.AddMessage("====================================")
	arcpy.AddMessage("Starting Sinkhole Identification Tool")
	arcpy.AddMessage("====================================")

	#setting environment variables from input DEM
	arcpy.env.snapRaster = DEM
	arcpy.env.extent = DEM
	DEM_sr = arcpy.Describe(DEM).spatialReference #get spatial reference from DEM
	#setting temp workspace in HOLV path
	HOLV_path = os.path.dirname(HOLV)
	workspace = HOLV_path + r"\temp_sinkhole_workspace"
	HOLV_basename = os.path.basename(HOLV) #takes filename from the HOLV path
	#if temp workspace exists, remove previous and create new directory
	if os.path.exists(workspace):
		arcpy.AddMessage("Removing previous temp workspace...")
		cleanup()
		os.mkdir(workspace)
	else:
		os.mkdir(workspace)

	# set workspace
	arcpy.env.workspace = workspace

	# print input and derived parameters
	arcpy.AddMessage("====================================")
```

```
arcpy.AddMessage("Input parameters:")
arcpy.AddMessage("DEM: %s" % DEM)
arcpy.AddMessage("Minimum depth threshold (d): %s" % d)
arcpy.AddMessage("Output shapefile: %s" % HOLV_basename)
arcpy.AddMessage("Temp workspace: %s" % workspace)

# create empty polygon layer in DEM projection
arcpy.CreateFeatureclass_management(HOLV_path, HOLV_basename, "POLYGON",
"", "", "", DEM_sr, "", "", "", "")

loop_num = 1
flag = True
while flag:
        arcpy.AddMessage("==============Iteration #%s============" %
        loop_num)

        # 1) [Fill Sinks] Fill sinks (DEM â€ ¡FIL)
        arcpy.AddMessage("Step 1: Filling sinks...")
        outFill = Fill(DEM)
        outFill.save("filled_dem")

        # 2) [Raster Calculator] Create a sink depth map (snk)
        arcpy.AddMessage("Step 2: Creating a sink depth map...")
        sink = Raster("filled_dem") - Raster(DEM)
        sink.save("sink")
        SNK = Con(("sink") > 0, "sink")
        SNK.save("snk")

        # 3) [Raster Calculator] Create mask layer of ones (MSK) for SNK
        arcpy.AddMessage("Step 3: Creating mask layer of ones for SNK")
        MSK = Con(SNK > 0, 1)
        MSK.save("msk")

        #4) [Raster to Polygon] Convert MSK to polygon (MSKV). Do not use
        â□œSimplify Polygonsâ€ •  option.
        arcpy.AddMessage("Step 4: Raster MSK to polygon MSKV...")
        arcpy.RasterToPolygon_conversion("msk", "mskv.shp", "NO_SIMPLIFY")

        # 5) [Zonal Statistics] Create a zone maximum raster (MAX), where MSKV
        polygons are the zones
        arcpy.AddMessage("Step 5: Creating zonal MAX of SNK where zones =
        MSKV.shp...")
        zonalmax = ZonalStatistics("mskv.shp", "ID", "snk", "MAXIMUM",
        "NODATA")
        zonalmax.save("MAX")
```

```
# 6) [Raster Calculator] Create hole indicator raster (HOL) for sinks having at least the minimum.
arcpy.AddMessage("Step 6: Creating hole indicator raster (HOL) for sinks with the specified min depth (d)...")
HOL = Con(Raster("snk") >= float(d), Con(Raster("snk") == Raster("MAX"), 1))
HOL.save("HOL")

# If the HOL raster is empty, terminate script.
nodata = arcpy.GetRasterProperties_management("hol", "ALLNODATA")
isnodata = nodata.getOutput(0)
if int(isnodata) == 1:
        arcpy.AddMessage(" No data in raster \"hol\". Process stopped.")

        arcpy.AddMessage("========================================
        ")
        arcpy.AddMessage("Sinkhole identifiation complete.")

        arcpy.AddMessage("========================================
        ")
        break

# 7) [Raster to Polygon] Convert HOL to polygon (HOLV1). Do not use â□œSimplify Polygonsâ□□ option.
arcpy.AddMessage("Step 7: Converting HOL to polygon (HOLV1)...")
arcpy.RasterToPolygon_conversion("HOL", "HOLV1.shp", "NO_SIMPLIFY")

# 8)
arcpy.AddMessage("Step 8: Checking number of polygons in HOLV1...")
num_records = int(arcpy.GetCount_management("HOLV1.shp").getOutput(0))
arcpy.AddMessage("  Number of records: %s" % (num_records))

# 9) Append HOLV1.shp to HOLV.shp
arcpy.AddMessage("Step 9: Appending HOLV to %s..." % HOLV_basename)
arcpy.Append_management("HOLV1.shp", HOLV, "NO_TEST")

# 10) [Raster Calculator] Create inverted sink depth raster with holes removed (DEM2):
arcpy.AddMessage("Step 10: Inverting sink depth raster and remove holes removed...")
DEM2 = Con(Raster("MAX") >= float(d), Con(Raster("snk") != Raster("MAX"), Raster("MAX") - Raster("snk")))
DEM2.save("DEM2")

# 11) Set DEM = DEM2 and go back to Step 1
DEM = "DEM2"
loop_num += 1
```

```
                arcpy.AddMessage("=====================================")

def cleanup():
        global workspace
        arcpy.AddMessage("Cleaning up intermediate files...")
        for filename in ["filled_DEM", "sink", "snk", "MAX", "msk", "DEM", "DEM2",
        "mskv.shp", "hol", "HOLV1.shp", "log", "info"]:
                if arcpy.Exists(filename):
                        arcpy.Delete_management(filename)
        arcpy.AddMessage("workspace is: %s" % workspace)
        os.rmdir(workspace)

# execute script
sinkhole_indentifier(DEM, d, HOLV)
cleanup()
```

Script 3: Zero Slope Procedure (ZS)

```
#Zero_Slope tool

#Extracts hydro-flattened water bodies from LiDAR-derived DEM
#Extracts all cell patches with slope = 0 and converts patches to polygons
#Applies a cell length buffer to adjust for perimeter cell loss

#Set workspace and processing extent
import arcpy
from arcpy.sa import *
from arcpy import env
arcpy.CheckOutExtension("Spatial")
env.overwriteOutput = True

#Parameters
#DEM - 2 meter filtered DEM
   #Set as raster layer in tool properties
#Output_shp - Zero Slope results shapefile
   #Set as string in tool properties
#Workspace - workspace
   #Set as folder in string properties
#Buffer_dist - buffer distance = cell size (2 Meters)
   #Set as string in tool properties

#get input parameters from Arc toolbox
DEM = arcpy.GetParameterAsText(0)
Output_shp = arcpy.GetParameterAsText(1)
Workspace = arcpy.GetParameterAsText(2)
Buffer_dist = arcpy.GetParameterAsText(3)

def Zero_Slope(DEM, Output_shp, Workspace):
   env.workspace = Workspace
   env.overwriteOutput = True
   env.extent = Raster(DEM)
   env.snapRaster = Raster(DEM)

   Raw = Raster(DEM)
   slope_dem = Slope(Raw)
   Out_DEM = SetNull(slope_dem  >  0,1)
   arcpy.RasterToPolygon_conversion(Out_DEM, "ZS_raw.shp", "NO_SIMPLIFY", "VALUE")
   arcpy.Buffer_analysis("ZS_raw.shp", Output_shp, Buffer_dist, "","","NONE")


#Execute Script
Zero_Slope(DEM, Output_shp, Workspace)
```

Script 4: Random Sampling for AA

```
#Function for random sampling of features for accuracy assessment
#Randomly selects a sample based on FID number and sorts in ascending order
#This operation is preceded by:
        #1)Selecting features that occur in all three datasets with ArcGIS select by location/
        intersect
        #2)Exporting the intersecting features from either NHD, TWIP, or ZS into a separate
        dataset
        #3)Identifying the maximum FID from the resulting dataset
#A sample size of 10 was chosen for each of the 5 drainages sampled

import random

def random_imps(fidMax, sampleSize):
   imp_IDs = random.sample(xrange(0, fidMax+1), sampleSize)
   imp_IDs.sort()
   return imp_IDs
```

Script 5: Total Catchment Area and Surface Area to Catchment Area Ratios

```
#SA:CA

#Calculates total catchment for each waterbody following the
 #dataset's use as pour points in watershed delineation
#This is necessary for accurate area measurement since catchments
 #can become fragmented if converted from raster to polygon
#Creates two new fields for the water body dataset
   #The first provides the total catchment area for each water body/ pour point
   #The second calculates a water body surface area to catchment area ratio
#This tool requires that the watersheds first be converted to polygons
 #and area calculated with the calculate areas tool of the spatial statistics toolbox
 #(this produces the "F_AREA" attribute for the catchments layer)
#This tool also requires that "F_AREA" has been calculated for the waterbodies
 #("F_AREA" for the value layer allows surface area to catchment area calculation)
#Matches water bodies to catchments based on FID and GRIDCODE


#Parameters
#focusLayer = water body dataset
   #Set as shapefile in tool properties
#valueLayer = watershed or catchment dataset
   #Set as shapefile in tool properties
#newFields = Catchment area and SA:CA fields
   #Set as string in tool properties
   #Script splits the string. E.g. "CA SA2CA"  ---> ["CA", "SA2CA"]
#workspace = workspace
   #Set as folder in tool properties

import arcpy
focusLayer = arcpy.GetParameterAsText(0)
valueLayer = arcpy.GetParameterAsText(1)
newFields = arcpy.GetParameterAsText(2)
workspace = arcpy.GetParameterAsText(3)

def SA2CA(focusLayer, valueLayer, newFields, workspace):

   #Set workspace

   from arcpy import env
   env.overwriteOutput = True
   env.workspace = workspace

   #add fields for CA and SA:CA ratio
   newFields = newFields.split()          #e.g., CA SA2CA -> ['CA', 'SA2CA'] with split()
```

```
    arcpy.AddField_management(focusLayer, newFields[0],"FLOAT","","",10)
    arcpy.AddField_management(focusLayer, newFields[1],"FLOAT","","",10)

    #create a feature layer for valueFC
    valLayer=arcpy.MakeFeatureLayer_management(valueLayer,"Value Layer")

    #Create new field list to include "FID"
    #fields = fieldInValueLayer.append(fieldInFocusLayer)
    fields = [newFields[0], newFields[1], "FID", "F_AREA"]

    #Select FID value
    fieldInValueLayer = ["F_AREA", "GRIDCODE"]
    cursorUpdate = arcpy.da.UpdateCursor(focusLayer, fields)
    for Row in cursorUpdate:
        FID = Row[2]
        #Select catchment fragments based on GRIDCODE = FID and sum CA Values
        statcursor = arcpy.da.SearchCursor(valLayer,fieldInValueLayer)
        for statrow in statcursor:
            if statrow[1] == FID:
                Row[0] = Row[0] + statrow[0]
                cursorUpdate.updateRow(Row)
            del statrow
        del statcursor
    del cursorUpdate

    #Calculate SA:CA ratio
    cursorUpdate = arcpy.da.UpdateCursor(focusLayer, fields)
    for Row in cursorUpdate:
        Row[1] = float(Row[3])/float(Row[0])
        cursorUpdate.updateRow(Row)
        del Row
    del cursorUpdate


#Execute Script
SA2CA(focusLayer, valueLayer, newFields, workspace)
```